



University of Ioannina
Department of Medicine
&
Foundation for Research and Technology
Biomedical Research Institute



Master Thesis
I.I.P.S. of Molecular and Cellular Biology and Biotechnology

Elucidating the role of the autism risk gene *CNTNAP2* in early cortical interneuron development using brain organoids

Student: Georgia Voudouri

Supervisor: Dr. Christos Gkogkas, Research Director

Ioannina, 2024-2025

Acknowledgements

The following thesis is part of attendance and completion of the Inter-institutional Interdepartmental Program of Postgraduate Studies (I.I.P.S.) titled “Molecular and Cellular Biology and Biotechnology”, which is a program of the department of Medicine of University of Ioannina.

The duration of the project was approximately a year. That project was assigned to me by Dr. Christos Gkogkas, Researcher at the Foundation of Research and Technology, and it was conducted in his lab in the Biomedical Research Institute of Ioannina.

First and foremost, I want to express my gratitude to Dr. Gkogkas not only for his trust and belief in me in undertaking this project, but also for mentoring me throughout. His help and guidance taught me how to be a better member of a lab and a part of a team.

Moreover, I would like to extend my profound thankfulness to Dr. Kleanthi Chalkiadaki, who supported me through this entire process. Her patience in explaining and teaching me new procedures, along with creating a comfortable and encouraging work environment, was invaluable.

At this point, I would also like to state my sincere appreciation for Dr. Karmel Sofia Gkika, whose support was especially invaluable during the final stages of my master's studies. Her patience in explaining combined with her ability to foster a comfortable and encouraging work environment, served as an example of what it means to be a dedicated and supportive team member.

Furthermore, I cannot exclude from the acknowledgements Elpida Statoulla and Maria Zafeiri, PhD candidates from the lab, whose help was invaluable both in the experimental part of my thesis and in fostering an enjoyable and seamless collaboration.

I sincerely extend my gratitude to the esteemed members of the examination committee, Professors Stathis Frillingos, Charalampos Labrakakis, George Leontaritis and Dimitris Liakopoulos, for accepting my invitation and willingly dedicating their time to reviewing my thesis. Their insightful feedback and valuable contributions have been instrumental in shaping this work.

Additionally, I would like to thank every member of the Institute for their help and goodwill.

Last but not least, I want to thank my family, especially my sister, and friends. They have always been my bulwark in both high and lows moments, including those I faced over the past year.

To conclude, I want to express my overall gratitude for the past year. The challenges, successes, failures, opportunities, and many other experiences encountered while working on a research project and being a member of a lab are unique and formative. I am thankful for these experiences, as they helped me become not only a better scientist but also a better person.

Abbreviations

2D Two-dimensional

3D Three-dimensional

4E-BP eIF4E binding protein

ADHD Attention Deficit Hyperactivity Disorder

AP Apical Progenitors

aRGC apical Radial Glial Cell

AS Alzheimer's disease

ASCL1 Achaete-Scute family bHLH transcription factor 1

ASCs Adult Stem Cells

ASD Autism Spectrum Disorder

BDNF Brain-derived neurotrophic factor

BMP Bone Morphogenic Protein

BP Basal Progenitors

CGE Caudal Ganglionic Eminence

CNS Central Nervous System

CNTN2 *Contactin 2*

CNTNAP2 *Contactin associated protein like 2*

CP Cortical Plate

CR Cajal-Retzius

CRISPR Clustered regularly interspaced short palindromic repeat

DEG Differentially Expressed Genes

DLX Distal-Less Homeobox family

EB Embryoid bodies

ECM Extracellular Matrix

eIF4E Eukaryotic translation Initiation Factor 4E

EMX1/2 Empty spiracles homeobox 1/2

ESCs	Embryonic Stem Cells
FGF	Fibroblast Growth Factor
FMR1	Fragile X Messenger Ribonucleoprotein 1
FOXP1	Forkhead Box G1
FOXP2	Forkhead Box P2
FXS	Fragile X Syndrome
GABA	γ -aminobutyric acid
GAD1	Glutamate Decarboxylase 1
GE	Ganglionic Eminence
GO	Gene Ontology
GPCRs	G Protein-Coupled Receptors
GSKβ	Glycogen Synthase Kinases β
GSX1/2	GS homeobox 1/2
hESCs	Human Embryonic Stem Cells
hiPSCs	Human Induced Pluripotent Stem Cells
hPSCs	Human Pluripotent Stem Cells
ICM	Inner Cell Mass
ID	Intellectual Disability
IP	Intermediate Progenitors
iPSCs	Induced Pluripotent Stem Cells
iSVZ	inner Subventricular Zone
IZ	Intermediate Zone
KD	Catalytic Kinase Domain
KLF4	Krüppel-like factor 4
LGE	Lateral Ganglionic Eminence
LHX	LIM homeobox family

LoF	Loss-of-function
MECP2	Methyl-CpG Binding Protein 2
MGE	Medial Ganglionic Eminence
mTOR	Mammalian target of rapamycin
mTORC1	Mammalian target of rapamycin complex 1
mTORC2	Mammalian target of rapamycin complex 2
MZ	Mantle Zone
NDD	Neurodevelopmental Disorder
NEC	Neuroepithelial Cell
Neurog1/2	Neurogenin 1/2
NKX2.1	NK2 Homeobox 1
NLGN	Neuroigin
NPC	Neural Precursor Cells
NRXN	Neurexin
NSC	Neural Stem Cell
OCD	Obsessive-Compulsive Disorder
OCT	Octamer-binding protein
oSVZ	outer Subventricular Zone
PAX6	Paired-box transcription factor 6
PCA	Principal Component Analysis
PCZ	Primitive Cortical Zone
PD	Parkinson's disease
PH	Pleckstrin Homology Domain
PI3K	Phosphoinositide 3-kinase
PIP₂	Phosphatidylinositol (4,5)-bisphosphate
PIP₃	Phosphatidylinositol (3,4,5)-triphosphate

PKB	Protein Kinase B
PRKCB	Protein Kinase C Beta
PTEN	Phosphatase and Tensin homolog
PV	Parvalbumin
RD	Regulatory Domain
RGC	radial glial cells
Rheb	Ras homolog protein enriched in brain
RTKs	Receptor Tyrosine Kinases
S6K	S6 Kinase
SCs	Stem Cells
SEM	Scanning electron microscopy
SEM	Standard Error of the Mean
SHANK3	SH3 And Multiple Ankyrin Repeat Domains 3
SHH	Sonic Hedgehog
SLC32A1	Solute Carrier Family 32 (GABA Vesicular Transporter) Member 1
SNPs	Short Neural Precursors
SOX2	SRY-related HMG-box transcription factor
SST	Somatostatin
SVZ	Subventricular Zone
TBR1	T-domain transcription factor
TGF-β	Transforming growth factor beta
TSC-1	Tuberous Sclerosis-1
TSC-2	Tuberous Sclerosis-2
UBE3A	Ubiquitin Protein Ligase E3A
VIP	Vasointestinal Peptide
VZ	Ventricular Zone

Abstract

Autism spectrum disorder (ASD) is a complex neurodevelopmental condition characterized by changes in social communication, repetitive behaviors, and cognition. The genetic basis of ASD has been extensively studied, with mutations in Contactin-associated protein-like 2 (CNTNAP2) emerging as a significant risk factor. CNTNAP2 plays a crucial role in neuronal development, particularly in neuronal migration, synaptic function, and interneuron differentiation. However, the precise mechanisms underlying CNTNAP2-related neurodevelopmental phenotypes remain poorly understood.

In this study, we investigated the role of *CNTNAP2* in early cortical interneuron development using human induced pluripotent stem cell (hiPSC)-derived brain organoids. By generating cerebral and ventral forebrain organoids from both control and CNTNAP2 knockout (KO) iPSC lines, we examined how CNTNAP2 loss-of-function impacts neuronal differentiation and the balance of excitatory and inhibitory neuronal populations. Immunofluorescence, confocal imaging, Western blotting, and RNA sequencing were employed to analyze the molecular and cellular consequences of *CNTNAP2* deletion.

Our findings revealed significant alterations in organoid morphology and ventricular zone organization in CNTNAP2 KO cerebral organoids. Notably, KO organoids exhibited an accelerated cell cycle and increased proliferation, coupled with a reduction in TBR1-expressing excitatory neurons. RNA sequencing identified a transcriptional shift favoring interneuron-associated genes, suggesting an imbalance in excitatory/inhibitory neuronal differentiation. In contrast, ventral forebrain organoids did not display significant changes in overall size at the examined time point, highlighting potential temporal and regional differences in CNTNAP2 function.

Given the involvement of the PI3K/AKT/mTOR signaling pathway in neurodevelopment and ASD pathophysiology, we further assessed its activation status in CNTNAP2 KO organoids. No significant differences in mTOR pathway effectors were detected at day 30, suggesting that CNTNAP2-related deficits may arise independently of this signaling cascade or may manifest at later developmental stages.

Together, these findings underscore the critical role of *CNTNAP2* in cortical development and interneuron specification. Our results contribute to the growing body of evidence linking CNTNAP2 dysfunction to ASD-associated neuropathology and emphasize the utility of brain organoids as a model system for studying neurodevelopmental disorders. Further studies incorporating longer differentiation timepoints and additional molecular analyses are necessary to fully elucidate the mechanisms underlying *CNTNAP2*-mediated neurodevelopmental deficits and their implications for ASD.

Περίληψη

Η Διαταραχή Αυτιστικού Φάσματος (ΔΑΦ) είναι μία σύνθετη νευροαναπτυξιακή διαταραχή που χαρακτηρίζεται από προβλήματα στην κοινωνική επαφή, από επαναλαμβανόμενες συμπεριφορές και από γνωστικές ελλείψεις. Η γενετική βάση του αυτιστικού φάσματος έχει μελετηθεί εκτενώς, με τις μεταλλάξεις στο γονίδιο *CNTNAP2* (*Contactin associated protein-like 2*) να φαίνεται να συνιστούν σημαντικό παράγοντα κινδύνου. Το γονίδιο *CNTNAP2* διαδραματίζει κρίσιμο ρόλο στην νευρωνική ανάπτυξη, ιδιαίτερα στη μετανάστευση των νευρώνων, στη λειτουργία των συνάψεων και στη διαφοροποίηση των ενδιάμεσων νευρώνων. Ωστόσο, οι ακριβείς μηχανισμοί που διέπουν τις νευροαναπτυξιακές δυσλειτουργίες που σχετίζονται με το *CNTNAP2* παραμένουν ελάχιστα κατανοητοί.

Στην παρούσα μελέτη, διερευνήσαμε τον ρόλο του γονιδίου *CNTNAP2* στην πρόιμη ανάπτυξη των φλοιικών διάμεσων νευρώνων χρησιμοποιώντας οργανοειδή εγκεφάλου που προέρχονται από ανθρώπινα επαγόμενα πολυδύναμα βλαστοκύτταρα (hiPSC). Δημιουργώντας οργανοειδή του εγκεφαλικού φλοιού και του κοιλιακού προσθίου εγκεφάλου από κυτταρική σειρά iPSC ελέγχου και *CNTNAP2* knock-out (KO) κυτταρική σειρά iPSC, εξετάσαμε πώς η απώλεια λειτουργίας του γονιδίου *CNTNAP2* επηρεάζει τη νευρωνική διαφοροποίηση και την ισορροπία μεταξύ διεγερτικών και ανασταλτικών νευρωνικών πληθυσμών. Για την ανάλυση των μοριακών και κυτταρικών επιπτώσεων της διαγραφής του γονιδίου της *CNTNAP2*, χρησιμοποιήθηκαν τεχνικές όπως η τεχνική ανοσοφθορισμού, η συνεστιακή απεικόνιση, η μέθοδος ανοσοαποτύπωσης και η αλληλούχιση RNA.

Τα αποτελέσματα έδειξαν σημαντικές μεταβολές στη μορφολογία των οργανοειδών και την οργάνωση της ζώνης νευρογένεσης στα *CNTNAP2* KO φλοιικά οργανοειδή. Συγκεκριμένα, τα KO οργανοειδή παρουσίασαν επιταχυνόμενο κυτταρικό κύκλο και αυξημένο κυτταρικό πολλαπλασιασμό, συνοδευόμενα από μείωση των διεγερτικών νευρώνων που εκφράζουν TBR1. Η αλληλούχιση RNA αποκάλυψε μια μεταγραφική μετατόπιση υπέρ των γονιδίων που σχετίζονται με τους διάμεσους νευρώνες, υποδηλώνοντας ανισορροπία στη διαφοροποίηση των διεγερτικών/ανασταλτικών νευρώνων. Αντίθετα, τα οργανοειδή του κοιλιακού προσθίου εγκεφάλου δεν παρουσίασαν σημαντικές αλλαγές στο συνολικό τους μέγεθος κατά το εξεταζόμενο χρονικό σημείο, υποδεικνύοντας πιθανές χρονικές και σημειακές διαφορές στη λειτουργία του γονιδίου της *CNTNAP2*.

Δεδομένης ανάμειξης του σηματοδοτικού μονοπατιού PI3K/AKT/mTOR στη νευροανάπτυξη και την παθοφυσιολογία της ΔΑΦ, εξετάσαμε περαιτέρω την ενεργοποίηση του στα *CNTNAP2* KO οργανοειδή. Στους κύριους ρυθμιστές του μονοπατιού δεν ανιχνεύθηκαν σημαντικές διαφορές την ημέρα 30, γεγονός που υποδηλώνει ότι οι *CNTNAP2*-σχετιζόμενες δυσλειτουργίες μπορεί να προκύπτουν ανεξάρτητα από αυτόν τον σηματοδοτικό καταρράκτη ή να εκδηλώνονται σε μεταγενέστερα στάδια ανάπτυξης.

Συνολικά, τα ευρήματά μας υπογραμμίζουν τον κρίσιμο ρόλο του *CNTNAP2* στην ανάπτυξη του φλοιού και την εξειδίκευση των διάμεσων νευρώνων. Τα αποτελέσματά μας συμβάλλουν στο αυξανόμενο σώμα ενδείξεων που συνδέουν τη δυσλειτουργία του *CNTNAP2* με την ASD και υπογραμμίζουν τη χρησιμότητα των οργανοειδών εγκεφάλου ως μοντέλου για τη μελέτη των νευροαναπτυξιακών διαταραχών. Περαιτέρω μελέτες με μεταγενέστερους χρόνους διαφοροποίησης και πρόσθετες μοριακές αναλύσεις είναι

απαραίτητες για την πλήρη κατανόηση των μηχανισμών που διέπουν τις CNTNAP2-μεσολαβούμενα νευροαναπτυξιακές δυσλειτουργίες και τις επιπτώσεις τους στην ASD.

Table of Contents

Acknowledgements.....	2
Abbreviations.....	3
Abstract.....	7
Περίληψη.....	8
Introduction.....	13
1. Stem cells	13
1.1. Potency	13
1.1.1. Totipotent stem cells	13
1.1.2. Pluripotent stem cells	13
1.1.3. Multipotent stem cells.....	14
1.1.4. Oligopotent or Unipotent stem cells.....	14
1.2. Types of stem cells	14
1.3. Molecular mechanisms that regulate self-renewal	15
2. Three-dimensional (3D) Models.....	16
2.1. Biological model systems.....	16
2.2. Organoids principles	17
2.2.1. Organoids applications.....	18
2.2.2. Types of organoids.....	18
2.3. Brain organoids.....	20
2.3.1. Cerebral organoids.....	22
3. Brain development	23
3.1. Cortical development	26
4. Cortical Neurogenesis	26
4.1. Neurons of neocortex.....	28
4.1.1. Excitatory cortical neurons	28
4.1.1.1. Origin of excitatory neurons	28
4.1.2. Inhibitory cortical neurons	29
4.1.2.1. Origin of interneurons	30
4.2. Genes expressed in cortical neurons used as markers to identify regions and developmental timepoints.....	31
4.3. Dysfunctional neurons and neurodevelopmental disorders	32
5. Autism spectrum disorders (ASD).....	33
5.1. Introduction to ASD Etiology	33
5.2. ASD and Cortical Organization	34
5.3. <i>CNTNAP2</i> and Brain Connectivity in ASD.....	35

6.	<i>Contactin associated protein like 2 - CNTNAP2</i>	35
6.1.	The role of <i>CNTNAP2</i> in neurodevelopmental disorders.....	37
6.2.	<i>CNTNAP2</i> and ASD.....	38
7.	PI3K-AKT/mTOR Signaling Pathway	38
7.1.	Main regulators of the pathway.....	39
7.1.1.	PI3K: Structure and Function.....	39
7.1.2.	AKT: Key Mediator of Cellular Function	39
7.1.3.	mTOR: Central Regulator of Cellular Homeostasis	40
7.2.	Roles of the PI3K-AKT/mTOR Signaling Pathway in Neurodevelopmental and Neurodegenerative Disorders	41
7.3.	PI3K/AKT/mTOR and ASD	42
	Motivation, Hypothesis and Aims	43
1.	Motivation	43
2.	Hypothesis.....	43
3.	Aims	43
	Materials and Methods	44
1.	iPSCs generation and cell culture.....	44
2.	Cerebral and Ventral forebrain organoids induction	44
2.1.	iPSCs thawing and culturing in Matrigel coated plates to D0	44
2.2.	Maintenance and passaging of cultured iPSCs	44
2.3.	Telencephalic organoids generation	45
2.4.	Fixation and Cryopreservation of organoids	45
3.	Immunofluorescence	46
3.1.	EdU click-it assay.....	47
4.	Immunoblotting.....	47
4.1.	Preparation of the samples and the protein extraction.....	47
4.2.	Preparation of polyacrylamide gels	47
5.	RNA sequencing and Bioinformatics Analysis	49
6.	Scanning Electron Microscopy (SEM).....	49
7.	Image Analysis	49
8.	Statistical Analysis	50
	Results.....	51
1.	A hiPSC model to study <i>CNTNAP2</i> gene loss-of-function using zinc finger nucleases	51
2.	<i>CNTNAP2</i> KO leads to decreased cerebral organoid size, VZ disorganization and accelerated cell cycle in cerebral organoids enriched for dorsal brain cells.....	53

3.	Pro-interneuronal transcriptional networks in CNTNAP2 KO cerebral organoids	55
4.	Imbalance of Inhibitory and Excitatory Marker Expression in CNTNAP2 KO Organoids	56
5.	Increased number of positive cells in additional interneuronal markers in KO dorsal Organoids.....	57
6.	<i>CNTNAP2</i> KO does not significantly affect ventral organoid size	57
7.	Increased number of cells expressing TBR1 in CNTNAP2 KO ventral organoids	58
8.	Increased number of GSH2 ⁺ cells in CNTNAP2 KO ventral organoids.....	59
9.	No significant changes in PI3K/mTOR signaling at D30 in dorsal or ventral telencephalic CNTNAP2 KO organoids	60
	Discussion.....	62
	References	65

Introduction

1. Stem cells

Stem cells (SCs) are undifferentiated cells that possess unique biological properties [1]. They are primarily characterized by two key abilities: self-renewal, which allows them to divide while maintaining their undifferentiated state, and differentiation, enabling them to develop into specialized cell types in response to specific signals [2].

Through self-renewal, a stem cell divides to generate one or two daughter cells, which are referred to as asymmetric division and symmetric division, respectively. Self-renewal is a specialized form of cell division in which at least one daughter cell retains the ability to remain in an undifferentiated state, thereby sustaining the stem cell pool [3]. While all stem cells are capable of proliferation, self-renewal refers to a situation in which at least one of the daughter cells retains developmental potential as the mother cells thus maintaining pluripotency and multipotency [4].

The regulatory microenvironment in which stem cells exist, termed the stem cell niche, is critical for preserving their undifferentiated state and controlling their function [5]. This niche comprises supporting cells, extracellular matrix components, and soluble factors that collectively influence stem cell fate. The extracellular matrix (ECM), in particular, serves as both a structural scaffold and a dynamic reservoir for molecular signals that modulate stem cell behavior [2,4]. As long as SCs remain attached to the supporting cells, self-renewal occurs and stemness is maintained. During cell division, one daughter cell remains in contact with the supporting cells, while the other adheres to the ECM, migrates from the niche, and generates a lineage of committed cells [2].

1.1. Potency

As stem cells undergo self-renew and differentiate, their potency - the ability to generate an entire organism from a single cell - gradually decreases. During specialization, developmental potency becomes more restricted, meaning that with each step, stem cells lose the ability to differentiate into a wide range of cell types. For example, pluripotent stem cells can give rise to nearly all cell types, whereas unipotent stem cells are limited to producing only a single cell type (Fig. 1) [1].

1.1.1. Totipotent stem cells

Totipotent stem cells of an embryo commit to two different cell fates, the embryonic cell lineage (the inner cell mass, ICM) and the extraembryonic cell lineage (the trophectoderm). These cells derived from fertilized egg (zygote/ early blastomeres) have the potential to give rise to the whole organism [6,7].

1.1.2. Pluripotent stem cells

Pluripotent stem cells (PSCs) form cells of all three germ layers (ectoderm, mesoderm, endoderm) (Fig. 1), but not extraembryonic structures, such as the placenta. During the process of embryogenesis, cells form aggregations germ layers each eventually giving rise to differentiated cells and tissues of the foetus and, later on, the adult organism. Embryonic stem cells (ESCs) are an example of PSCs. ESCs, including human embryonic stem cells (hESCs), are derived from the inner cell mass of preimplantation embryos. Another example

is induced pluripotent stem cells (iPSCs) derived from the epiblast layer of implanted embryos. The pluripotency of stem cells allows them to form any cell of the organism [1].

1.1.3. Multipotent stem cells

Multipotent stem cells have a narrower spectrum of differentiation potential than PSCs, but they can still generate specialized cell types within specific lineages. In the case of hESCs, once they differentiate into the three germ layers, they transition into multipotent stem cells, which are then limited to producing cell types specific to their respective germ layer. This transition occurs over a brief period during human development. One example is a neural stem cell, which can develop into nerve cells and their supporting cells—oligodendrocytes and astrocytes [1,8].

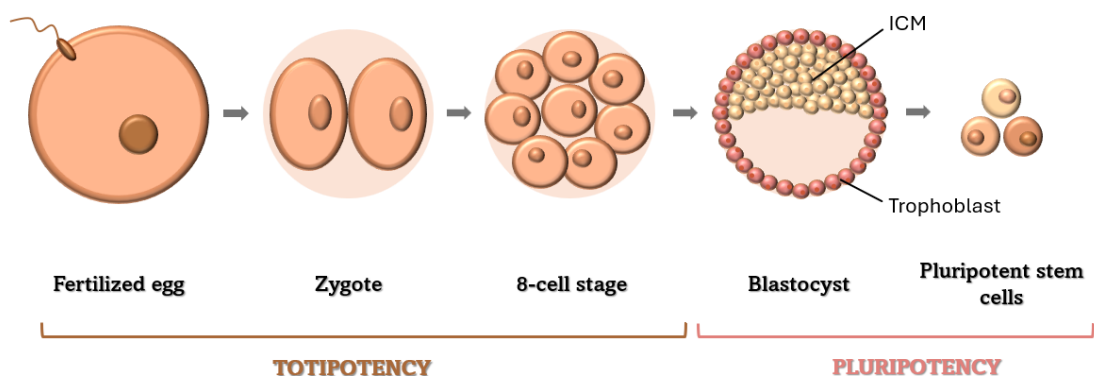
1.1.4. Oligopotent or Unipotent stem cells

Oligopotent or Unipotent stem cells are characterized by the narrowest differentiation capabilities and a special property of dividing repeatedly. They can differentiate into several cell types of given tissues when the tissue contains only one lineage of cells. Hence, these cells are only able to form one cell type [1].

1.2. Types of stem cells

There are several categories of stem cells, based on their source and the tissue they are typically generated from, as well as the stage during which they appear in the lifetime of the organism. Two main categories include the pluripotent stem cells, which are divided into ESCs, iPSCs, and the nonembryonic or somatic stem cells, known as adult stem cells (ASCs).

- I. ESCs are derived from embryonic sources and from the inner cell mass of preimplantation blastocysts. They possess the ability for indefinite self-renewal, and can eventually differentiate and generate all cell types within the body, a characteristic known as pluripotency [2,4].
- II. iPSCs arise from genetic reprogramming of somatic differentiated cells into a dedifferentiated state, which resembles embryonic stem cells [2]. Reprogramming involves the activation of oncogenes such as *MYC* and *KLF4*, processes that will be described below [1].
- III. ASCs are undifferentiated cells and found among differentiated cells in the whole body after development. They are multipotent progenitor cells that can be isolated from a variety of adult tissue including bone marrow, blood vessels, skin and muscles [2]. They possess extensive, but limited, self-renewal potential.



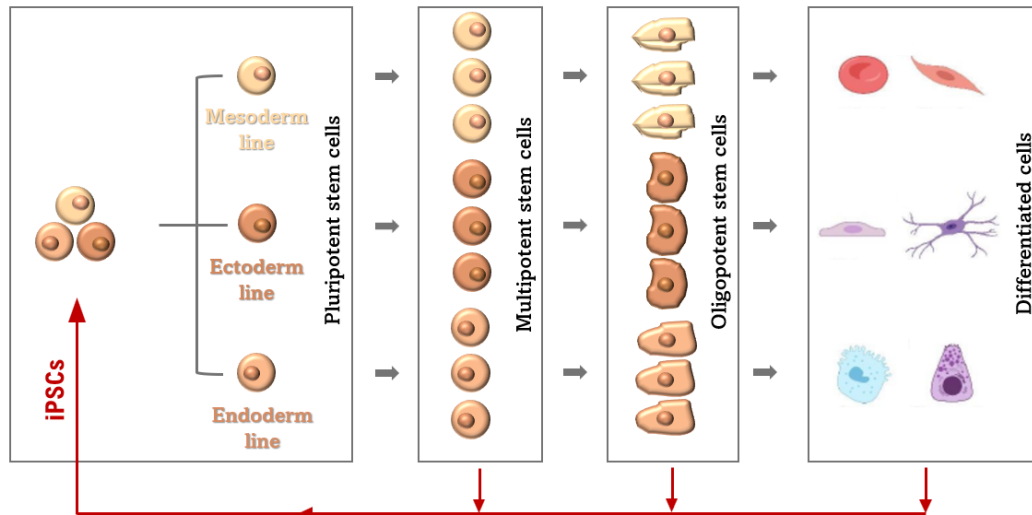


Figure 1 | The stem cell hierarchy progresses, from pluripotent stem cells (PSCs) which originate from inner cell mass (ICM) to fully differentiated cells, passing through intermediate stages of multipotent and oligopotent, with the potential of dedifferentiation [9].

1.3. Molecular mechanisms that regulate self-renewal

The traditional developmental dogma follows the differentiation of totipotent stem cells into PSCs, which then progress to multipotent, unipotent and finally mature cells. During the transition both self-renewal capacity and differential potential decrease [6]. However, the discovery of nuclear reprogramming methods such as somatic cell nuclear transfer method and use of transcriptional factors to induce pluripotency in any cell type, can reverse this hierarchy [10].

Pluripotency of cells is mainly regulated by number of molecular mechanisms that control the expression of genes responsible for maintaining the primitive state and preventing differentiation [11]. Somatic cells can be reprogrammed to achieve a totipotent or pluripotent state and iPSCs generated from patients have proven potential for disease modeling and regenerative medicine [6].

Several transcription factors, including *OCT3/4*, *SOX2*, *NANOG* and others, play key roles in the maintenance of pluripotency in both early embryos and ES cells [12]. Additionally, several genes frequently upregulated in tumors, including *STAT3*, *E-RAS*, *c-MYC*, *KLF4* and *β-CATENIN* contribute to the long-term ES cell phenotype maintenance and the rapid proliferation of ES cells in culture [6].

Cellular reprogramming into an induced pluripotent state is achieved through the ectopic expression of key transcription factors, collectively referred to as the Yamanaka factors (*OCT4*, *SOX2*, *KLF4*, and *c-MYC*). These factors orchestrate the activation of pluripotency-associated genes while repressing differentiation pathways, thereby converting somatic cells into a pluripotent state with characteristics similar to embryonic stem cells [6,13].

OCT4 (Octamer-binding protein 4), a transcription factor of POU transcription factor family, is essential for establishing and maintaining pluripotency. Its expression is restricted to pluripotent lineages and represses differentiation to the trophoblast, while it works with other factors to maintain the undifferentiated state [14].

SOX2 (SRY-related HMG-box transcription factor Sox2) is important for various development processes, and its key role is the regulation of pluripotency, and the determination of cell fate. It works alongside OCT4 to activate genes required for maintaining the undifferentiated state [6,15].

KLF4 (Krüppel-like factor 4) supports the regulation of NANOG expression by interacting with OCT4 and SOX2 further reinforcing the pluripotent state [6].

c-MYC facilitates an active chromatin environment conducive to cell proliferation, enhancing transcription initiation and elongation [6].

2. Three-dimensional (3D) Models

2.1. Biological model systems

Throughout evolution, biological mechanisms have remained largely conserved, allowing researchers to use model organisms to study fundamental processes in biomedical research. Ideal model species are those that exhibit rapid growth, high reproductive rates, and can be maintained cost-effectively in laboratory settings. Commonly used models include *S. cerevisiae*, *C. elegans*, *D. melanogaster*, zebrafish, mice, and human cell lines, all of which have been instrumental in advancing our understanding of cellular signaling, drug discovery, and disease mechanisms [16].

The development of human induced pluripotent stem cell (hiPSC) technology, along with advancements in ASC culture methods, has enabled the creation of personalized in vitro models. By reprogramming somatic cells into iPSCs and directing their differentiation into specialized cell types such as neurons or cardiomyocytes, researchers have established two-dimensional (2D) monolayer cultures as a standard approach in experimental studies [11]. Despite their broad applications and numerous advantages, these models still face limitations that may impact their utility [11,16]. Additionally, 2D culture models, though useful, are much simpler in terms of their physiological and developmental complexity. They cannot capture the intricate process that occurs between different cell types in an organ or organism, limiting their ability to provide a comprehensive understanding of complex processes such as embryonic development, cellular differentiation, tissue regeneration, and disease progression (Fig. 2) [17].

In the case of animal models, studies have identified biological processes unique to humans that cannot be accurately replicated in other animals. These include processes like brain development, metabolism and drug efficacy testing. For example, plenty of biological phenomena that are specific to humans are difficult to reproduce in animal models. The human brain is notably more complex than that of a mouse counterpart, in part due to unique development events and mechanisms. Also, the inaccessibility of this tissue and the lack of human in vitro models also impede research on the brain [18]. Looking closer, neurons in the human cortex arise from a cell type, outer radial glia, which is either absent or present in negligible amounts in rodents [19]. Furthermore, generating animal models for specific diseases often requires prior knowledge of the conditions or genes implicated in a disease examined. Animal models are usually developed by subjecting animals to harmful conditions or by manipulating the genes associated with the disorder, something that gives rise to ethical concerns, which subsequently lead to limited use of animal models in disease

modeling and drug screening [16]. Moreover, differences in microbiota and pathogen composition between animal models and humans, as well as the failure of some phenomena observed in mice to translate directly to humans, limit the applicability of animal models in human disease research (Fig. 2) [17].

To improve model precision, researchers have developed in vitro three-dimensional (3D) culture techniques that utilize stem cells derived from various human tissues. Differentiating hiPSCs into multiple specialized cell types allows these cultures to form structured tissue-like assemblies, overcoming several limitations of conventional 2D models. This innovation has positioned 3D culture systems as a promising tool for biomedical research [17]. So, 3D cell models can be generated directly from patients without prior knowledge of the genes responsible for the disease. In this context, human organoids, which emerged in the early 2010s, represent a novel experimental model that bridges the gap between animal models and human biology (Fig.2) [19].

	2D cell culture	<i>C.elegans</i>	<i>D. melanogaster</i>	<i>D. rerio</i>	<i>M. musculus</i>	PDX	Human organoids
Ease of establishing system	✓/✗	✓	✓	✓	✓	✓	✓
Ease of maintenance	✓	✓	✓	✓	✓	✓	✓
Recapitulation of developmental biology	✗	✓	✓	✓	✓	✗	✓
Duration of experiments	✓	✓	✓	✓	✓	✓	✓
Genetic manipulation	✓	✓	✓	✓	✓	✗	✓
Genome-wide screening	✓	✓	✓	✓	✗	✗	✓
Physiological complexity	✗	✓	✓	✓	✓	✓	✓
Relative cost	✓	✓	✓	✓	✓	✓	✓
Recapitulation of human physiology	✓	✓	✓	✓	✓	✓	✓

✓ Best
✓ Good
✓ Partly suitable
✗ Not suitable

Figure 2 | Comparison of organoids with other model systems [19].

Despite their advantages, 3D models also present certain challenges. One significant limitation is cost, while in most cases are generally less expensive than vertebrate models such as mice or fish, organoids remain more costly compared to traditional models like cell lines, yeast, or invertebrate organisms. Scalability is another concern, as modeling whole-organ functions remains difficult. Additionally, heterogeneity, resulting from individual biological variability and differences in protocols across laboratories, can lead to inconsistencies in organoid formation and experimental reproducibility. Developing standardized methodologies for organoid generation and quality control is essential to enhance the reliability of these models [19,20].

Still, organoid models are at the forefront of research, offering more and greater advantages than drawbacks. As a result, research efforts are increasingly focused on overcoming the constraints of this model to fully harness its potential and make it more effective for scientific and medical applications.

2.2. Organoids principles

Organoids are self-organizing, 3D culture systems that mimic the structure and function of human organs. In some cases, they exhibit histological features that are nearly identical to

their *in vivo* counterparts [21]. A key characteristic of all organoids is that they are derived from either PSCs or ASCs (also known as tissue stem cells) by replicating human development or organ processes *in vitro* (Fig. 3) [22]. Studying organoid formation offers valuable insights into the mechanisms governing human development and organ regeneration, underscoring their significance for basic biological research, as well as their potential applications in pharmaceutical testing and molecular medicine [19,23].

3D organoids are capable of multi-lineage differentiation, giving rise to a diverse population of cells that self-organize into complex, tissue-like structures. Processes such as cell migration, segregation, and spatially restricted lineage determination are key to tissue self-organization during organogenesis [17].

In conclusion, organoids represent a significant advancement in model system generation, featuring cell types and environmental conditions that more accurately reflect those found in the human body.

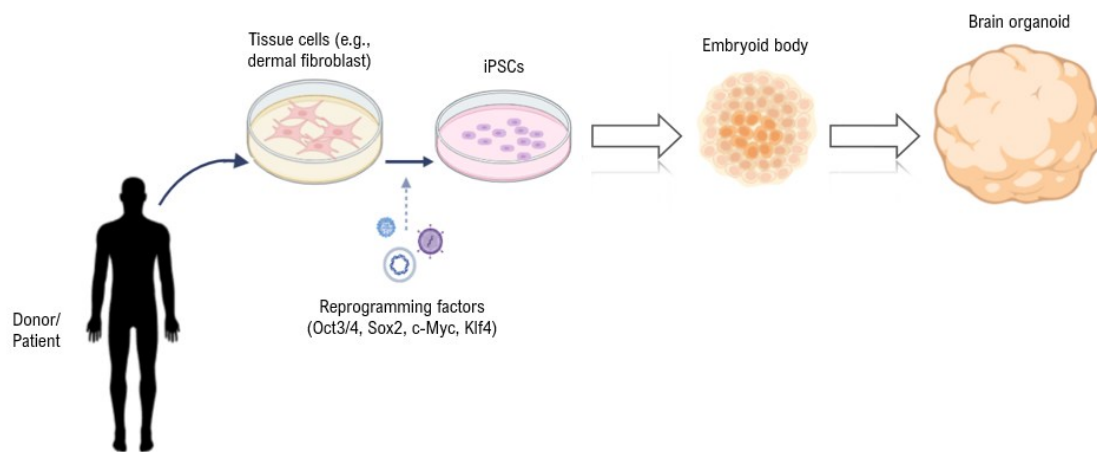


Figure 3 | Organoid formation from hiPSCs.

2.2.1. Organoids applications

Organoid-based methods are highly effective for exploring regulatory and pathological mechanisms at the molecular level due to their wide range of applications. 3D organoids have numerous uses in therapeutic and pharmaceutical testing, including studying host-microbe interactions, conducting transcriptome profiling to identify biomarkers of interest, modeling cancer and metastasis, screening drugs, and modeling diseases through mutational reversion, which can be targeted in cell-based therapies [17,24,25]. Overall, organoids have paved the way to model disease conditions more accurately in comparison to prior models. Thus, organoids could be an excellent experimental model [16].

2.2.2. Types of organoids

Various differentiation protocols have been developed to generate a wide range of organoid types *in vitro*, such as intestinal, kidney, brain, retinal, pancreatic, and liver organoids (Fig.4) [19]. By directing hPSCs to differentiate into the three germ layers, progenitors from these different lineages can be aggregated and further differentiated into the specific cell types and tissues of interest [26]. This approach allows the modeling of complex diseases associated with various organs using these different forms of organoids. For instance, brain

organoids can be used to model congenital brain malformations, primary microencephaly, autism/macrocephaly, Alzheimer's disease, Parkinson's disease. Pancreatic organoids can be utilized to study cystic fibrosis and pancreatic ductal adenocarcinoma, while lung organoids can model fibrotic lung disease. Retinal organoids are valuable for studying conditions such as retinitis pigmentosa, age-related macular degeneration and Leber congenital amaurosis (LCA) [17].

Reprogramming cells to a pluripotent state is typically achieved through the forced expression of a defined set of transcription factors, allowing the resulting pluripotent cells to subsequently differentiate into specific cell types. iPSC has revolutionized research by enabling the generation of patient-specific stem cells, providing an unlimited supply of human stem cells and stem cell-derived tissues [22]. Additionally, iPSC technology has facilitated the establishment of patient-derived stem cell banks. Line-to-line variability, arising from human genetic heterogeneity, has been addressed through the use of isogenic controls generated via genetic engineering tools such as CRISPR–Cas9 [27]. These advancements have allowed researchers to employ iPSC-derived specialized cell types, including neurons, cardiomyocytes, hematopoietic progenitor cells, and pancreatic β -cells, for disease modeling and drug screening. Notably, just over a decade after their introduction, 3D organ culture methods have significantly expanded the applications of human iPSCs [17].

Human PSC-derived organoids are generated using guided differentiation protocols that emulate developmental processes identified through *in vitro* and *in vivo* studies. While it remains nearly impossible to precisely replicate all biochemical cues that drive cell differentiation and 3D tissue assembly—including their timing, spatial distribution, and molecular concentrations—cells *in vitro* tend to follow a semi-autonomous differentiation trajectory similar to their *in vivo* counterparts [19].

Organoid formation follows three essential steps. First, key signaling pathways involved in developmental patterning are either activated or inhibited using commercially available morphogens and signaling inhibitors to establish the correct regional identity during stem cell differentiation. This is typically guided by signaling events identified in murine models that regulate cell fate *in vivo*. Second, optimized media formulations are developed to support the terminal differentiation of specific cell types within the organoid (Fig.18). Finally, cultures are grown under conditions that promote three-dimensional expansion, either by aggregating cells into 3D structures or embedding them in a supportive extracellular matrix [19].

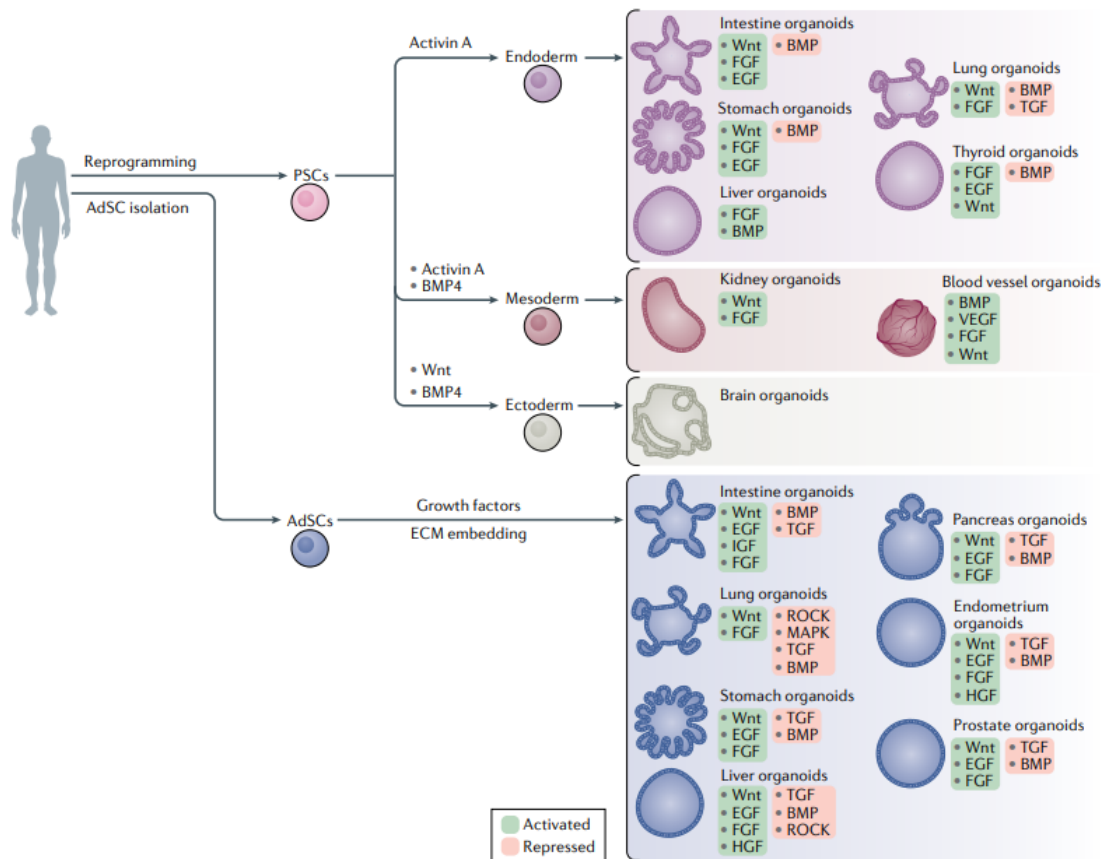


Figure 4 | Process for the establishment of human PSC-derived and ASC-derived organoids [19].

In the case of brain organoids, human PSCs are initially guided to differentiate into embryoid bodies before further differentiation towards the neuroectodermal lineage. Once the cell aggregates contain the developmental precursors for brain tissue patterning, the rest of the developmental steps occur spontaneously.

2.3. Brain organoids

Until the last decade, available models to study human brain development included post-mortem tissues at different stages of development, derivations from animal models, and in vitro mono- or co-culture models of cell types present in the brain, each presenting their own advantages and limitations. In the past decade, the quest for more complex and physiologically relevant human in vitro models for disease modelling and drug discovery culminated in the development of brain organoids [28]. These in vitro models that are derived from human pluripotent stem cells cultured in 3D have emerged as a new model system that could bridge the gap between patient studies, cell cultures and animal models [29]. Ever since and after the first report of generation of 3D self-organized human cortical tissue, various methods are used to generate brain organoids, many of which aim to model the development of the human brain and to recapitulate human disease [30,31]. Organoids have been generated to model various parts of the brain, including the forebrain, midbrain, cerebellum, cortex and hippocampus (Fig. 5). Thus, brain organoids, which simulate brain development, function as an excellent model system for studying neurodevelopmental [32].

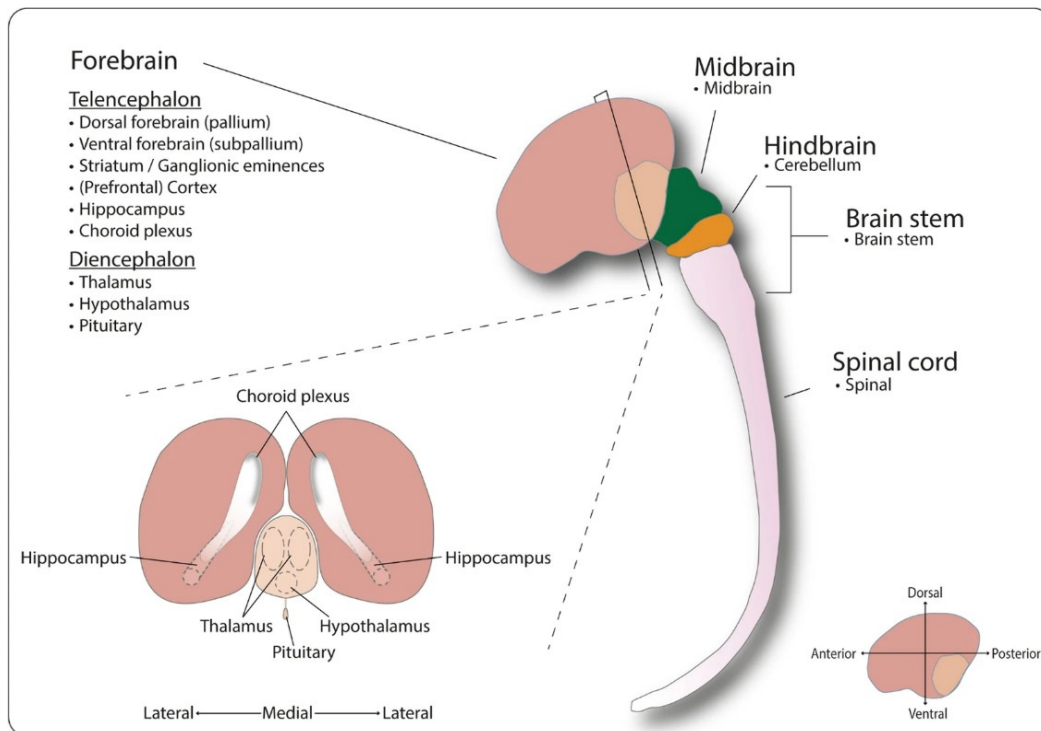


Figure 5 | Schematic overview of the currently available brain organoid models representing different regions of the human developing central nervous system [28].

Human brain organoids are self-organizing 3D tissue models derived from PSC that can reflect early brain organization and replicate specific aspects of human brain development and physiology, including various cell types and brain regions. This structure allows cells to interact with one another and with the extracellular matrix, thereby creating a physiological microenvironment. The 3D shape accurately emulates the natural, *in vivo* environment. As a result, the gene expression and morphology of these organoids closely resemble those of the human foetal brain, extending up to the last trimester of gestation [32]. Human brain organoids provide a unique opportunity to model with precision different cellular facets of human brain development and disease, such as cellular proliferation, differentiation, and survival. Additionally, they can offer insights into the migratory trajectories of specific cell types *in vivo*, such as the migration of interneurons from the ventral forebrain into the dorsal forebrain [28].

Brain organoids can be generated using either guided or non-guided approaches. In both cases, hPSCs or hiPSCs are initially cultured in 3D spheres called embryoid bodies (EB) which have the capability to differentiate into the three embryonic germ layers [33]. During the development of brain organoids, they differentiate into diverse specific regional identities following an endogenous trajectory. EBs are then directed towards an ectodermal fate and further differentiated into neural ectoderm giving rise to neural precursor cells (NPC, neural stem cells and neural progenitors). NPCs further differentiate into the diverse neuronal and glial cell types (e.g., neurons, astrocytes, and oligodendrocytes) while organizing into region-specific structures that mimic different regions of the human brain (Fig. 6) [32]. Due to their ectodermal origin, organoids typically lack non-ectodermal cell types such as microglia and vasculature [28].

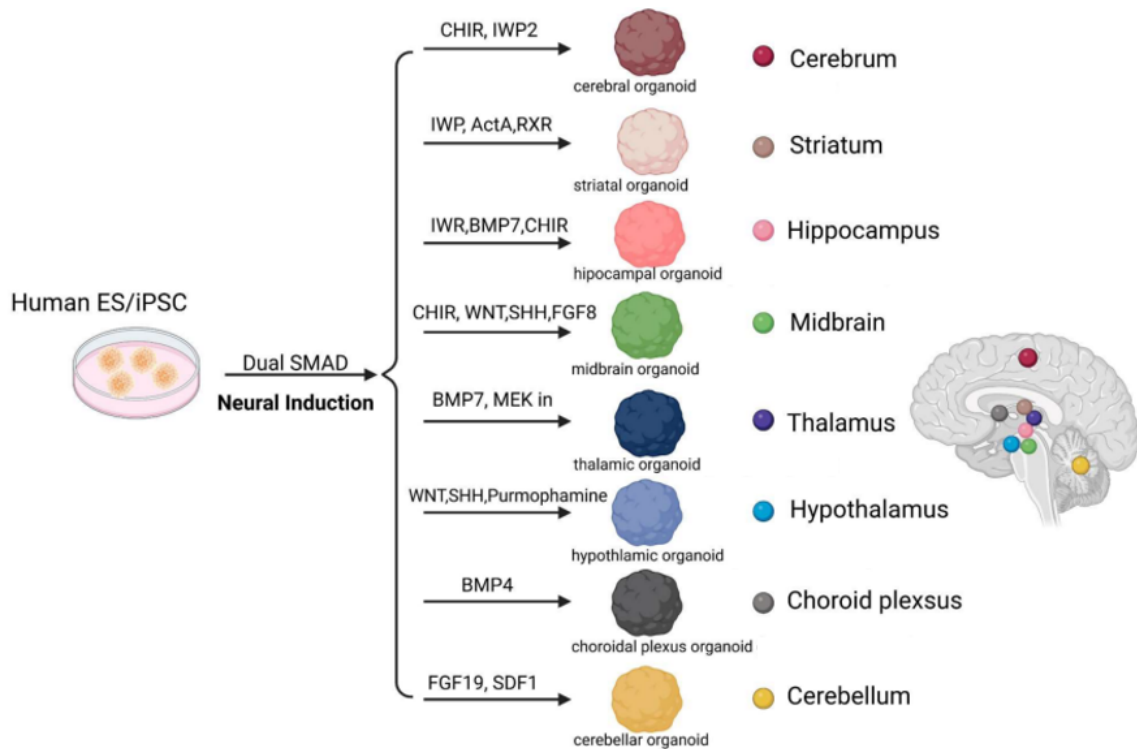


Figure 6 | Brain region-specific organoids through patterned differentiation [32].

2.3.1. Cerebral organoids

It originates from the dorsal telencephalon of the anterior forebrain and represents the largest brain structure, playing a key role in complex behaviors such as perception and episodic memory. During development, the cerebral cortex exhibits a layered organization, consisting of the ventricular zone, subventricular zone, outer subventricular zone, intermediate zone, subplate, cortical plate, marginal zone, and outer cortical layers [34,35].

The ventricular zone contains neural stem cells that express the paired-box transcription factor 6 (PAX6) and SOX2, which are essential for neurogenesis. The induction of the cerebral cortex from dorsal telencephalic regions is highly dependent on extrinsic signaling cues, including Bone Morphogenic Proteins (BMPs), WNT, Fibroblast Growth Factors (FGFs), and Sonic Hedgehog (SHH). Additionally, dorsal telencephalic neural progenitors exhibit high expression of pro-neural transcription factors such as Neurog1/2-Neurogenin 1/2, EMX1/2-empty spiracles homeobox 1/2, LHX2-LIM/homeodomain, and PAX6 [34,35].

In contrast, neural progenitors in the ventral telencephalon rely on distinct molecular pathways. Unlike their dorsal counterparts, they do not depend on BMP and WNT signaling and instead express a unique set of pro-neural transcription factors, including ASCL1-achaete-scute family bHLH transcription factor 1, GSX1/2-GS homeobox 1/2, DLX1/2/5/6-Distal-Less Homeobox family, LHX6/8, and NKX2.1- NK2 Homeobox 1, which are critical for ventral identity and interneuron specification [34,35].

There are several approaches for generating human cortical organoids. Cortical organoids are first induced to neural fate with inhibitors of WNT, BMP and/or Transforming growth factor beta (TGF- β) signaling. After differentiation, insulin and Brain-derived neurotrophic factor (BDNF) promote maturation (Fig. 7) [34].

Cerebral organoids recapitulate many aspects of embryonic cortical development including the generation of diverse cell types corresponding to different brain regional identities. For instance, cerebral organoids can produce dorsal and ventral forebrain progenitors that generate excitatory neurons and inhibitory interneurons, respectively. Moreover, cerebral organoids can be generated from hiPSCs and used for functional genomic studies of neurological disorders such as microcephaly and Autism. Therefore, cerebral organoids represent an exemplary experimental system to study the role of neurological disease-associated genes in brain development [36].

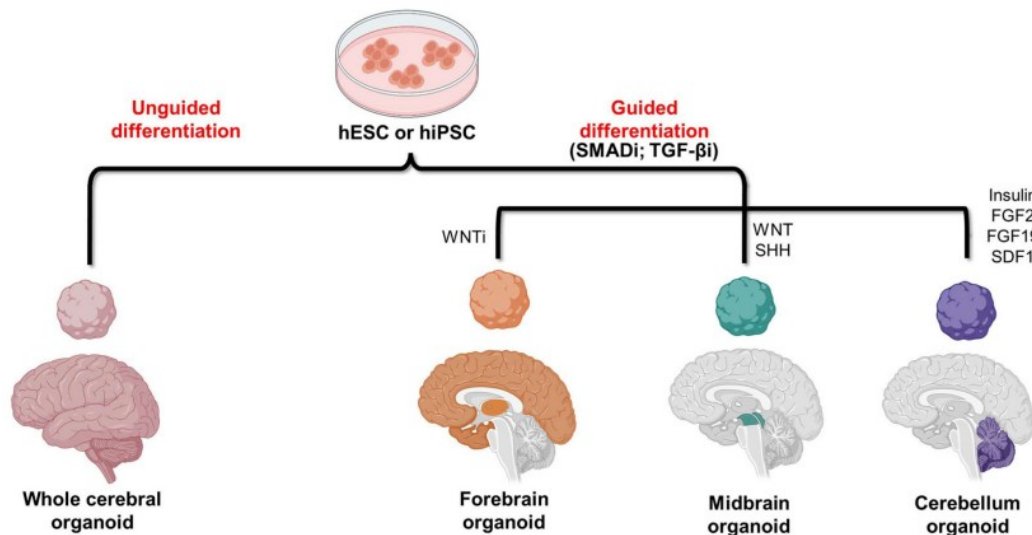


Figure 7 | Methods of generating brain organoids [16].

3. Brain development

Human brain development follows a highly organized sequence of cellular and molecular events, orchestrated by genetic instructions, to form an organ responsible for complex cognitive and behavioral functions, including memory, language, and emotion. While many of these developmental mechanisms are conserved across mammalian species, research using traditional animal models has been crucial in uncovering their genetic basis. However, evolutionary adaptations have introduced species-specific traits that may underlie the advanced cognitive capabilities unique to humans [36,37].

The brain is arguably the most complex organ in the human body. The exquisite process of human brain formation, in the duration of which a microscopic tube of neuroepithelial cells forms a complex structure of billions of cells of diverse types and numerous synaptic connections, is a result of coordinated cellular and molecular steps. The development of the mammalian brain follows conserved spatiotemporal patterns that regulate its cellular organization, progressing from pluripotent stem cells to a differentiated and intricately complex mature nervous system [38].

The formation of the human brain begins in the third week after conception and extends into early adulthood. Initially, the process involves a sequence of developmental milestones, including neurulation, during which the neural tube forms, followed by ventral induction,

where the primary brain vesicles emerge. These steps ultimately lead to the regional patterning and structural organization of the brain (Fig. 8) [29].

A huge number of steps complete the development of nervous system and subsequently the development of the brain, starting with the individualization of the neural plate (at the beginning of the 3rd week post conception until adolescence), continuing with late neurogenesis and ending with some persisting neuronal production for life [39].

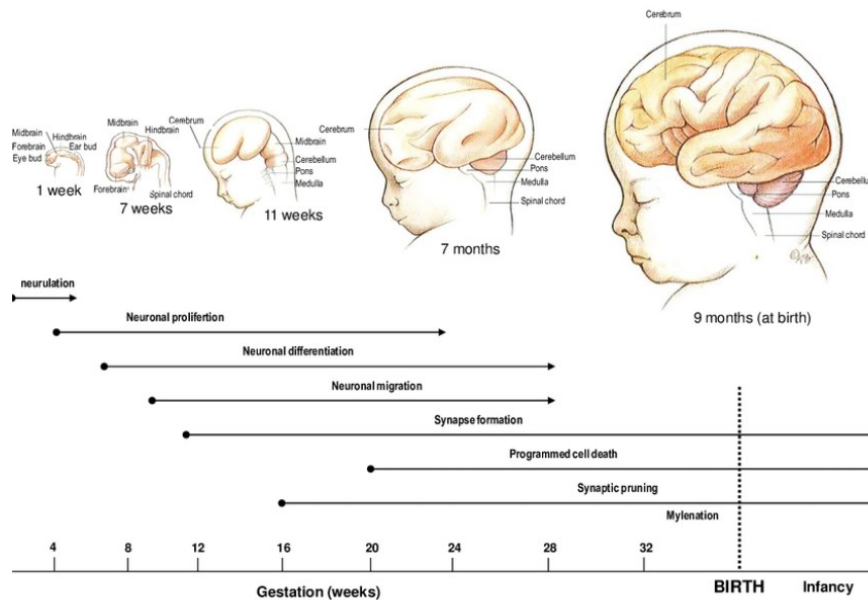


Figure 8 | The principal stages of brain development before birth [40].

The initial event of nervous system development is the formation of the three germ layers during a procedure called gastrulation, where epiblast cells migrate. Primitive stimuli lead to gastrulation, such as the secretion of fibroblast growth factor 8 (FGF8). Now epiblast cells migrate to take their place and form endoderm, mesoderm, and ectoderm. A group of cells called notochord and have endoderm origin induces the neuroectoderm to become the neural plate through various signals (e.g. increasing the FGF and inhibiting the bone morphogenic protein-BMP4) [41].

As neural development progresses, the edges of the neural plate rise to form neural folds, while the central region creates the neural groove. These folds eventually converge and fuse, giving rise to the neural tube, a structure essential for the formation of the central nervous system. Concurrently, a subset of cells at the boundary between the neural plate and the ectoderm differentiates into neural crest cells, which subsequently migrate to various embryonic regions and contribute to multiple cell lineages. Initially, the neural tube remains open at both ends, with the anterior neuropore closing by day 25 (18–20 somite stage) and the posterior neuropore sealing by day 28 (25 somite stage) (Fig. 9) [41].

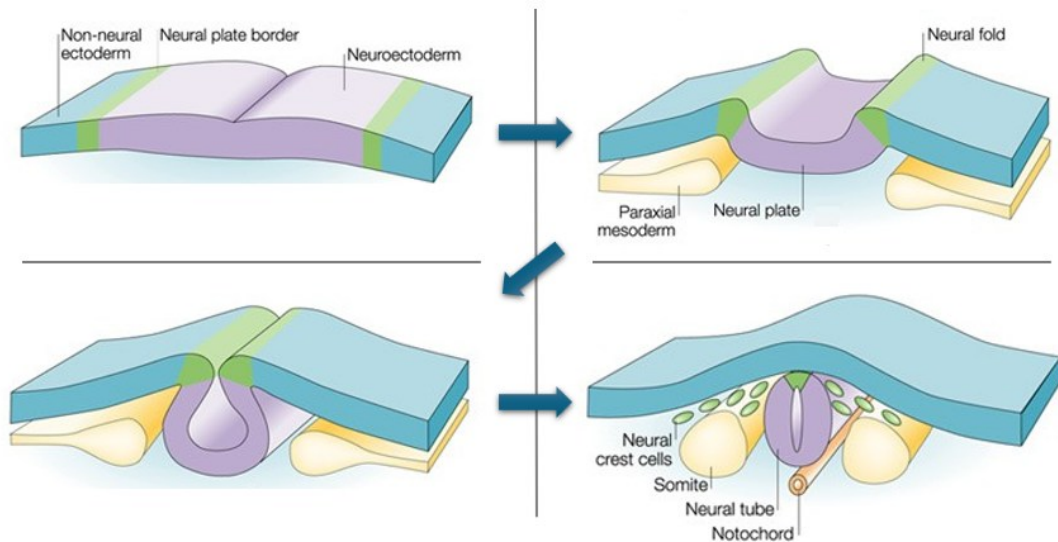


Figure 9 | Formation of neural tube [42].

The upper part of the neural tube, which becomes the adult brain, gives rise to three primary areas of it. The forebrain (Prosencephalon), the midbrain (Mesencephalon), and the hindbrain (Rhombencephalon) are about to constitute the adult brain. The forebrain is divided further into Telencephalon and Diencephalon, while hindbrain divides into the Metencephalon and Myelencephalon. The lower part of the neural tube is going to be the adult spinal cord (Fig. 10) [41,43].

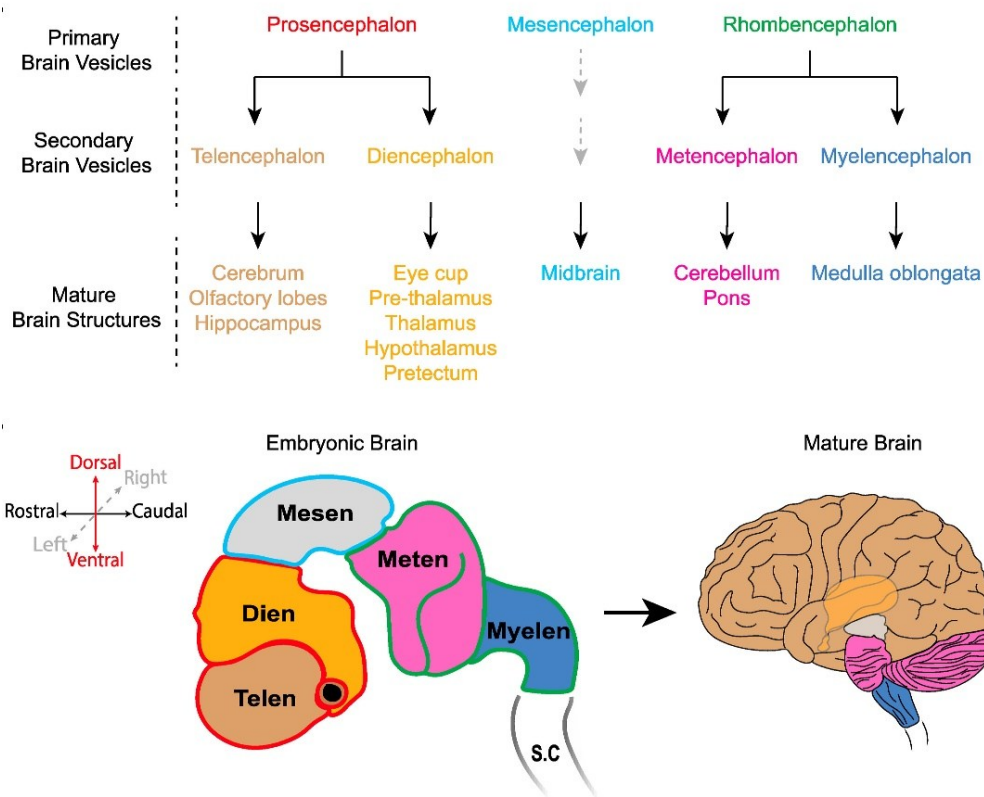


Figure 10 | Schematic of brain vesicle differentiation during neural tube development [34].

Some essential events can be considered as principal stages of brain development. The induction of the ectoderm, the formation of the neural tube followed by the formation of the telencephalon along with the neurogenesis, which is referred to the production of neuronal progenitors and then of mature neurons, and neural migration can be considered as some of those. Also, the programmed neural death, the generation of neurites, the synaptogenesis, the angiogenesis, gliogenesis and myelination are some more. Intrinsic factors, determined genetically, control these various stages of brain development and maturation. Extrinsic environmental factors modulate the intrinsic signals and involve the epigenetic factors. All these synchronized stimuli ensure the normal progression of the development. Any derangement of those events could lead to deficit in brain growth and/or brain malformation. The functional consequences to children depend on the developmental stage in question [39].

3.1. Cortical development

The cerebral cortex is critical for memory formation, language, perception, attention, and other intellectual activities. These functions are supported by six layered neuronal structures, which are composed of excitatory and inhibitory neurons [44].

As is already mentioned, the telencephalon, at the rostral end of the developing neural tube, is the embryonic precursor to the cerebral hemispheres. Through the telencephalic development process, the different areas of it provide the necessary cues for neurons so they generate their complex networks of connections and finally form the mature cerebral cortex. Even at this earliest stage, the telencephalon shows evidence of patterning, such as the restricted expression domains of certain genes. For example, the homeobox genes *GSH2*, *PAX6*, and *EMX2* are each expressed in specific regions of the telencephalon and are essential for its normal patterning. In addition to being defined by specific patterns of gene expression, the various telencephalic regions also exhibit different rates of cell proliferation, differentiation, and programmed death, leading to distinct morphologies [45].

The telencephalon is divided into dorsal and ventral regions, contributing to the generation of specific neuronal populations. The dorsal telencephalon (pallium) is responsible for producing glutamatergic excitatory neurons, which integrate into structures such as the neocortex and hippocampus. In contrast, the ventral telencephalon (subpallium) gives rise to GABAergic inhibitory neurons, originating from the medial, lateral, and caudal ganglionic eminences (MGE, LGE, CGE, respectively), which later form the striatum and globus pallidus [45,46].

4. Cortical Neurogenesis

The mature cerebral cortex is the result of a developmental process that ends with the maturation of neural connections and the refinement of functional circuit assemblies. It all begins during embryogenesis, when a relatively limited number of neural stem cells (NSCs) generates the vast numbers and diversity of cortical neurons, a process called neurogenesis, followed by the generation of a rich diversity of glial cells [47].

Neuroepithelial cells (NECs) serve as the earliest cortical progenitors during embryonic development. They form a monolayered neuroepithelium and exhibit a highly polarized morphology, extending two thin processes away from the soma. The radial processes

connect both the apical neuroepithelial surface (apical process) and the basal lamina (basal process) [47]. In the early stages, NECs undergo symmetric divisions to expand their population before shifting to asymmetric divisions, giving rise to radial glial cells (RGCs), which reside in the ventricular zone (VZ) and act as key neural progenitors [48]. Similarly to NECs, RGCs maintain bipolar morphology with apical and basal processes. RGCs form apical adherent junctions and become apical Radial Glial Cells (aRGCs). The transition of NECs to apical RGCs binds their neural fate. aRGCs are the primary type of cortical progenitor cell, divide at the apical surface, express the PAX6 and their lineage gives rise to all cortical excitatory neurons. aRGCs anchor to the apical domain and this defines the primary germinal layer of cortical primordium, the Ventricular Zone (VZ). The VZ contains the cell body of aRGCs and Short Neural Precursors (SNPs), a second and less frequent type of apical progenitor cell with either no basal process or a short one restricted to the VZ [47].

Throughout embryonic cortical development, RGCs undergo extensive divisions within the VZ to sustain self-renew and later to produce neurons. Neuronal generation can occur directly via apical radial glial cells (aRGCs) or indirectly through transient amplifying progenitors. These second progenitors migrate from the apical surface toward the basal border of the VZ, where they divide, hence they are called Basal Progenitors (BP) or Intermediate Progenitors (IPs). BPs typically establish a secondary germinal zone, the Subventricular Zone (SVZ), which consists of an inner (iSVZ) and outer (oSVZ) subventricular zones, containing basal radial glial cells (bRGCs) or outer radial glial cells (oRGCs) [47,49].

As corticogenesis proceeds, immature neurons emerge from the lower layers of the developing cortex by using the radial glial processes from RGCs as scaffolds that extend to the basal surface. Thus, attaching through cell adhesion mechanisms migrate radially to the intermediate zone (IZ) and finally to the developing cortical plate (CP). There they will mature and establish synaptic connections to start developing cortical circuits (Fig. 11) [50].

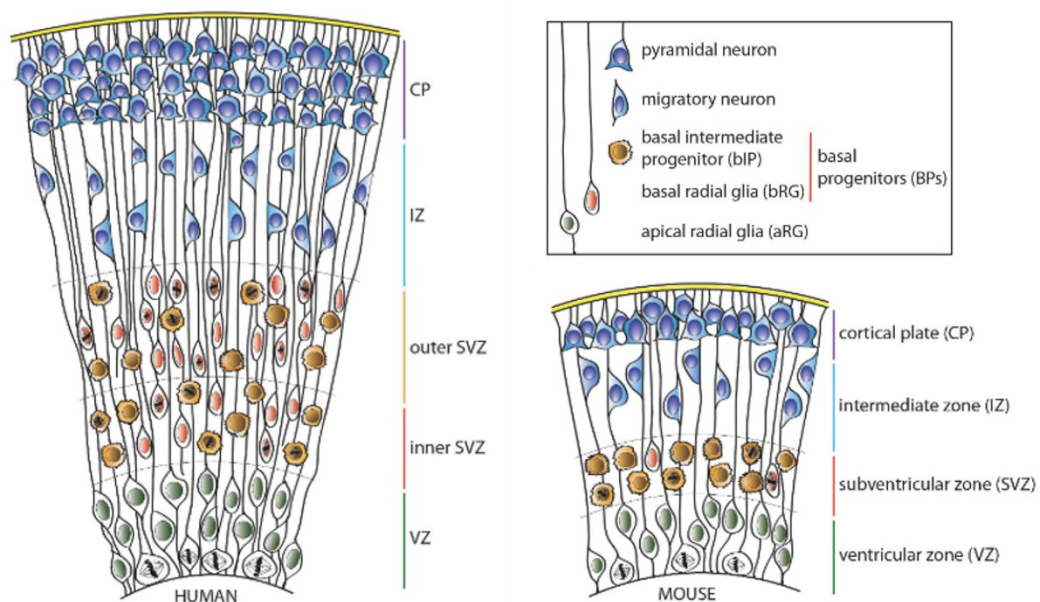


Figure 11 | Schematic representation of the cytoarchitecture of the developing neocortex in mouse and human [51].

In the mature neocortex the foresaid layers contain two major populations of neurons, the cortical projection neurons, which are generated locally and interneurons, which migrate into the neocortex from the ganglionic eminences [51].

4.1. Neurons of neocortex

The neocortex is a key brain region responsible for high-order cognitive functions such as learning, memory, and sensory processing. The cerebral cortex is composed of two primary neuronal populations: excitatory pyramidal neurons and inhibitory interneurons. Cortical function relies on a delicate excitatory/inhibitory (E/I) balance to regulate neural circuitry. Pyramidal neurons, which constitute the majority of excitatory cells, release glutamate to stimulate intracortical and subcortical targets. In contrast, GABAergic interneurons release γ -aminobutyric acid (GABA), exerting inhibitory control either locally within the same cortical column or via long-range projections to distant brain regions [52].

4.1.1. Excitatory cortical neurons

Excitatory projection neurons represent the major output neurons of the neocortex. They are generated from neural progenitors in the dorsal telencephalon and originate from the ventricular zone of the dorsal telencephalon and migrate radially to the cortical plate [53]. Pyramidal neurons are characterized by their distinct apical and basal dendritic trees and the pyramidal shape of their soma [54]. These neurons are usually classified into various subtypes according to their location within different cortical layers and regions, to their axonal projections to distinct intracortical, subcortical, and subcerebral targets, to dendritic morphologies and to the distinct expression of different neuron type-specific genes [55,56].

Their firing activity is locally regulated by GABAergic inhibitory interneurons. Although projection neurons and interneurons originate from different germinal zones, they ultimately integrate and coexist in the cortex, forming local microcircuitry. This process relies on the coordinated migration and development of these two broad neuronal populations [55].

4.1.1.1. Origin of excitatory neurons

The development of cortical excitatory neurons from their progenitors is well documented. Excitatory neurons are generated by progenitors located dorsally in the developing cortex and migrate radially to occupy their terminal positions in the cortical plate [57]. They are derived from neural progenitor cells in the cortical VZ, they divide symmetrically to amplify self-renewing stem cells and then in the neurogenic period asymmetrically to give one RG cell and one neuron or IP. Both neurons and IPs migrate toward the sub-VZ (SVZ), retracting their apical and basal processes. As multipolar neurons, they initiate axon formation and start radial migration along RG fibers extending a leading process in front and a long trailing process, a nascent axon, at the rear. They initially migrate in locomotion mode, *videlicet* repeated saltatory movements, but finally change to terminal translocation mode, a move quickly along the shortening leading process, by anchoring the leading process to the marginal zone (MZ). Underneath the MZ, postmigratory neurons are densely packed, forming the primitive cortical zone (PCZ). The mode change allows newly arrived neurons to integrate into the PCZ (Fig. 12). Neuron–RG cell adhesion disappears during the terminal phase of migration [44].

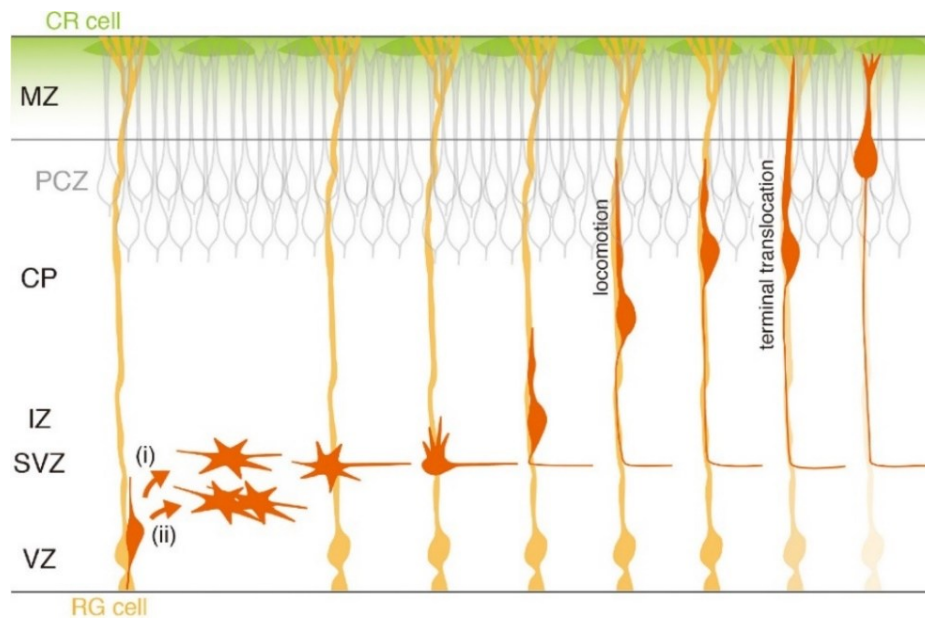


Figure 12 | Neurogenesis, migration, and migration termination of excitatory cortical neurons (i) Direct neuron production from RG cells (ii) indirect neuron production from RG cells via intermediate neuronal progenitors [44].

4.1.2. Inhibitory cortical neurons

The ventral telencephalon is a developmental site for γ -aminobutyric acid inhibitory neurons, which constitute 20-30% of all cortical neurons [59]. The GABA-ergic interneurons of the cerebral cortex are a diverse population of cells. Their variety appears in their different morphological, molecular-neurochemical and electrophysiological features [58]. Examples of the morphological features are the shape, the size, the orientation of the soma, the structure of the dendrites and the axons and the form of the connections. The molecular features include the transcription factors, neurotransmitters, neuropeptides, calcium binding proteins, cell-surface markers, ionotropic or metabotropic receptors, connexins and others. Lastly, the action potential, the firing patterns, the response to hyperpolarization, postsynaptic response etc. belong to physiological features (Fig.13) [50]. This diversity of subtypes of interneurons accentuates the highly specialized role the interneurons play in cortical circuits [52].

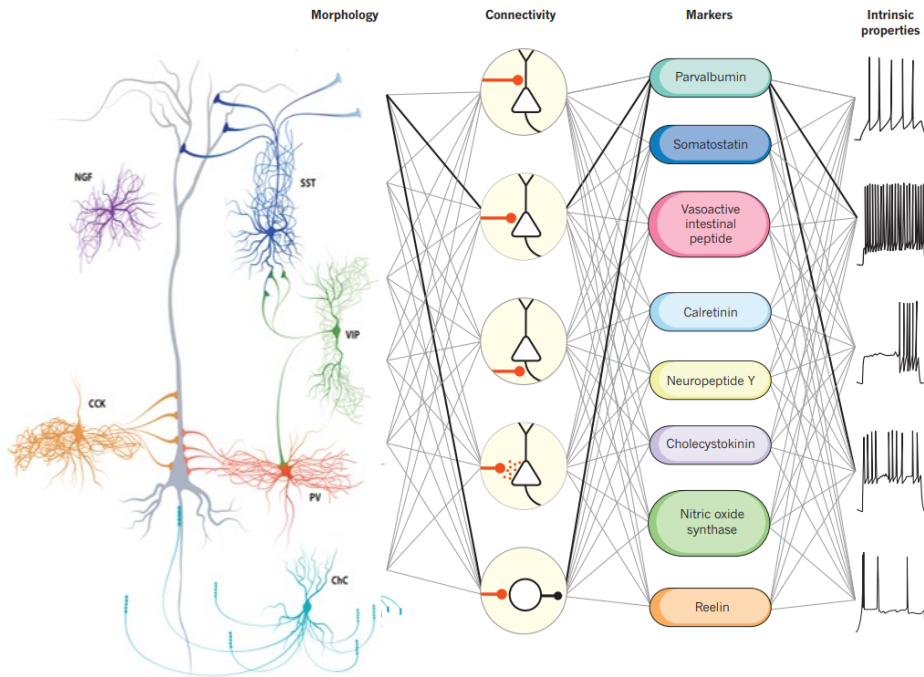


Figure 13 | The diversity of interneurons [59,60].

4.1.2.1. Origin of interneurons

Most cortical interneurons originate outside the cortex, specifically within the ganglionic eminences (GEs) of the ventral telencephalon. These transient subpallial progenitor zones include the medial, lateral, and caudal ganglionic eminences. In mammals, interneurons destined for the cerebral cortex and hippocampus arise from three primary regions within the basal telencephalon: the MGE, CGE, and the preoptic area (POA) [61]. Interneuron progenitors of the telencephalon undergo incredibly complex patterns of dispersion [59]. Cortical interneurons travel long and complex tangential migratory routes to their final settling positions throughout the forebrain to the cerebral cortex, and finally integrate into local neural networks (Fig. 14) [53,62].

Similar to the dorsal telencephalon, each of the GEs contains three primary regions: VZ, SVZ, and MZ. VZ is the most apical portion of the GE that lines the ventricle and contains neural progenitors called Apical Progenitors (APs). APs have bipolar morphology with basal and apical processes, as it is described above, and divide at the VZ surface both symmetrically to expand the AP population, as well as asymmetrically, to produce another AP and a neurogenic BP. The SVZ is located between the VZ and MZ, and contains BPs, which can further divide symmetrically to produce two neuronal precursor cells. The MZ largely contains migratory postmitotic cells that are thought to be committed to particular cell fates (e.g. to PV- or SST-expressing interneurons) [43].

The medial ganglionic eminence (MGE) serves as the primary source of cortical interneurons, generating approximately 60% of the total interneuron population. These interneurons are broadly categorized into two major classes. The first group consists of parvalbumin (PV)-expressing interneurons, which display fast-spiking activity and include basket cells, chandelier cells, and translaminal interneurons. The second group comprises somatostatin (SST)-expressing interneurons, which predominantly form dendritic-targeting synapses. SST-positive interneurons can be further classified into Martinotti cells, non-Martinotti cells, and

long-range GABAergic projection neurons [61]. The CGE produces relatively rarer subtypes, including neurogliaform, bipolar, vasointestinal peptide (VIP)-expressing multipolar interneurons and Reelin-expressing cortical interneurons. The LGE gives rise to olfactory bulb interneurons and the medium spiny projection neurons of the striatum [62].

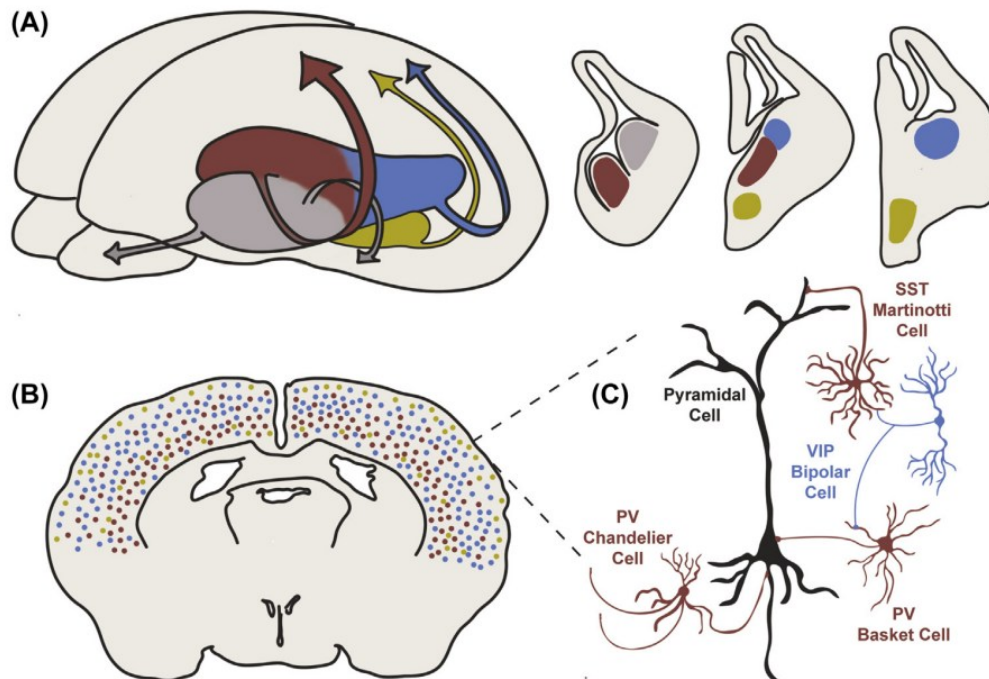


Figure 14 | **A.** Trajectories cortical interneurons follow during embryonic development. The medial ganglionic eminence (MGE-red), the caudal ganglionic eminence (CGE-blue), the lateral ganglionic eminence (LGE-grey) and the preoptic region-POA (yellow). **B.** In the adult cortex, their distribution varies, with MGE-derived interneurons predominantly in deeper layers and CGE-derived interneurons more common in superficial layers. These interneurons exhibit diverse structural forms and establish connections with specific compartments of excitatory pyramidal neurons and other interneuron subclasses, highlighting their functional specialization [63].

Throughout embryonic and postnatal stages, GABA signaling is required for cell migration, axonal and dendritic remodeling and synapse formation, thus, interneurons are key modulators of cortical development and plasticity, in addition they play a crucial role in shaping the spatiotemporal pattern of neuronal activity [52].

It is not surprising that disruption in interneuron activity has been associated with various neurological diseases. Realizing the critical role of interneurons in shaping brain development and in the etiology of multiple neurological disorders have been developed methods to generate interneuron-enriched neural culture from hPSCs [52].

4.2. Genes expressed in cortical neurons used as markers to identify regions and developmental timepoints

The telencephalon is characterized by distinct molecular markers that define the dorsal and ventral regions, reflecting their developmental roles. In the dorsal telencephalon, markers such as PAX6 and EMX1 are prominently expressed. PAX6, a homeobox transcription factor, plays a crucial role in neural progenitor proliferation and cortical neurogenesis, while EMX1

delineates dorsal progenitors [45]. Additionally, TBR1, T-domain transcription factor, and downregulation of PAX6, serves as a marker for excitatory neurons [64].

In contrast, the ventral telencephalon expresses markers like NKX2.1, a critical regulator of MGE development and interneuron specification [36,45]. Loss of *NKX2.1* has been shown to redirect MGE-derived interneurons toward CGE and LGE fates [62]. Other ventral markers include DLX2, a homeobox transcription factors, widely expressed throughout subpallium, is broadly required for GE progenitors to migrate and differentiate into GABAergic interneurons and *GSH2* (also known as *Gsx2*), another homeobox transcription factor gene, which is essential for ventral progenitor identity [45,56]. Furthermore, *LHX6*, LIM/homeodomain gene, is expressed in a subregion of the MGE and is key to the differentiation of ventral-derived interneurons, including somatostatin- and parvalbumin-expressing subtypes [61,65]. Broadly spanning the embryonic telencephalon, *FOXG1*, a Forkhead Box G1 transcription factor gene, also plays an essential role in delineating regional identity and ensuring proper forebrain development [45]. Expression of *GAD1*, glutamic acid decarboxylase, indicates GABA (γ -aminobutyric acid)-ergic identity [66]. Together, these markers underscore the molecular and functional distinctions that shape the development of dorsal and ventral telencephalic regions (Fig. 15).

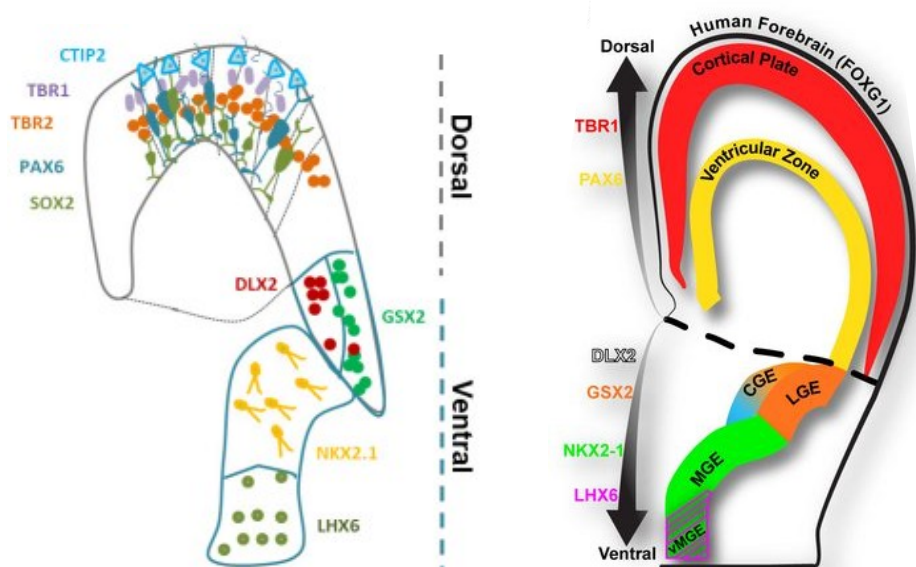


Figure 15 | Schematic overview of the two forebrain regions of the mammalian cortex presenting the characteristic markers/populations for dorsal and ventral regions [36,65]

4.3. Dysfunctional neurons and neurodevelopmental disorders

Impaired neurogenesis and disruptions in fundamental neural mechanisms are strongly associated with the development of neurodevelopmental and neurological disorders. Dysfunction or reduced interneuron populations have been implicated in various conditions, including epilepsy, autism spectrum disorder (ASD), Alzheimer’s disease, and schizophrenia [55]. Deficits in the GABAergic system, which is critical for maintaining excitatory/inhibitory balance in the brain, are frequently observed in neurodevelopmental disorders. Dysregulation of GABAergic cortical interneurons has been implicated in the pathophysiology

of schizophrenia, epilepsy, and ASD, suggesting a shared vulnerability across these disorders. These findings underscore the central role of interneuron function in cortical development and highlight the potential of targeting GABAergic pathways for therapeutic interventions [52].

5. Autism spectrum disorders (ASD)

Autism spectrum disorder (ASD) is one of the most well-recognized and frequently occurring neurodevelopmental conditions. It is described as a complex and pervasive neurodevelopmental disorder, characterized by core symptoms including difficulties in social cognition and communication (such as impaired language development), repetitive behaviors and hypersensitivities to external stimuli [67,68]. ASD is the most prevalent neurodevelopmental disorder in children, which has been steadily increasing in the past two decades [69]. In 2000, the Center for Disease Control's Autism and Developmental Disabilities Monitoring (ADDM) Network estimated the prevalence of ASD at 1 in 150 children. By 2016, the National Health Center for Health Statistics reported a significant increase, indicating that ASD was diagnosed in as many as 1 in 36 children [70]. ASD encompasses a range of heterogeneous clinical syndromes, defined by these hallmark features. According to the Centers for Disease Control and Prevention, ASD currently affects approximately 1 in 44 children, with boys being 4.2 times more likely to be diagnosed than girls [71]. Diagnosis of ASD is challenging not only because the symptoms are variable, but also because children present with varying degrees of symptom severity [72]. Furthermore, over 70% of individuals with ASD experience comorbid conditions including attention-deficit hyperactivity disorder (ADHD), epilepsy, anxiety, depression, bipolar disorder, Tourette syndrome and tic disorders, gastrointestinal problems, and intellectual disability, sleep disturbance, gastrointestinal and immune problems [72,73].

The significant heterogeneity in the clinical and genetic aspects of ASD poses a major challenge to understanding its genetic and pathological mechanisms [73]. Emerging evidence suggests that ASD manifestations may stem from disruptions occurring during the second trimester of fetal development—a critical period for the specification of inhibitory cortical interneurons. This makes studying GABAergic interneuron development particularly relevant to ASD [74]. Furthermore, an imbalance between excitatory and inhibitory signaling, often attributed to interneuron dysfunction, has long been regarded as a key underlying factor in ASD pathophysiology. Human post-mortem studies strongly support the involvement of both GABAergic and glutamatergic dysfunction in the etiology of ASD [67].

5.1. Introduction to ASD Etiology

The exact etiology of ASD remains elusive despite extensive research efforts. Both genetic and environmental factors are believed to contribute to the development of ASD [71,75]. Experiments in animal models have confirmed the below. For example, experimental ASD mouse models have been divided into environmental and genetic models. Environmental models were developed based on studies that link prenatal environmental exposure to future ASD [72]. Additionally, novel technologies and large population-based studies have provided new insight into the risk architecture of ASD and the possible role of environmental factors in etiology. Twin studies provide a unique platform to study the relative contribution of genetic and (shared and non-shared) environmental factors to the variability of a certain

trait or disorder. According to recent evidence, up to 40–50% of variance in ASD liability might be determined by environmental factors [76]. On the other hand, genetic models were also developed by first identifying ‘ASD risk genes’ in humans from single-gene syndromes with ASD phenotypes [72]. From mouse and other animal model studies, it is found that ASD is highly heritable, with hundreds of genes linked to an increased risk. The most studied ASD-related single gene mutations are *Shank3*, *Mecp2*, *Fmr1*, *Nlgn*, *Cntnap2*, *Tsc*, *Ube3A* and *Pten*. The role of these genes can be grouped into several categories, including synaptic stability (*Shank3*, *Nlgn3*, *Cntnap2*), neural circuitry balance (*Fmr1*), and cell homeostasis (*Mecp2*, *Tsc1*, *Ube3A*, *Pten*); regardless, all play a role in the development and regulation of synaptic function [71,72]. Abnormalities in synaptic proteins involved in cell adhesion, scaffolding, or signaling such as neuroligins (NLGN) and neuroligins (NLGN), are considered key contributors to ASD. Variants in genes encoding these proteins have been associated with the disorder [73].

Currently, ASDs are classified according to their etiology into syndromic ASDs (S-ASDs), which are associated with described clinical syndromes and are caused by the known genetic abnormalities (genetic diseases), non-syndromic ASDs (NS-ASDs), which are not associated with these syndromes, but have identified genetic causes, and idiopathic ASDs (I-ASDs), for which no genetic or other causes have been established [77].

Findings from genetics, neuropathology, and therapeutic studies highlight several common molecular and cellular pathways implicated in ASD. These include dysregulation of the PI3K/mTOR signaling pathway, alterations in oxytocinergic signaling, and defective synaptic functioning [73]. The PI3K/mTOR pathway regulates synaptic protein synthesis and is closely associated with the activation of neuron surface receptors, such as N-methyl-D-aspartic acid (NMDA) receptors, metabotropic glutamate (mGluR) receptors, and AMPA-type glutamate receptors. Dysregulation of this pathway has been linked to ASD, with evidence that mTOR inhibitors, such as rapamycin and everolimus, can ameliorate behavioral deficits in certain animal models [73]. Mutations in genes associated with tuberous sclerosis (*TSC1*, *TSC2*) or the *PTEN* tumor suppressor gene, which are involved in the PI3K/mTOR pathway, also contribute to ASD. Although these mutations result in broader symptoms, including benign malformations and tumors, autistic traits are a prominent feature [68].

5.2. ASD and Cortical Organization

Clinical, neuropathological and neuroimaging studies suggest that ASD involves abnormalities in neuronal-cortical organization, ranging from defects in neuronal migration to synaptic dysfunction [74,78]. The cerebral cortex plays a central role in cognitive and emotional processes, including attention, social behavior, and language [73]. Neurons in each cortical layer form distinct connections within the cortex and with subcortical structures, such as the basal ganglia and amygdala, which are also implicated in ASD. Disruptions in these processes, such as synaptic connectivity or cortical-cortical and cortical-subcortical circuits, may result in the behavioral deficits observed in ASD. Identifying the specific circuits involved and targeting molecular mechanisms could inform the development of pharmacological treatments [79].

5.3. *CNTNAP2* and Brain Connectivity in ASD

The clinically and genetically heterogeneous nature of ASD has made it challenging to identify causative genes. No single gene has been found to be solely responsible for the disorder. Instead, numerous genes with either common variants of small effect or rare variants with larger effects have been implicated. This heterogeneity underscores the need to understand the biological pathways influenced by these genes, as this could provide a unifying framework for understanding ASD pathophysiology and guiding targeted treatment strategies [79].

The *CNTNAP2* (*Contactin-associated protein-like 2*, also known as *CASPR2*) gene has emerged as a significant risk factor for ASD and related neurodevelopmental disorders [80]. Structural magnetic resonance imaging (MRI) studies, though limited by small sample sizes and control matching difficulties, provide evidence of brain structural and functional alterations associated with psychiatric disorders, including ASD. Brain connectivity has been proposed as a unifying abnormality in ASD, with disruptions in processes such as neuronal migration, dendritic maturation, axon pathfinding, and synapse formation leading to disconnection of brain areas critical for higher-order cognitive functions. Disconnection linked to the *CNTNAP2* genotype is considered a risk factor for ASD, although it may not be sufficient on its own to cause the disorder [79].

In summary, ASD arises from a complex interplay between genetic factors and brain development, with multiple molecular pathways contributing to its etiology. This complexity highlights the need for further research to uncover potential therapeutic targets and develop strategies to mitigate the effects of this disorder.

6. *Contactin associated protein like 2 - CNTNAP2*

Contactin associated protein like 2 (CNTNAP2), is one of the largest genes in the human genome, spanning approximately 2.3 Mb, located on chromosome 7q35-36.1 (Fig. 16) [81]. It was first identified in rodents in 1999 as a member of the neurexin superfamily and specifically as the mammalian homolog of the fruit fly (*Drosophila melanogaster*) neurexin IV, which plays a role in neuron–glia interactions in myelinated axons [79]. *CNTNAP2* encodes 1331 amino acid protein, also known as *CASPR2*, which functions as a presynaptic type 1 transmembrane protein. Its large extracellular domain and smaller intracellular segment facilitate cell–cell adhesion and synaptic interactions [82].

CNTNAP2 is widely expressed throughout both the developing and adult central nervous system (CNS) [83], with high expression levels in the frontal and temporal lobes, striatum, dorsal thalamus, and specific cortical layers [82]. As part of the neurexin family, *CNTNAP2* participates in synapse formation and function by interacting with its postsynaptic partners, neuroligins, although not all neurexins share the same role [79].

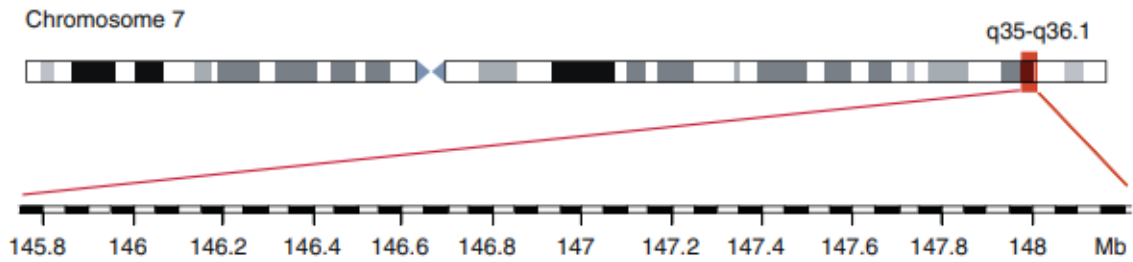


Figure 16 | Schematic representation of the *CNTNAP2* gene spanning 2.3 Mb on chromosome 7 [79].

Beyond synapse formation, *CNTNAP2* regulates multiple neurodevelopmental processes, including synaptic spines growth, synaptic communication, neural circuits formation, and neuronal network activity [82,84]. Studies in *CNTNAP2* KO mice and human cell lines suggest that *CNTNAP2* is involved in neuronal migration, myelination, and neurotransmission, with a notable reduction in both GABAergic inhibitory interneurons and excitatory neurotransmission [85,86].

In myelinated axons, *CNTNAP2* localizes to the juxtaparanodal regions, where it forms part of a protein complex that secures the glial myelin sheath to the axon and helps to segregate Na^+ and K^+ channels, facilitating efficient nerve impulse propagation [87]. The ectodomain of *CNTNAP2* binds contactin-2 (*CNTN2*) at axo-glial contact points, forming a molecular bridge, while its cytoplasmic tail helps recruit K^+ channels [87,88]. Additionally, *CNTNAP2* has an emerging role at synapses, particularly at inhibitory synapses, where it localizes to the presynaptic membrane, interacting with *CNTN2* at the postsynaptic membrane to form a trans-synaptic bridge spanning the synaptic cleft (Fig. 17) [89].

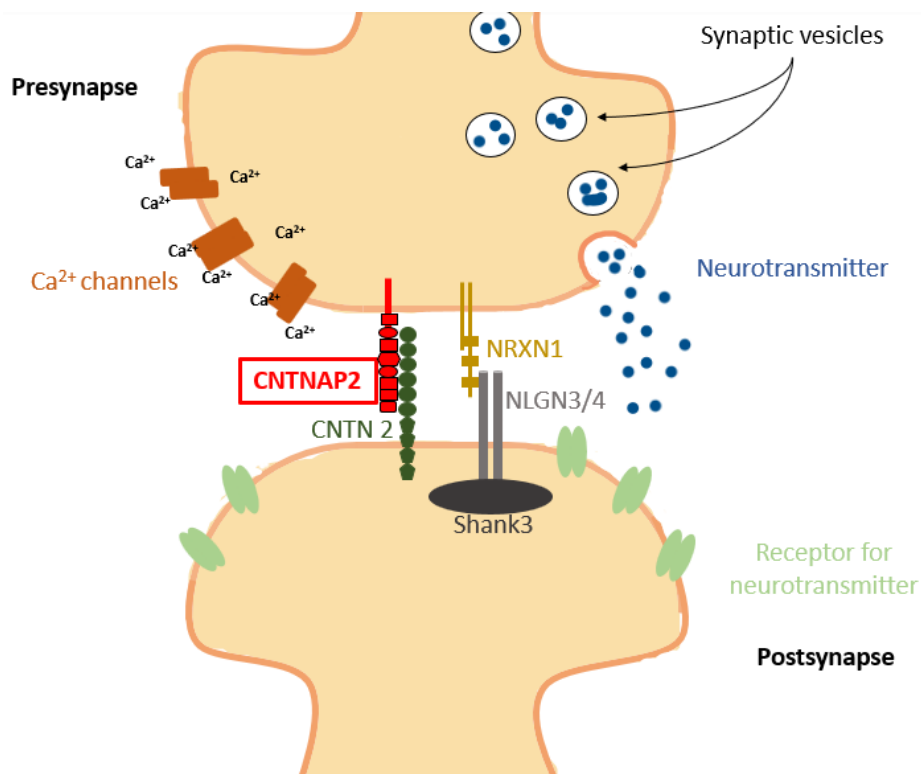


Figure 17 | Schematic representation of *CNTNAP2* localization at synapses

The human genome contains five *CNTNAP* genes (*CNTNAP1–CNTNAP5*), with *CNTNAP1* being crucial for axon–glial junction formation through its interaction with *CNTN2*. However, the other *CNTNAP* proteins do not interact with *CNTN* and instead exhibit diverse functions at neuron–glia interfaces. *CNTNAP2* is specifically involved in clustering K^+ channels at the juxtaparanodal region of the nodes of Ranvier, a critical process for axon conduction [79].

6.1. The role of *CNTNAP2* in neurodevelopmental disorders

Extensive research has linked *CNTNAP2* mutations to a range of neurodevelopmental and neurological disorders. Pathogenic mutations in *CNTNAP2* are associated with a spectrum of clinical phenotypes including autism spectrum disorder (ASD), intellectual disability (ID), epilepsy, language disorders, behavior disorders, schizophrenia spectrum and other psychotic disorders, obsessive–compulsive disorder (OCD), Gilles de la Tourette syndrome and attention deficit hyperactivity disorder (ADHD) [90–92].

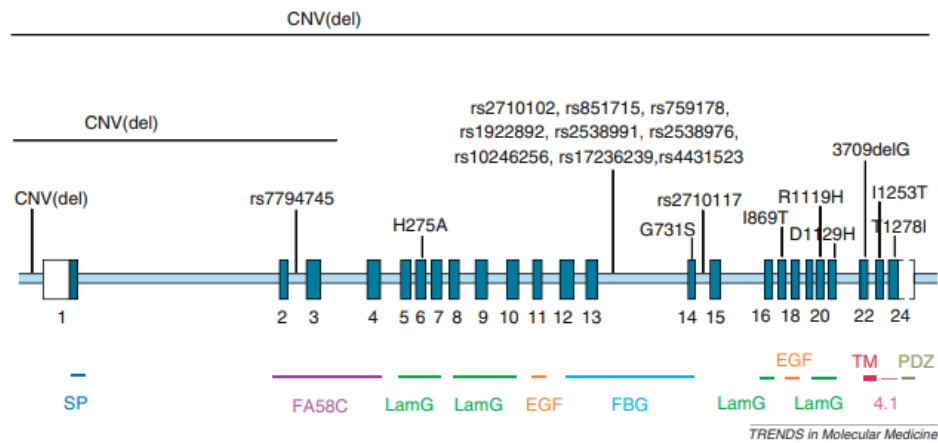


Figure 18 | Schematic representation of the location of *CNTNAP2* mutations associated with neurodevelopmental disorders. Exons are depicted as numbered dark blue boxes, introns as a light blue line. Variants are indicated above and protein structural domains encoded by the specific exons are presented below. SP, signal peptide; FA58C, coagulation factor 5/8 C terminal domain; LamG, laminin G; EGF, epidermal growth factor; FBG, fibrinogen-like domain; TM, transmembrane domain; 4.1, protein 4.1B binding domain; PDZ, PSD95/DlgA/ZO-1 homology protein–protein interaction domain [79].

RNA interference (RNAi)-mediated knockdown of *CNTNAP2* in neuronal cultures has been shown to impair dendritic arborization and spine development, leading to decreased neural network activity. Loss-of-function (LoF) in *CNTNAP2* is also associated with reduced rapid and saltatory conduction in hippocampal myelinated axons, likely due to decreased voltage-gated potassium channel activity [81].

Studies using *Cntnap2*^{-/-} mice further reveal neuronal migration defects, including mislocated cortical neurons and a decreased number of GABAergic interneurons in the cortex, hippocampus, and striatum [93–95]. Loss of *CNTNAP2* function further leads to abnormal cortical layer patterning and impaired synaptic transmission, resulting in an imbalance between excitatory and inhibitory (E/I) synapses. Additionally, reduced *CNTNAP2* expression in the prefrontal cortex has been linked to fewer functional excitatory-inhibitory

synapses and altered neuronal connectivity. However, the precise cellular mechanisms underlying these deficits remain unclear [73,91].

6.2. *CNTNAP2* and ASD

To elucidate the role of *CNTNAP2* in ASD, researchers developed *Cntnap2* KO homozygous KO (*Cntnap2*^{-/-}) mouse models, which exhibit key ASD-like behaviors, including deficits in social interaction, repetitive behaviors, and impaired communication [96]. These mice also exhibit neuronal migration abnormalities, reduced numbers of GABAergic interneurons, and hyperactivity, supporting the hypothesis that E/I imbalance contributes to ASD pathophysiology [83].

The embryonic expression of *CNTNAP2* and its role in postnatal myelination, combined with increasing evidence linking *CNTNAP2* mutations to ASD, suggests its involvement in early brain development. In humans, *CNTNAP2* is predominantly expressed in the brain and spinal cord. In situ hybridization studies of the human fetal brain show that *CNTNAP2* is highly expressed in a cortico-striato-thalamic circuit, which regulates higher-order cognitive functions. Within the cortex, *CNTNAP2* expression is enriched in the frontal and prefrontal regions during development, a pattern that persists into adulthood [79]. The critical role of *CNTNAP2* in regulating key processes during brain development makes it a major candidate in ASD pathogenesis. Since atypical brain function arises long before neurons and their connections fully mature—preceding experience-dependent circuit modifications during critical plasticity periods—*CNTNAP2* dysfunction may contribute to early neurodevelopmental abnormalities associated with ASD [74].

Knocking out the *CNTNAP2* gene in mice results in a range of phenotypic alterations, including deficits in social behavior, communication, learning, and memory. Complete KO leads to epileptic seizures, a reduction in interneuron numbers, impaired neuronal migration, and abnormal neural network activity [79]. Additionally, a study using rats a models has demonstrated the crucial role of the autism-risk gene *CNTNAP2* in behaviors associated with ASD, including substantial alteration in social behaviors, an increased repetitive actions, and disruptions in sensory processing [97]. In cultured iPSCs, *CNTNAP2* LoF has been shown to reduce neurite branching and simplified complex neuronal networks, further highlighting its importance in neurodevelopment [98].

7. PI3K-AKT/mTOR Signaling Pathway

The phosphoinositide 3-kinase (PI3K)-protein kinase B (AKT)/mammalian-mechanistic target of rapamycin (mTOR) pathway is a highly conserved signaling cascade that plays a central role in regulating cell proliferation, survival and metabolism [99,100]. It functions as a complex, non-linear phosphorylation network interacting with multiple pathways through crosstalk and feedback loops [101]. Due to its regulatory significance, dysfunction of this pathway has been implicated in various human diseases, including cancers, neurodegenerative and neurodevelopmental disorders, diabetes, cardiovascular diseases and others making it a focal point of extensive research [100].

7.1. Main regulators of the pathway

7.1.1. PI3K: Structure and Function

PI3K is a member of lipid kinase family classified into three main classes (I, II, and III) based on structural and functional differences and respective phosphoinositide substrates. The most studied class, Class I PI3K, consists of a regulatory subunit (p84, p85, or p101) and a catalytic subunit (p110 α , p110 β , p110 γ , or p110 δ). PI3K activation occurs through G protein-coupled receptors (GPCRs) and receptor tyrosine kinases (RTKs) upon stimulation by ligands such as hormones, cytokines, and growth factors. Activated RTKs interact with regulatory subunits of Class IA PI3Ks, whereas Class IB PI3Ks are activated through GPCR signaling. This cascade leads to the phosphorylation of phosphatidylinositol(4,5)-bisphosphate (PIP₂), generating phosphatidylinositol(3,4,5)-trisphosphate (PIP₃), a crucial second messenger in AKT activation (Fig. 19). Unlike class I PI3Ks expressed as heterodimers, class II PI3Ks are monomers having only a catalytic subunit without a regulatory subunit. Only one class III PI3K exists, named Vps34. Vps34 is the only PI3K found in yeast and is conserved across species from yeast to humans [100].

The pathway is negatively regulated by PTEN (phosphatase and tensin homolog), a lipid phosphatase which dephosphorylates PIP₃ back to PIP₂, thereby inhibiting AKT/mTOR signaling [99]. PTEN plays a critical role in brain development, and it is a key regulator of cell growth and proliferation. In humans, mutations in PTEN have been associated with macrocephaly, epilepsy, intellectual disabilities, ASD, and mental retardation and seizures [99,102]. Studies in PTEN knockout (KO) mice reveal phenotypes resembling human autism, including social deficits, seizures, anxiety-like behaviors, and cognitive impairments [102].

7.1.2. AKT: Key Mediator of Cellular Function

AKT, also known as protein kinase B (PKB), is a serine/threonine kinase that regulates cell survival, metabolism, apoptosis, and neuronal integrity. It exists in three homologous isoforms: AKT1 (PKB α), AKT2 (PKB β), and AKT3 (PKB γ). While AKT1 governs cell survival and growth, AKT2 regulates glucose metabolism, and AKT3 is predominantly expressed in the brain, playing a crucial role in neuro-inflammation and neuronal maintenance [100].

AKT3 is expressed at higher levels than AKT1 and AKT2 in the human fetal brain and the adult mouse brain. As the predominant isoform, AKT3 is present throughout all regions of the adult mouse brain, accounting for approximately half of the total AKT protein in adult brain tissue [103].

AKT comprises three distinct functional domains: a pleckstrin homology (PH) domain in the N-terminus, a central catalytic kinase domain (KD), and a C-terminal regulatory domain (RD). The activation of AKT involves two major phosphorylation events: (1) Thr308 phosphorylation by phosphoinositide-dependent kinase 1 (PDK1), another PH domain-containing kinase and (2) Ser473 phosphorylation by mammalian target of rapamycin complex 2 (mTORC2). These modifications facilitate downstream signaling, promoting neuronal differentiation, migration, and synaptic function. AKT1 and PDK1 are both recruited by PIP₃ and co-localize on the membrane surface (Fig. 19). PDK1 further causes the phosphorylation of KD at Thr308 in AKT1, which is crucial for the activation of AKT1. Then, a secondary phosphorylation of AKT1 at the C-terminal hydro-phobic motif Ser473 is mediated

by mTORC2. AKT2 (Thr309/Ser474) and AKT3 (Thr305/Ser472) are also regulated by the corresponding residues [100].

7.1.3. mTOR: Central Regulator of Cellular Homeostasis

mTOR is a serine/threonine kinase that integrates extracellular signals to regulate cell homeostasis through key molecular processes including autophagy, metabolism, lipid biogenesis, cytoskeleton organization, mRNA translation and synaptic plasticity. mTOR is an essential kinase found in all forms of eukaryotic cells, including neurons. mTOR is highly expressed in brain regions such as the hippocampus, striatum, amygdala, and prefrontal cortex, and forebrain where it contributes to neuronal growth, proliferation, and synapse formation [101,102]. It also exerts a significant impact on axonal regeneration, the expression of ion channels and receptors, dendritic arborization, and the growth of spinal dendrites [102].

mTOR functions in two distinct complexes known as mTOR complex 1 (mTORC1) and complex 2 (mTORC2), two physically and functionally different forms [104]. mTORC1 regulates cell growth and metabolism protein synthesis via downstream targets such as ribosomal protein S6 kinase 1 (S6K1) and eukaryotic translation initiation factor 4E-binding protein 1 (4EBP1) [101,105]. It is positively regulated by nutrients, growth factors, energy, and stress of the cell, in contrast, tuberous sclerosis complex (TSC) 1 (hamartin) and TSC2 (tuberin) are negative regulators of mTORC1 [1]. mTORC2 controls cytoskeletal dynamics and AKT activation (Fig. 19) [101].

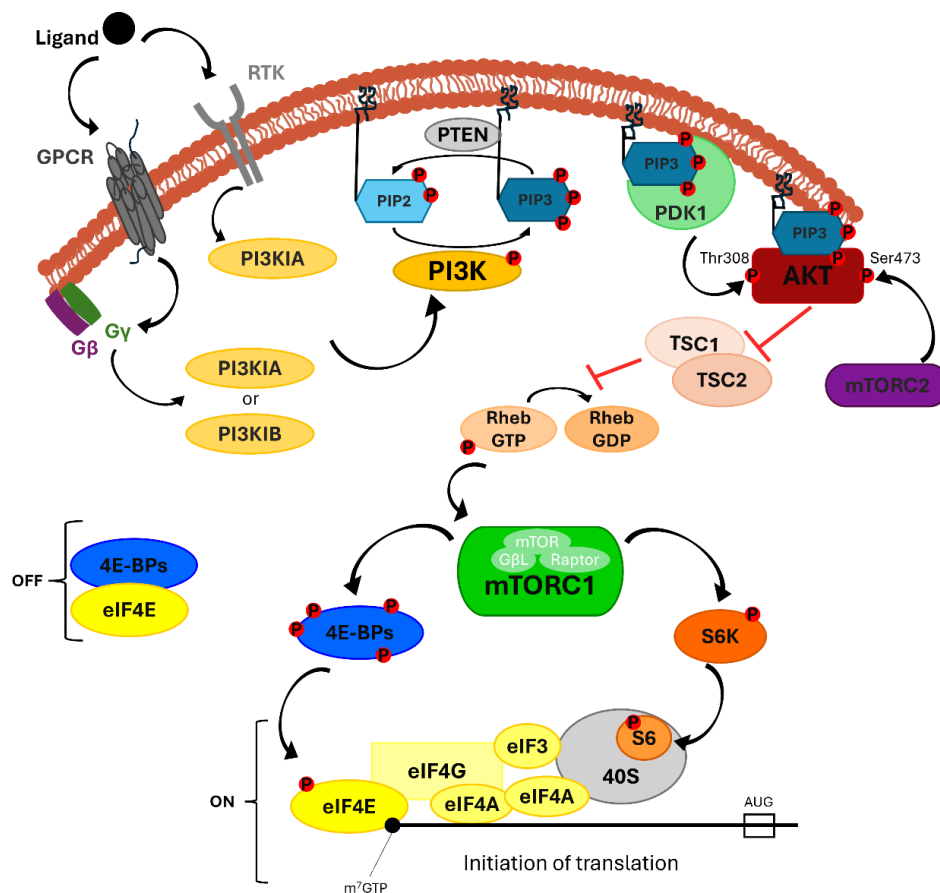


Figure 19 | Molecular mechanisms of PI3K-AKT-mTOR signaling cascade and its role in translational control.

7.2. Roles of the PI3K-AKT/mTOR Signaling Pathway in Neurodevelopmental and Neurodegenerative Disorders

The occurrence and development of various neurodegenerative disorders are strongly associated with the PI3K/AKT/mTOR signaling pathway due to its important functions in cellular proliferation, suppression of oxidative stress, apoptosis, autophagy, and control of different downstream components [100]. Dysregulation of the PI3K-AKT/mTOR signaling pathway is implicated in both neurodevelopmental and neurodegenerative disorders, with distinct clinical phenotypes, including Parkinson's disease (PD) brain trauma, epilepsy, down syndrome, tuberous sclerosis complex (TSC), Fragile X Syndrome (FXS), mental retardation, Rett syndrome, depression, brain injury, schizophrenia, Alzheimer's disease (AD), and a range of brain malformations [102,103].

By regulating protein synthesis, the PI3K/PTEN/AKT/mTOR pathway modulates key processes such as neuronal proliferation, axon and dendrite growth, synapse formation, and cortical development [102]. It is also crucial for establishing and maintaining neuronal polarity. Genetic mutations leading to pathway dysregulation have been implicated in cortical malformations and impaired neuronal connectivity [105].

Research indicates that hyperactivation of mTORC1 contributes to neuronal hypertrophy, altered cortical organization, and impairments in synaptic plasticity. Mouse models with ectopic mTORC1 activation exhibit changes in neuronal morphology, size, and laminar positioning, resembling features of cortical malformations. Additionally, alterations in mTOR signaling have been linked to glial scaffold disruption in primary cortical cultures and brain organoids [106].

Loss-of-function mutations in PTEN, TSC1, and TSC2 result in overactivation of PI3K-AKT/mTOR signaling, leading to axonal dysregulation, megalencephaly, neuronal overgrowth, and increased synaptic excitation. The overexpression of PI3K/AKT in neurons has several harmful consequences, including depolarization of the membrane, mitochondrial, neuronal apoptosis and reduced oxidative phosphorylation and ATP production [102].

Increased activity in the PI3K-AKT/mTOR signaling pathway in neurons has been associated with autistic behaviors, deficits in memory and learning, disruption in serotonin signaling, epilepsy, and synaptic abnormalities. Studies have identified mutations in the AKT/mTOR pathway (PTEN, TSC1, TSC2, and PI3K-related genes) as significant risk factors for ASD [102].

Studies have established associations between various brain disorders and specific genetic and molecular pathways, as well as corresponding structural brain changes and patient phenotypes all related with PI3K-AKT/mTOR signaling. In ASD, mutations in NLGN3, NLGN4, TSC1, and TSC2, along with dysregulation of the PI3K-mTORC1 and ERK pathways, have been linked to macrocephaly, reduced postcentral gyrus volume, and aberrant Purkinje cell morphology in the cerebellum. These alterations contribute to core ASD phenotypes, including persistent social interaction deficits and restricted repetitive behaviors. Moreover, epilepsy is associated with dysregulation of the eEF2K/eEF2 and mTOR/MAPK pathways, leading to increased neuronal proliferation and manifesting as seizures, abnormal sensory experiences, and episodes of impaired awareness. Similarly, schizophrenia has been linked to dysfunction in the AKT-mTOR pathway, resulting in decreased neuronal proliferation and reduced gray matter volume, which underlie clinical symptoms such as psychosis, hallucinations, delusions, and severely disordered thinking and behavior [104].

Conventional and conditional ablation of key components of the PI3K-Akt-mTOR pathway in mouse, such as Pten, Pdk1, Tsc1/2, mTOR, and Raptor contributes to mechanistic research and development of therapies for these devastating disorders [103].

7.3. PI3K/AKT/mTOR and ASD

Accumulating evidence implicates the PI3K/AKT/mTOR pathway in ASD pathogenesis. Whole-genome studies, copy number variation screening and SNP analyses, have led to identified AKT/mTOR-related genes (PTEN, TSC1, TSC2, and FMR1) as ASD risk factors [107].

Akt-mTOR signaling participates in the pathogenesis of ASD. Dysfunctional mTOR signaling has been observed in ASD mouse models (*Tsc1*^{+/-}, *Tsc2*^{+/-}, *Pten*^{-/-} and *Fmr1*^{-/-}). Additionally, pharmacological inhibition of mTOR was shown to increase the PI3K/Akt/mTOR-mediated autophagic pathway and to improve social interactions in ASD-like animal models. The inhibitor of mTOR signaling, rapamycin, has been demonstrated to be an effective therapeutic for impaired social interaction in *Tsc1*^{+/-}, *Tsc2*^{+/-}, *Pten*^{-/-} mice and pharmacological induced ASD animal model [108]. Notably, *Pten* KO mice exhibit behavioral abnormalities reminiscent of human autism, including learning deficits, seizures, and social impairments [107]. *Fmr1* KO mice, a model of FXS, exhibit the development of autism spectrum disorder (ASD)-associated symptoms upon stimulation of the PI3K/Akt/mTOR signaling cascade. This is likely due to upregulated protein translation at the synapses and an elevated excitatory/inhibitory (E/I) ratio in critical neuronal pathways [109]. Mice deficient in synaptic genes implicated in ASD, including *Cntnap2*, *Neuroligins* and *Shanks*, demonstrate core autism-related deficits. Research has shown that *Cntnap2*^{-/-} mice display hyperactive Akt-mTOR signaling in the hippocampus [108].

Alterations in GABAergic and glutamatergic circuits were observed in ASD patients [110]. Autophagy has been identified as a key factor linking mTOR hyperactivity, the dysregulation of the neuronal excitation/inhibition balance, and ASD-like behaviors, while it is proven that the levels of glutamate and GABA vary in autistic children [107].

Motivation, Hypothesis and Aims

1. Motivation

Evidence from diverse model systems highlights *CNTNAP2* as a critical regulator of cortical interneuron development, which is notably implicated in the pathophysiology of ASD [74,111]. Loss of *CNTNAP2* leads to abnormal neuronal migration and an altered distribution of GABAergic interneurons in both mouse and zebrafish [83,111], while also reducing neurite branching and overall complexity in developing human excitatory neurons [112]. Moreover, *Cntnap2* deletion in mice has been shown to activate the Akt/mTOR pathway, and pharmacological inhibition of this signaling cascade can rescue core autism-like symptoms [113]. Together, these findings underscore the potential link between *CNTNAP2* dysfunction, disrupted interneuron and excitatory neuron development, and aberrant PI3K/AKT/mTOR pathway activity in ASD.

2. Hypothesis

Loss-of-function mutations in *CNTNAP2* disrupt early human forebrain development by altering excitatory and inhibitory neuronal balance across dorsal and ventral regions. This disruption may involve aberrant PI3K/AKT/mTOR signalling. Human iPSC-derived brain organoids offer a powerful model to investigate these region-specific effects and the underlying molecular mechanisms during critical early developmental stages.

3. Aims

- a. To model early human cerebral development using iPSC-derived brain organoid models
- b. To utilize cerebral organoids to examine the effects of *CNTNAP2* ablation on early human brain development
- c. To assess the activity of the PI3K/AKT/mTOR signaling pathway

Materials and Methods

1. iPSCs generation and cell culture

For the current experiments two lines of iPSCs (46, XY cell line, reprogrammed from skin fibroblasts, collected from healthy donors, using defined factors) were used. The two commercially available cell lines were: XCL1 control cell line, and XCL1-*CNTNAP2*^{-/-} cell line. The bi-allelic *CNTNAP2* KO line was generated with the Zinc Finger Nuclease (ZFN) method. In allele 1 and 2 of *CNTNAP2* gene an insertion of 4bp and a deletion of 2bp were introduced in exon 17, respectively (RxCell Science, Canada).

Confirmation of *CNTNAP2* mutations was performed by Sanger sequencing-based genotyping. Pluripotency tests were frequently performed, by measuring the expression of pluripotency markers (*OCT3/4* and *NANOG*) with qPCR and fluorescent ICC. Karyotype analysis was conducted every ~10 passages using the CGH-array method. All the above aim to confirm the pluripotency of both cell lines to move on to cerebral organoid induction.

2. Cerebral and Ventral forebrain organoids induction

2.1. iPSCs thawing and culturing in Matrigel coated plates to D0

For maintenance and culture of iPSCs coating of plates with Corning® Matrigel® Matrix® (Thermo Fisher Scientific, cat #354277) was required to ensure cell adhesion. Matrigel (light-sensitive) and diluted in DMEM-F12-antimycotic/antibiotic. The Matrigel/medium mixture was then added to each well and incubated at room temperature for 1h prior to thawing the cells.

iPSCs vials were thawed from liquid nitrogen. Tubes were centrifuged at 10,000 rpm for 5 min. The supernatant was then removed, and cells were reconstituted in mTeSR™Plus (Stem Cell Technologies, cat #05825) -ROCK inhibitor (ROCKi, Y-27632, 10 μm, Stem Cell Technologies) before plating. Matrigel was removed and cells were washed with DMEM-F12 prior to cell plating. At this point, cells were considered to be at D0.

2.2. Maintenance and passaging of cultured iPSCs

At D1 culture medium was aspirated and replaced with mTeSR™plus without ROCKi. Media changes were performed every 2 days. Plates were incubated at 37°C, 5% CO₂. At 60-70% confluency, cells were considered ready for splitting.

To split and re-seed cells old medium was aspirated, and cells were washed once with DMEM-F12. Non-enzymatic cell dissociation medium (0.05mM EDTA in PBS) was then added to cells, aspirated, and washed twice with DMEM-F12. Cells were then scrapped, centrifuged (800rpm for 5min) and resuspended in mTeSR™plus with ROCKi. Plates were then incubated at 37°C, 5% CO₂. The next day, culture medium was replaced with mTeSR™plus without ROCKi.

2.3. Telencephalic organoids generation

When hiPSCs reached 80-90% confluency, ventral and dorsal neural induction was initiated. The neural induction and organoid formation protocol was based on the protocol by Gomes et al.

Before induction, hiPSCs were incubated with ROCKi, then treated with Accutase® solution (Sigma-Aldrich, cat #A6964), which is an enzymatic method for cell detachment of the cells, for 5 min at 37°C. Cells were then scrapped and collected via mild centrifugation (5min at 200-300 x g). The pellet was resuspended in mTeSR™Plus-ROCKi. Cell viability was checked by using Countess 3 Automated Cell Counter, and the amount of the needed cells, floating in the suspension, was calculated, we only used cells if viability was >97%. Cells were seeded at 9,000 cells/well in 96 well U-bottom plates (Corning #7007) with mTeSR™plus supplemented with 10 µM ROCKi. Embryoid bodies (EBs) were formed within 24 hours, considered as day 1 (D1), and full expansion medium was replaced to mTeSR™plus without ROCKi.

For the dorsal forebrain patterned organoids, EBs were kept in the 96-well plate for 6 days. Medium changes were performed on day 2 (D2) and day 4 (D4). On D6, EBs were transferred to ultra-low attachment 24-well plates (Corning, #3473) in neural induction medium, supplemented with 10µM SB431542 (Selleck Chemicals, #S1067) and 100nM LDN-193189 (Selleck Chemicals, #S2618). D10 EBs were embedded on Matrigel GFR® (Corning, #354230) droplets and cultured in cerebral organoid differentiation medium. Embedded EBs were kept on stationary culture for 24hrs, followed by transfer to an orbital shaker (Heathrow Scientific, #5003396).

For the ventral patterned organoids, EBs were kept in the 96-well plate for 5 days. On day 5 (D5) EBs were collected and transferred to ultra-low attachment 24-well plates (Corning, #3473) in neural induction medium supplemented with 10µM SB431542 (Selleck Chemicals, #S1067) and 100 nM LDN-193189 (LDN) (Selleck Chemicals, #S2618). Half medium exchanges were made at days 0, 3 and 5. Media supplemented with 2.5 µM IWP2 (Sigma Aldrich, # I0536), 100 nM SAG (Biogems, #9128694) and 10 µg/ml Heparin (Sigma Aldrich, #H3149) was used for half-medium exchanges on D7 and D13. The ventral organoids were kept on an orbital shaker (Heathrow Scientific, #5003396).

At day 30 the dorsal and ventral organoids were collected for experimentation.

2.4. Fixation and Cryopreservation of organoids

D30, telencephalic brain organoids were preserved for future experiments through two different procedures. 1) D30 organoids were transferred from culture plates. For each biological replicate, 3-5 organoids were pooled in microtubes. They were briefly rinsed in ice-cold DPBS (PAN-Biotech, #P04-36500), flash-frozen in liquid nitrogen, and stored in -80°C until further processing. 2) Alternatively, for immunofluorescence studies organoids were cryopreserved as follows. D30 organoids were fixed in 4% (w/v) paraformaldehyde solution in PBS for 1 hour at room temperature (RT), then cryoprotected in 30% (w/v) sucrose in PBS, overnight (O/N), or until they sank, at 4°C. The organoids were embedded in optimal cutting temperature (O.C.T.) compound (Shakura Finetek USA Inc, #4583) and frozen with a dry ice/ethanol bath and stored at -80°C until further use.

3. Immunofluorescence

Immunofluorescence was performed to stain and detect specific markers/proteins in ventral and dorsal organoid sections from different batches. The protocol which was used included the following. The sections were thawed from -80°C freezer and treated with PBS. The slides were incubated in blocking solution (10% NGS IN 0.3% Triton X-100 PBS), for 1-2 hours at room temperature and then incubated in primary antibody solution overnight in 4°C (Table 1).

Table 1 | List of the primary antibodies used in Immunofluorescence experiments. Host and target species, dilution used, supplier and catalogue number.

<i>Primary antibody</i>	<i>Biological source</i>	<i>Dilution</i>	<i>Supplier</i>	<i>Cat. Number</i>
Anti- Microtubule Associated Protein 2 (MAP2)	Rabbit	1:200	Cell Signaling Technology	#4542
Anti- Microtubule Associated Protein 2 (MAP2)	Mouse	1:50	Sigma-Aldrich	#M4403
Anti-T box, brain 1 (TBR1)	Rabbit	1:250	Cell Signaling Technology	#49661S
Anti – β 3 Tubulin (TUJ1)	Mouse	1:200	Santa Cruz Biotechnology	#sc-80005
Anti -TTF-1/Thyroid Transcription Factor 1/ NK2 Homeobox 1 (NKX2.1)	Mouse	1:200	Santa Cruz Biotechnology	#sc-53136
SRY-related HMG-box transcription factor 2 (SOX2)	Mouse	1:200	Santa Cruz Biotechnology	#sc-365823
Anti-Gutamic acid decarboxylase 67kDa (GAD67)	Mouse	1:2000	Sigma -Aldrich	#MAB5406
Anti – GS Homeobox 2 (GSH2)	Rabbit	1:500	Abcam	#ab229239

Prior to and after incubating with the secondary antibody solution (Table 2), the slides were washed with 1X PBS (3 times; 8 minutes/wash). The slides were incubated with a nuclear marker, DAPI (in 1X PBS at 1:2000) (Abcam, #ab228549). The slides were briefly rinsed with 1X PBS, covered with coverslips, and allowed to dry for at least 24 hrs prior to imaging. Imaging was carried using Nikon A1R HD confocal microscope, using a 20X air objective (whole slices). Five organoids per batch were imaged, for which a minimum of 3 sections per organoid were imaged and analyzed.

Table 2| List of the secondary antibodies used in Immunofluorescence experiments. Host and target species, dilution used, supplier and catalogue number.

<i>Secondary antibody/Conjugate</i>	<i>Host</i>	<i>Target species</i>	<i>Dilution</i>	<i>Supplier</i>	<i>Cat. Number</i>
-------------------------------------	-------------	-----------------------	-----------------	-----------------	--------------------

IgG (H+L) Secondary Antibody, Alexa Fluor™ 488, Invitrogen	Goat	Mouse	1:1000	Thermo Fisher Scientific	#A-11017
IgG (H+L) Secondary Antibody, Alexa Fluor™ 568, Invitrogen	Goat	Mouse	1:1000	Thermo Fisher Scientific	#A-11004
IgG (H+L) Secondary Antibody, Alexa Fluor™ 488, Invitrogen	Goat	Rabbit	1:1000	Thermo Fisher Scientific	#A-21244
IgG (H+L) Secondary Antibody, Alexa Fluor™ 568, Invitrogen	Goat	Rabbit	1:1000	Thermo Fisher Scientific	#A-11011

3.1. EdU click-it assay

D30 organoids were incubated in in 10 μ M 5-ethynyl- 2'-deoxyuridine (EdU) (Invitrogen, #C-10337, Component A) diluted in cerebral organoid differentiation medium, for 2hrs. Four organoids per genotype were collected and processed as described previously (1.2.4. Fixation and Cryopreservation of organoids), for immunofluorescence experiments. EdU click-it assay was performed in organoid cryosections per manufacturer's instructions (EdU kit Invitrogen, #C-10337) followed by immuno-staining for Ki67. The Edu+ /Ki67+ ratio was measured, and cell cycle length was calculated using the formula $T_c = T_s / (Edu+ / Ki67+)$ (T_c =cell cycle length, T_s = S phase length). A minimum of 3 slices/organoid were imaged and analyzed.

4. Immunoblotting

Immunoblotting was performed to identify specific proteins of interest. The identification is based on the separation of the proteins according to their molecular weight. Immunoblotting is considered as a semi-quantitative method, as it mediates a relative comparison of protein levels, but it does not provide the exact protein abundance.

4.1. Preparation of the samples and the protein extraction

Tissue was homogenized in the suitable volume of RIPA buffer with protease and phosphatase inhibitors (diluted 1:100) in an ultrasonic homogenizer. The samples were centrifuged for 20min at 16000 x g at 4°C to obtain soluble protein fractions. Pierce BCA Protein Assay Kit (Thermo Fisher Scientific, #23225) was used to determine protein concentration. The loading samples contained 45ug of protein, 4x SDS loading buffer and ddH₂O. The samples were heated (5min at 95°C), vortexed, spun down and kept in ice or froze at -80°C for future use.

4.2. Preparation of polyacrylamide gels

For the studies presented, the following stacking and resolving gels were prepared: 4% stacking gel (30% Acrylamide/bis, 0.5M Tris-HCl pH=6.8, ddH₂O, 10% SDS, TEMED, 10% APS, 0.01% Bromophenol Blue) and 10% resolving gel (30% Acrylamide/bis, 1.5M Tris-HCl pH=8.8, ddH₂O, 10% SDS, TEMED, 10% APS, 0.01% Bromophenol Blue). The cassette was assembled,

the resolving gel 10% was poured, after its polymerization, the stacking gel 4% was poured and immediately the combs were inserted and after its polymerization, the gels were placed in the tank, which was filled with 1x Running Buffer. For running the gel, the ladder and the samples were loaded on the gel and the right setting were placed (20mA for 45 min and then 140V until the desired bands were resolved). Nitrocellulose membrane was used for protein transfer. The transfer sandwich was assembled and placed in the tank filled with 1x Transfer Buffer. The electrophoresis device was set at 100V for 90min. Following protein transfer the membrane was briefly washed with dH₂O and incubated for 5 min in a Ponceau stain. The nitrocellulose membrane was destained with dH₂O and incubated with Blocking Buffer (5% BSA in TBS-T 1X) on a rocker for 1h at RT. Following an overnight incubation at 4°C with primary antibody (in 1% BSA in TBS-T, 0.02% Azide Na) (Table 3) the membrane was used with 1 X TBS-T.

Table 3 | List of the primary antibodies used in western blot experiments. Host and target species, dilution used, supplier and catalogue number.

<i>Primary antibody</i>	<i>Biological source</i>	<i>Dilution</i>	<i>Supplier</i>	<i>Cat. Number</i>
Phospho-S6 Ribosomal Protein (Ser240/244)	Rabbit	1:1000	Cell Signaling Technology	#2215
Phospho-Akt (Thr473)	Rabbit	1:1000	Cell Signaling Technology	#9271
Ribosomal Protein-S6	Mouse	1:1000	Santa Cruz Biotechnology	#sc-74459
Akt	Rabbit	1:1000	Cell Signaling Technology	#9272

The membrane was incubated with the secondary antibody (in 1% BSA in TBS-T, 0.02% Azide Na) (Table 4) at RT for 1h on a rocker. The membrane was scanned and developed using Azure equipment (Azure Biosystems) for protein visualization and quantification.

Table 4 | List of the secondary antibodies used in Immunofluorescence experiments. Host and target species, dilution used, supplier and catalogue number.

<i>Secondary antibody</i>	<i>Host</i>	<i>Target species</i>	<i>Dilution</i>	<i>Supplier</i>	<i>Cat. Number</i>
IgG (H+L) Polyclonal Antibody conjugated to IRDye® 6800RD	Goat	Mouse	1:5000	LI-COR Biosciences	#926-68070
IgG (H+L) Polyclonal Antibody conjugated to IRDye® 800CW	Donkey	Rabbit	1:5000	LI-COR Biosciences	#926-68070

When required, NaOH (0.1M-1M) was used to strip the membrane, allowing the incubation with other antibodies.

5. RNA sequencing and Bioinformatics Analysis

On day 30, organoids were transferred from culture plates to 1.5ml tubes and briefly washed with ice-cold DPBS. For each biological replicate, 3 to 4 organoids were pooled in a single tube. After removing DPBS, organoids were homogenized using QIA shredder homogenizers (Qiagen, #79656). Total RNA was extracted using the RNeasy Micro kit (Qiagen, #74004) following manufacturer's instructions. The extracted RNA was dissolved in RNase-free water, and its concentration and purity were assessed using a Nanodrop spectrophotometer (ThermoFisher, Nanodrop One C). Library preparation and RNA sequencing were performed as a service by GENEWIZ/AZENTA, with sequencing performed on a Novaseq 6000 platform (Illumina).

Sequence reads were trimmed to remove possible adapter sequences and nucleotides with poor quality using Trimmomatic v.0.36. The trimmed reads were then aligned to the Homo sapiens GRCh38 reference genome from ENSEMBL using the STAR aligner v.2.5.2b, generating BAM files. Gene hit counts were calculated using featureCounts from the Subread package v.1.5.2, only including unique reads mapped to exon regions. These counts were summarized and reported according to gene IDs in the annotation file.

Differential gene expression analysis was performed using DESeq2. Gene expression differences between KO and control samples were evaluated, with the Wald test used to calculate p-values and log₂ fold changes. Genes with an adjusted p-value < 0.05 were considered differentially expressed. To gain insight into the biological processes associated with these genes, gene ontology (GO) analysis was performed using GeneSCF v.1.1-p2. The goa_human GO list was used to group genes based on their biological functions and assess statistical significance.

6. Scanning Electron Microscopy (SEM)

Scanning electron microscopy (SEM) images were obtained using a JEOL JSM-6510 LV SEM Microscope (JEOL Ltd., Tokyo, Japan) equipped with an X-Act EDS-detector by Oxford Instruments, Abingdon, Oxfordshire, UK (an acceleration voltage of 20 kV was applied). Prior to SEM analysis, the samples (control and KO cerebral organoids) were coated with an Au/Pd thin film (4–8 nm) in a sputtering equipment (SC7620, Quorum Technologies, Lewes, UK). SEM imaging was performed in collaboration with Prof. Apostolos Avgeropoulos from the Department of Materials Science Engineering, University of Ioannina, Ioannina, Greece.

7. Image Analysis

Bright-field images were obtained using an EVOS TM XL Core microscope (Invitrogen). Organoid surface area was quantified in ImageJ software, by outlining the perimeter of each organoid. For fluorescent images, cell counting was conducted using the cell counter tool in ImageJ, with the cell fraction for each marker calculated as a percentage of the total nuclei measured. Immunoblot images were processed in Image Studio, where protein expression bands were selected and quantified following background definition. All measurements obtained were retained for the statistical analysis. For the VZ analysis, SOX2 and MAP2 staining was used to manually define the VZ boundaries. Area and perimeter of each VZ was measured using Image J (Analyze/Measure tool). Disorganisation of the VZ was calculated using MAP2 staining as an indicator; a VZ containing MAP2+ cells was scored as disorganised,

while absence of MAP2+ cells (clear boundaries) assigned a VZ as organised. For each organoid, a minimum of 5 VZ from at least 3 separate slices were measured and analyzed.

8. Statistical Analysis

Statistical analyses were conducted using GraphPad Prism 8.0 (GraphPad Software, San Diego, CA, USA). Data are presented as mean \pm SEM (SEM: Standard Error of the Mean). The normality of sample distributions was assessed using the Shapiro-Wilk test ($\alpha=0.05$), with statistical significance established a priori at $p<0.05$. No randomization was applied in this study and experimenters were blinded to genotype during the analysis. N number corresponds to biological replicates (single organoid, or pooled organoids). Data were derived from 4 to 7 biological replicates per batch, across a total of 3 batches, with each biological replicate further comprising more than 3 technical replicates. Statistical significance was a priori set at $p < 0.05$.

For distributions that met the normality criteria, as assessed by the Shapiro-Wilk test ($p > 0.05$), an unpaired *t*-test was employed for sample analysis under the assumption of equal standard deviations. If the Shapiro-Wilk test indicated a deviation from normality ($p < 0.05$), where variances were considered significantly different, and the assumption of equal standard deviation was disregarded, a non-parametric alternative, such as the Mann-Whitney U test, was used instead. In these instances, the Unpaired *t*-test was conducted with Welch's correction.

Details for statistical tests used are provided within figure legends.

Results

1. A hiPSC model to study *CNTNAP2* gene loss-of-function using zinc finger nucleases

In this study we aimed to investigate the role of *CNTNAP2* in early brain development. To achieve this, we obtained *CNTNAP2* knockout induced pluripotent stem cells (iPSCs) from XCell Science (Canada), which were generated through zinc-finger nuclease-mediated genome editing (Fig. 20), targeting both alleles in the XCL1 male human pluripotent stem cell line. These knockout iPSCs, alongside the unedited XCL1 control iPSCs, were employed to examine the potential alterations caused by *CNTNAP2* loss-of-function mutations.

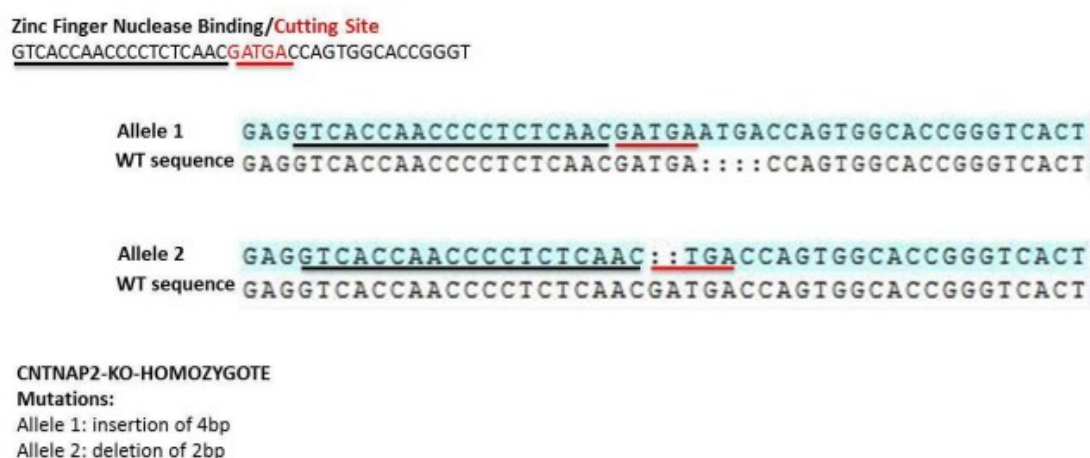


Figure 20 | Bi-allelic *CNTNAP2* KO iPSCs generation with the insertion of 4bp (allele1) and the deletion of 2bp (allele 2), in exon 17, using Zinc Finger Nuclease. Black lines depict binding sites of nucleases and red lines the cutting site.

Both the *CNTNAP2* knockout (KO) iPSCs and the isogenic XCL1 control iPSCs exhibited a normal karyotype, as confirmed by comparative genomic hybridization (CGH) array analysis (Fig. 21 D). Pluripotency of these lines was validated through the expression of OCT-3/4 and NANOG, assessed using immunofluorescence and RT-qPCR (Fig. 21A, B). Cerebral organoids were subsequently derived from both control and KO iPSCs using a modified organoid differentiation protocol [114].

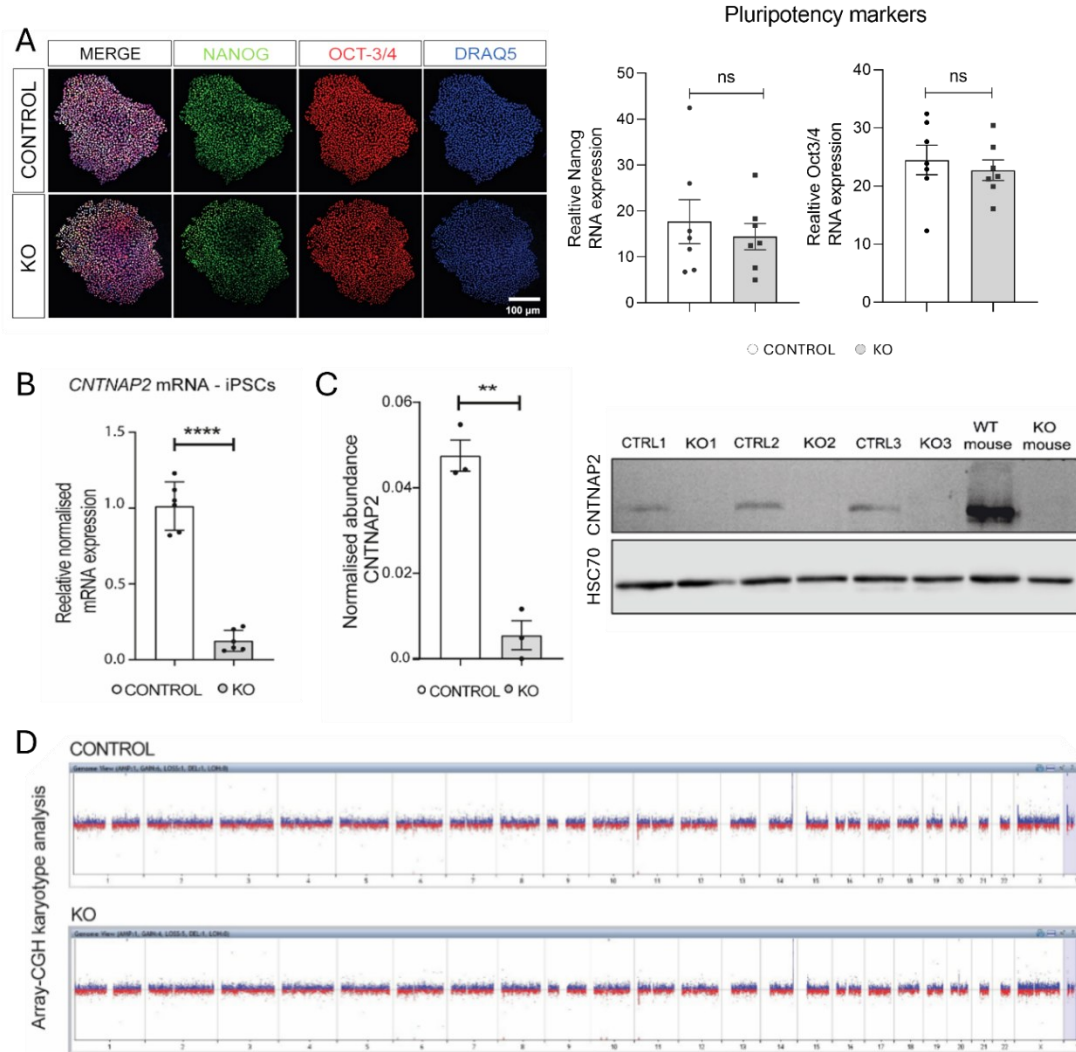


Figure 21 | **A**. Representative fluorescent images (left) from control and KO iPSC and quantitative RT-qPCR analysis (right) of the pluripotency markers NANOG (green) and OCT-3/4 (red) expression, confirming the pluripotency of both cell lines. DRAQ5⁺ (blue) was used for nuclear staining. **B**. Quantitative RT-qPCR analysis of *CNTNAP2* expression in control and KO iPSCs, showing significantly decreased *CNTNAP2* mRNA expression (n=2 biological replicates/genotype and 2-4 technical replicates/genotype). **C**. Western blot analysis that shows *CNTNAP2* expression in D30 control organoids, and absence in D30 KO organoids. Each lane corresponds to one biological replicate. **D**. CGH-array karyotype analysis of control and KO iPSCs that confirms the normal karyotype of both cell lines. For **(A)** One-way ANOVA with Dunnett's post hoc analysis Control: 17.69 ± 4.8 ; KO: 14.42 ± 2.854 ; $p=0.911$ for relative NANOG mRNA expression and Control: 24.5 ± 2.56 ; KO: 22.74 ± 1.76 ; $p=0.92$ for relative OCT3/4 mRNA expression **(B)** Student's *t*-test analysis Control: 1.019 ± 0.0713 ; KO: 0.11 ± 0.034 ; **** $p < 0.0001$ and **(C)**, Student's *t*-test analysis Control: 0.0475 ± 0.036 ; KO: 0.0055 ± 0.0033 ; ** $p < 0.001$

2. *CNTNAP2* KO leads to decreased cerebral organoid size, VZ disorganization and accelerated cell cycle in cerebral organoids enriched for dorsal brain cells

Cerebral organoids were derived from both control and *CNTNAP2* knockout (KO) hiPSCs using a modified protocol (detailed in the Materials and Methods section) (Fig. 22 A). These organoids are enriched in dorsal forebrain cell types (mainly excitatory) but also contain a small number of ventral brain cells (inhibitory) (Lancaster, 2013) [114]. Confocal imaging of immunofluorescence-labeled organoid sections at day 30 revealed the prominent expression of key markers characteristic of early brain development. We detected a substantial number of cells positive for the neural progenitor markers SRY-box 2 (SOX2) and PAX6, localized within ventricular zone (VZ)-like structures in organoid sections from both genotypes. In contrast, more mature neurons expressing β -Tubulin III (TUJ1) and MAP2 were observed outside these VZ-like structures (Fig. 22 C). Bright-field microscopy further demonstrated that D30 KO organoids were noticeably smaller compared to their control counterparts (by $\approx 8\%$) (*Mann Whitney* test, $P=0.024$) (Fig. 22 B).

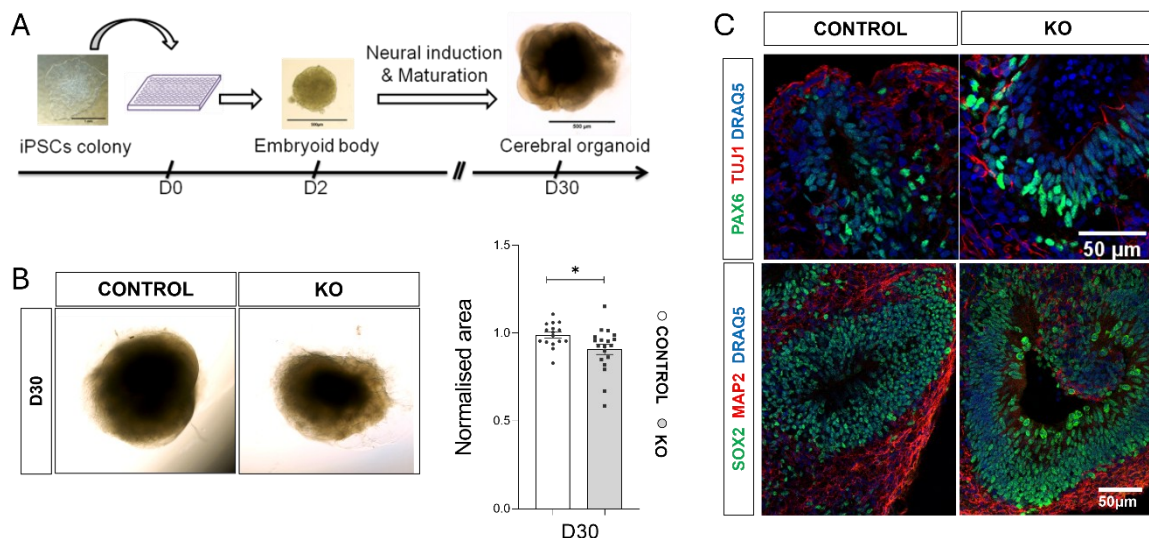
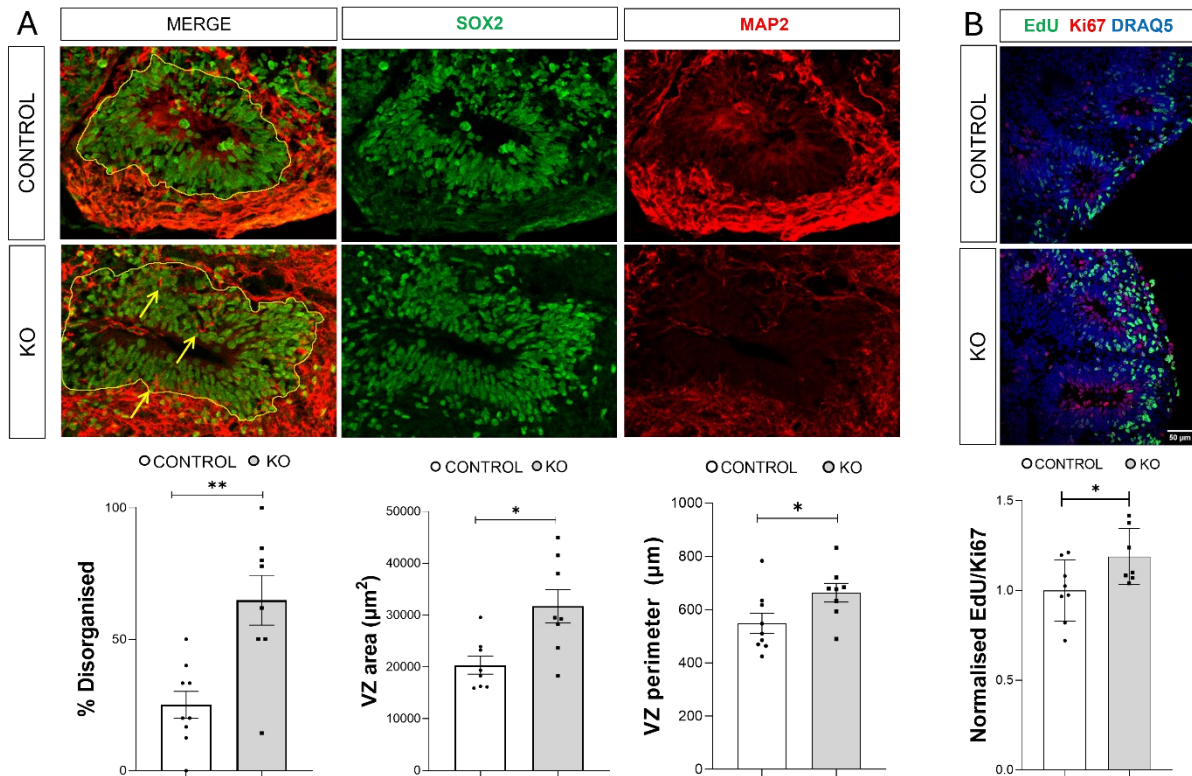


Figure 22 | A cerebral organoid model harboring *CNTNAP2* targeted deletion. **A**. Schematic overview of the cerebral organoid protocol development until day 30 of differentiation. **B**. Representative bright field images from control and KO organoids (left) and normalized projected surface area measurements showing a decrease in size in KO organoids on day 30 (right). **C**. Representative images from control and KO organoids with SOX2 (green)-TUJ1 (red) and PAX6 (green)-MAP2 (red). DRAQ5⁺ (blue) was used for nuclear staining. For **(B)** *Mann Whitney* test, Control: 1 ± 0.037 ; KO: 0.907 ± 0.029 $*p < 0.05$.

Given the difference in size at D30, we assessed proliferation during early organoid development by measuring cell cycle length through co-labeling with EdU (to measure de novo DNA synthesis during the S-phase of the cell cycle) and the proliferative marker Ki67, followed by confocal imaging. On day 30 (D30), *CNTNAP2* knockout organoids exhibited a higher EdU/Ki67 ratio ($\approx 20\%$), indicating increased proliferative potential in neural progenitor cells (NPCs) and shorter cell cycle durations (Fig. 23B). To further investigate size and surface folding abnormalities, D30 organoids were sectioned, and the size and organization of VZ-like structures were examined with immunofluorescence and confocal imaging. The VZ boundaries were delineated by SOX2-positive NPCs and MAP2-positive neurons. KO

organoids demonstrated a significantly increased VZ area ($\approx 56\%$) and perimeter ($\approx 20\%$) compared to control organoids. Additionally, the extensive presence of MAP2-positive cells within the VZ-like zones suggested a disruption in cellular organization (Fig. 23A). Such disorganization in VZ-like structures could impair corticogenesis, consistent with findings on



other ASD-related mutations modeled using brain organoids.

Figure 23 | **A.** Representative images from control and KO organoids with SOX2 (green) and MAP2 (red) immunostaining, demonstrating increased size and disorganisation of the VZ-like structures in KO organoids. Yellow line delineates the VZ region and yellow arrows emphasize the presence of MAP2 positive neurons inside the VZ. Quantification of the area and perimeter of VZ and the occurrence of organised versus disorganised VZ regions in control and KO organoids, based on SOX2 and MAP2 staining patterns ($n=9$ for control and $n=8$ for KO organoids, 4 separate organoid batches per genotype). Student's *t* test analysis (% Disorganised VZ - Control: 25.09 ± 5.121 ; KO: 64.83 ± 9.475 ; $**p < 0.01$, VZ Area - Control: 20345 ± 1721 ; KO: 31699 ± 3213 ; $*p < 0.05$, VZ Perimeter - Control: 548.2 ± 37.53 ; KO: 663.2 ± 35.02 ; $*p < 0.05$). **B.** Representative images from EdU (green), Ki67 (red) and DRAQ5⁺ (blue) immunostaining of D30 organoids. Bar graph showing increased EdU/Ki67 immunofluorescence signal ratio in KO organoids ($n = 7$ /group, 3 separate organoid batches per genotype, KO values are normalized to the control mean). Quantification of cell cycle length was performed using the formula $T_c = T_s / (\text{EdU}^+ / \text{Ki67}^+)$. KO organoids showed shorter cell cycle length than control organoids. Student's *t* test analysis (Control: 1 ± 0.06 ; KO: 1.19 ± 0.059 ; $*p < 0.05$).

Indeed, when we examined organoid surface folding using Scanning electron microscopy (SEM), we observed that D30 cerebral organoids, which had previously been coated with gold/palladium, exhibited an 82% increase in surface folding (Fig. 24). The folding of the surface of brain organoids reflects the emergence of structural complexity and is reminiscent of human cortical folding, which enables complex neural connectivity and increase the surface of the brain [115].

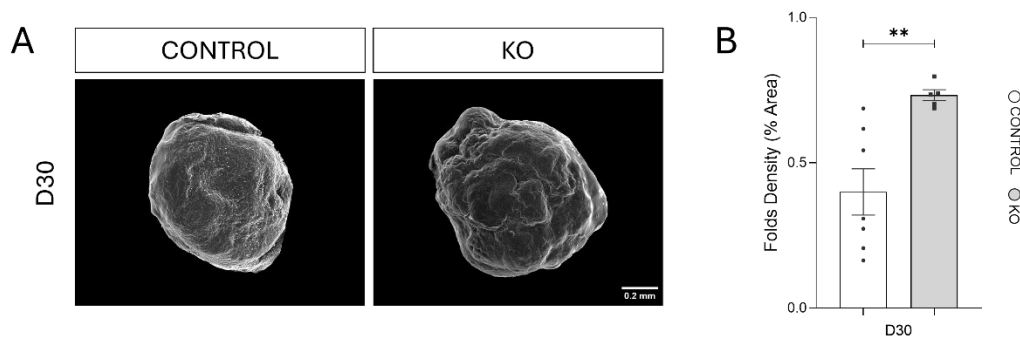


Figure 24 | **A.** Representative scanning electron microscopy images from control and KO organoids at D30. **B.** Quantification of surface fold density showing increased surface folding in KO-derived organoids at D30 (n=7 for control, n=5 for KO D30, 2 separate organoids batches per genotype, Control: 0.398 ± 0.079 ; KO: 0.732 ± 0.018 ; Student's *t* test analysis $**p < 0.01$).

3. Pro-interneuronal transcriptional networks in CNTNAP2 KO cerebral organoids

To gain a better understanding of the potential mechanisms underlying the phenotypes observed in CNTNAP2 KO organoids, bulk RNA sequencing was performed on mRNA extracted from day 30 organoids (control and KO).

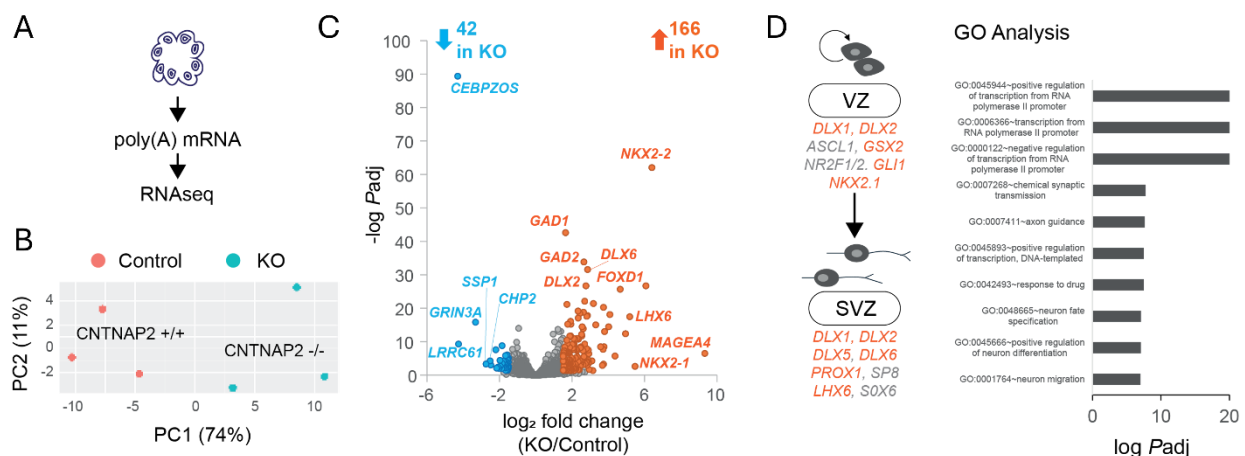


Figure 25 | RNAseq data from cerebral organoids. **A.** Illustration of cerebral organoid poly(A) mRNA isolation and RNAseq. **B.** Principal Component Analysis (PCA) for RNAseq biological (n=3) replicates of CNTNAP2 control (+/+) or KO (-/-) organoids (1 organoid batch per genotype). Scatter plot visualising the proportion of explained variance, with Principal Component 1 (PC1) accounting for the majority (74%) of the variance. PC2 explains a smaller portion of the variance (11%). **C.** Volcano plot of D30 RNAseq experiment highlighting upregulated (orange) and downregulated (cyan) DEG in KO samples. X-axis demonstrates the log₂-transformed fold change in abundance (KO/control) and the Y-axis indicates the negative log-transformed *P*_{adj} (adjusted *P*) values associated with individual mRNAs. A cut-off of $-\log P_{adj} > 1.3$, $1.5 < \log_2 \text{fold change} < -1.5$ was applied. **D. Left:** Illustration of pro-interneuron mRNAs upregulated (in orange) in CNTNAP2 KO RNAseq DEG, showing genes participating in VZ and

SVZ neurogenesis, cell-fate commitment, and tangential migration (in grey). *Right*: GO analysis of DEG using GeneSCF v1.1-p2. Significantly enriched GO categories with adjusted P value <0.05 (Fisher exact test). DEG, differentially expressed genes; VZ, ventricular zone; SVZ, subventricular Zone.

A total of 208 differentially expressed genes (DEGs) were identified, including 42 downregulated and 166 upregulated genes ($-\log P_{adj} > 1.3$, $1.5 < \log_2 \text{fold change} < -1.5$). Gene Ontology (GO) analysis revealed significant enrichment in pathways related to transcriptional regulation, synaptic transmission, axon guidance, neuron fate specification, and neuron differentiation (Fig. 25 D). Among the top DEGs, notable upregulation was observed in transcription factors associated with cortical interneuron development, such as DLX family genes (DLX1, DLX2), NKX2.1, and LHX6. These genes are implicated in VZ-neurogenesis, cell fate determination, and SVZ cell fate commitment and tangential migration.

4. Imbalance of Inhibitory and Excitatory Marker Expression in CNTNAP2 KO Organoids

Given the extensive transcriptional remodelling in CNTNAP2 KO eliciting pro-interneuronal transcriptional networks, we hypothesized that deletion of CNTNAP2 may engender an imbalance in Glutamatergic (excitatory) over GABAergic (inhibitory) cells in the developing organoids at D30. To verify this, we performed immunofluorescence analysis and confocal imaging of day 30 control and KO cerebral organoids and assessed GAD1, a key inhibitory neurotransmitter, and TBR1, a transcription factor in excitatory neurons.

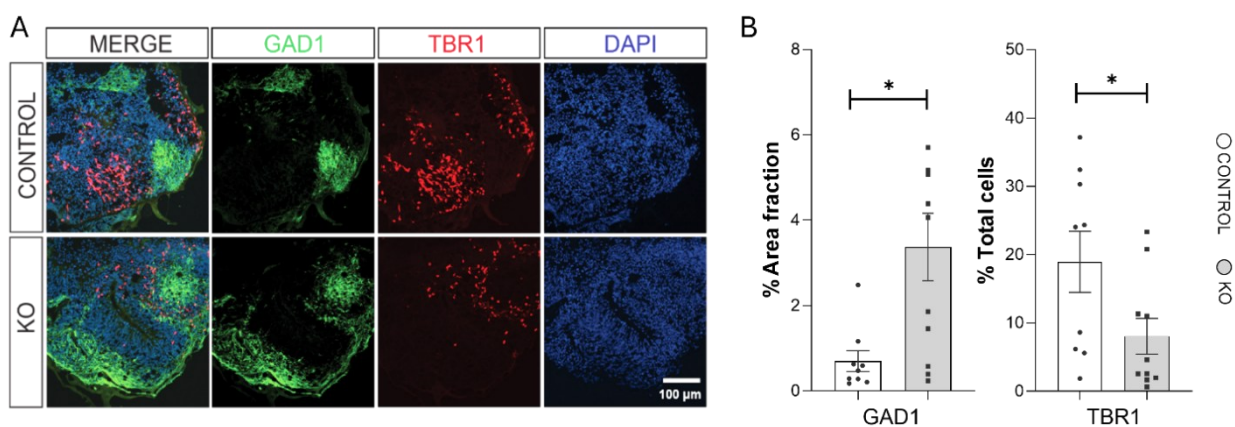


Figure 26 | **A.** Representative images of immunostaining of TBR1⁺(red) postmitotic Glutamatergic neurons and GAD1⁺(green) mature GABAergic interneurons, depicting the increased GAD1 expression in D30 KO cerebral organoids. **B.** Quantification of TBR1⁺ cell fraction and GAD1 expression (% area fraction) in D30 cerebral organoids. Total cells were estimated by counting DAPI⁺ nuclei (3-6 separate organoid batches per genotype, n=1- 3 organoids/batch). Mann Whitney test analysis was performed for GAD1 expression (Control: 0.699±0.245; KO: 3.373±0.791; * $p < 0.05$) and for TBR1 expression (Control: 18.94±4.468; KO: 8.047±2.623; * $p < 0.05$).

Compared with control, KO organoids exhibited significantly increased GAD1 expression ($\approx 380\%$ increased in area fraction). Conversely, KO organoids displayed an decreased number of TBR1 positive cells compared with control ($\approx 59\%$ decrease in cell number) (Fig. 26).

5. Increased number of positive cells in additional interneuronal markers in KO dorsal Organoids

Given the apparent increase in GAD1 expression, a marker typically associated with inhibitory interneurons, we further examined other markers known to be expressed in interneurons.

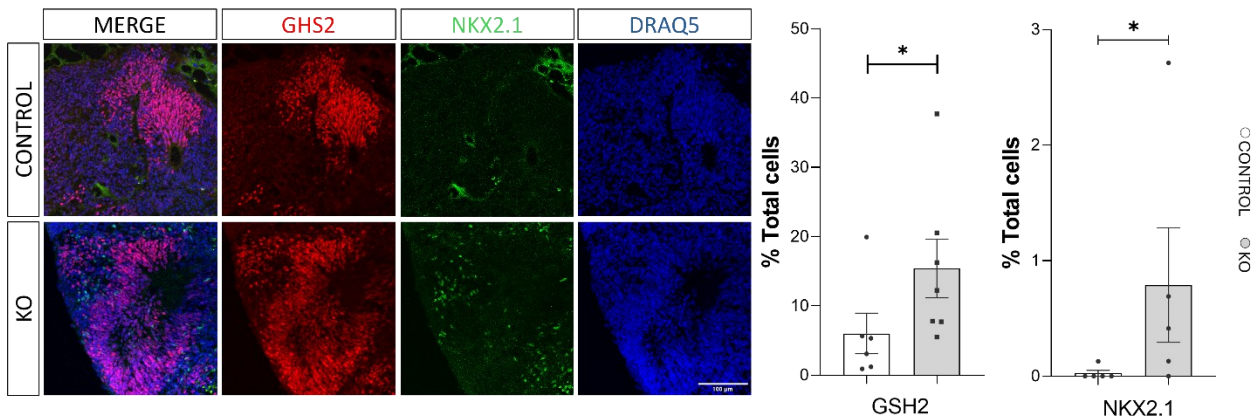


Figure 27 | Representative images from D30 control and KO organoids with GABAergic neuron progenitor markers NKX2.1 (green) and GSH2 (red) immunostaining. Quantification NKX2.1⁺ and GSH2⁺ cell fraction, in D30 cerebral organoids. Total cells were estimated by counting DRAQ5⁺ nuclei. Mann Whitney test analysis was performed for NKX2.1 expression (Control: 0.0257±0.0257; KO: 0.789±0.495; **p* < 0.05) and for GSH2 expression (Control: 6.018±2.901; KO: 15.4±4.225; **p* < 0.05).

Both NKX2.1; a transcription factor that marks the MGE which expression is essential for the specification of interneuron subtypes, and GSH2; a homeobox gene marking the LGE, which contributes to the development of striatal projection neurons and some interneuron populations; display increased number of cells expressing these markers in KO organoids compared with control by ≈79% and ≈158% respectively (Fig. 27). The increase in those markers' expression could underscore a broader dysregulation in the patterning and specification of ventral progenitor domains.

6. CNTNAP2 KO does not significantly affect ventral organoid size

Building on the findings of transcriptomic analyses and IF of CNTNAP2 KO cerebral organoids, we reasoned that disruptions in the molecular mechanisms underlying interneuron development and the imbalance between excitatory and inhibitory neuronal populations are key contributors to the observed phenotypes. The altered expression of ventral telencephalic markers, such as NKX2.1 and GSH2, and the role of these regions in interneuron generation highlight the need for a model that can further investigate interneuron development in isolation. To address this, we developed ventral telencephalic organoids following a published protocol, Gomes et al., 2020 [65].

Ventral organoids were derived from both control and CNTNAP2 knockout hiPSCs (Fig. 28 A). Organoid sections at day 30 were immunofluorescently-labeled and used for confocal imaging to investigate the expression of key markers specific for early ventral brain development. We detected prominent expression of the early neuron progenitor marker SOX2 within VZ-like zones in both control and KO organoids (Fig. 28 C). Bright-field microscopy was employed to assess organoid size as in Fig. 22. D30 KO ventral organoids had no significant differences in size (based on their projected area) compared with control (*Mann Whitney test, P=0.6196*) (Fig. 28 B).

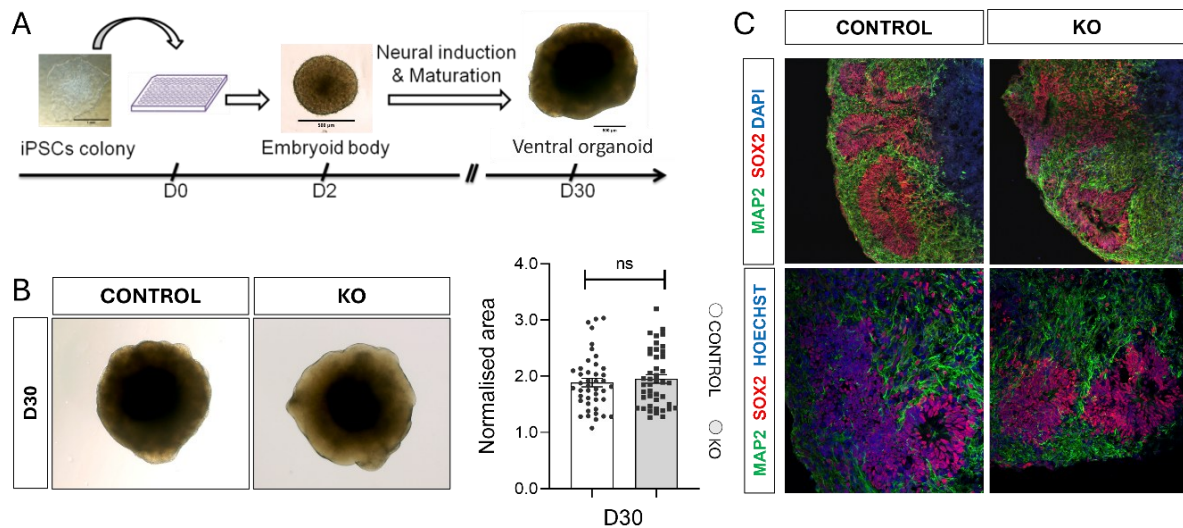


Figure 28 | A summary of the ventral organoid model that hosts *CNTNAP2* targeted deletion. **A.** Schematic overview of the cerebral organoid protocol development until day 30 of differentiation. **B.** Representative bright field images from control and KO organoids (left) and normalized projected surface area measurement in size in KO organoids on day 30 (right). Mann Whitney test analysis, Control 1.888 ± 0.07541 ; KO 1.952 ± 0.07719 ; $p=0.6196$. **C.** Representative images from control and KO organoids with SOX2 (green)-MAP2 (red) immunostaining, demonstrating no difference at the size and disorganisation of the VZ-like structures in KO organoids.

7. Increased number of cells expressing TBR1 in CNTNAP2 KO ventral organoids

Our analysis revealed that the number of cells that express TBR1, a transcription factor predominantly expressed in excitatory neurons in deep cortical layers, was significantly increased in KO ventral organoids compared with controls ($\approx 350\%$). This suggests a possible shift toward excitatory neuron specification or altered maturation pathways in the absence of CNTNAP2 (Fig. 29).

In contrast, the expression of GAD1, a key enzyme involved in the synthesis of GABA and a marker for inhibitory interneurons, showed no significant difference between KO and control organoids. This finding indicates that while *CNTNAP2* deletion appears to influence excitatory neuron development, its effect on the generation or maturation of inhibitory interneurons may be more subtle or dependent on additional factors (Fig. 29).

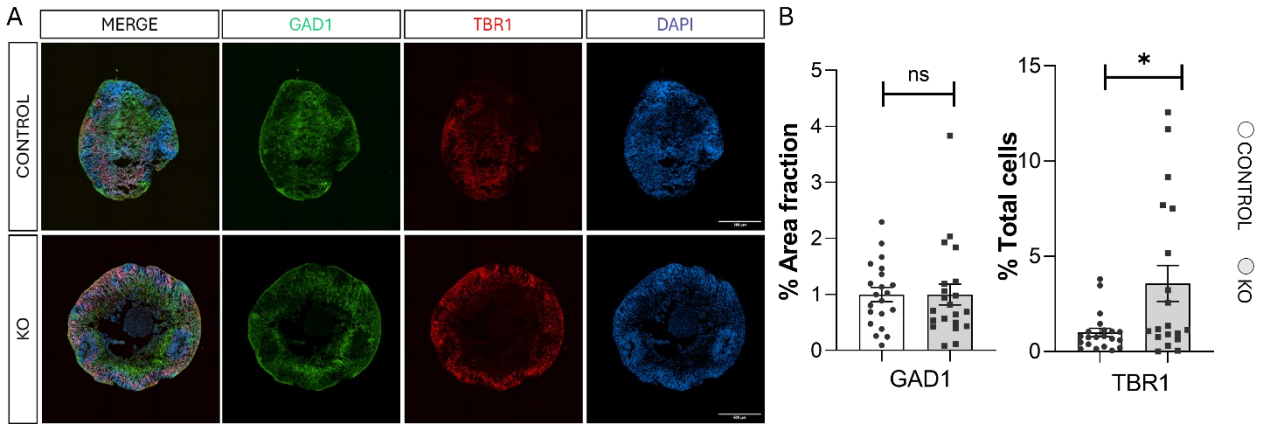
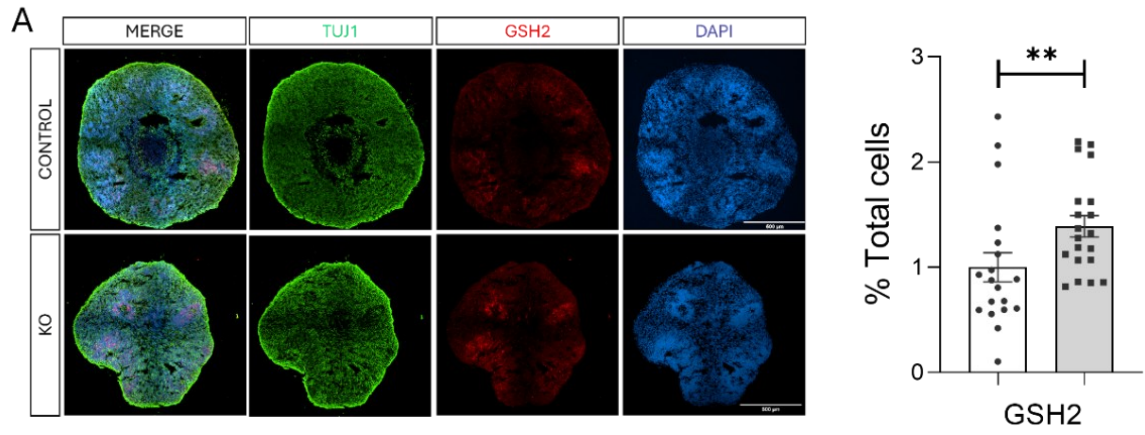


Figure 29 | **A.** Representative images of immunostaining of TBR1⁺ (red) and GAD1⁺ (green) mature cells, in D30 KO cerebral organoids. **B.** Quantification of TBR1⁺ cell fraction and GAD1 expression (% area fraction) in D30 ventral organoids. Total cells were estimated by counting DAPI⁺ (blue) nuclei. Mann Whitney test analysis was performed for GAD1 expression (Control 1±0.1254; KO 0.9986±0.1853; *p* = 0.5499) and for TBR1 expression (Control 1±0.2177; KO 3.572±0.9411; **p* < 0.05).

8. Increased number of GSH2⁺ cells in CNTNAP2 KO ventral organoids

We examined the expression of GSH2 and NKX2.1 in ventral telencephalic organoids. Our results revealed that the number of GSH2⁺ cells was significantly increased in CNTNAP2 KO ventral organoids compared with controls (~40%) (Fig. 30 A), suggesting an alteration in the regional specification or progenitor dynamics of the ventral telencephalon. In contrast, the number of NKX2.1⁺ showed no significant difference between KO and control ventral organoids (Fig. 30 B), indicating that MGE progenitor identity might remain largely unaffected despite the observed changes in GSH2 expression.



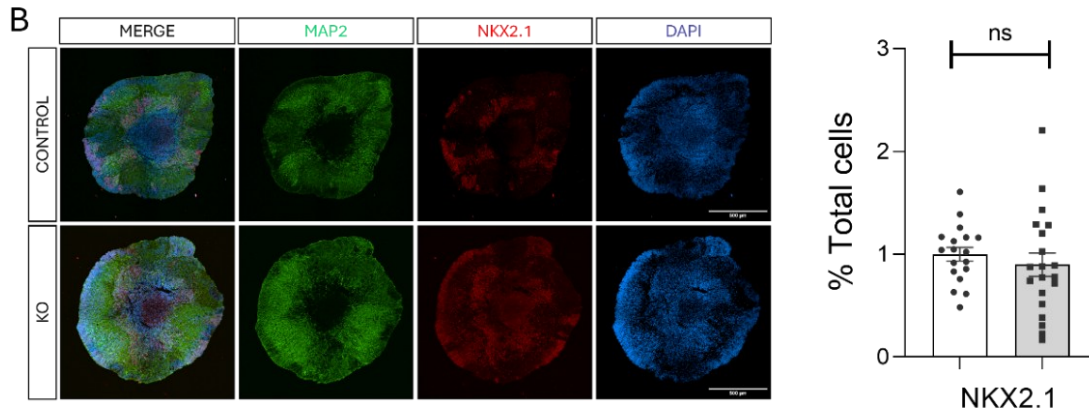


Figure 30 | **A.** Representative images of immunostaining of GSH2⁺ (red) cells in D30 control and KO ventral organoids sections compared with the quantification of GSH2 expressions in D30 ventral organoids. Total cells were estimated by counting DAPI⁺ (blue) nuclei. Mann Whitney test analysis was performed for GSH2 expression (Control 1 ± 0.1394 ; KO 1.389 ± 0.1018 ; $**p < 0.01$). **B.** Representative images of immunostaining of NKX2.1⁺ (red) cells in D30 control and KO organoids slides along with the quantification of NKX2.1 cell fraction, in D30 ventral organoids. Total cells were estimated by counting DAPI⁺ (blue) nuclei. Mann Whitney test analysis was performed for NKX2.1 (Control 1 ± 0.06662 ; KO 0.8982 ± 0.1132 ; $p = 0.4560$).

9. No significant changes in PI3K/mTOR signaling at D30 in dorsal or ventral telencephalic CNTNAP2 KO organoids

Recent studies have highlighted the critical role of mTOR signaling in ensuring the fidelity of cortical development, with posttranscriptional regulatory mechanisms identified as key contributors to this process [106]. For example, *PTEN*^{-/-} cerebral organoids exhibit increased AKT signaling and disrupted cortical development [116], while *Cntnap2*^{-/-} adult mice show enhanced AKT/mTOR activity, implicating this pathway in neurodevelopmental disorders [113].

Thus, we aimed to investigate whether similar alterations in AKT/mTOR signaling occur in CNTNAP2 KO ventral organoids. Using Western blotting, we measured the expression of key phosphoproteins, effectors of this pathway, including: phospho-AKT (S473) and phospho-ribosomal protein S6 (rpS6, S240/244). Consistent with findings from cerebral (enriched in dorsal brain cells) organoids at D30, no significant differences were detected in the expression levels of AKT/ effectors between control and KO ventral organoids (Fig. 40).

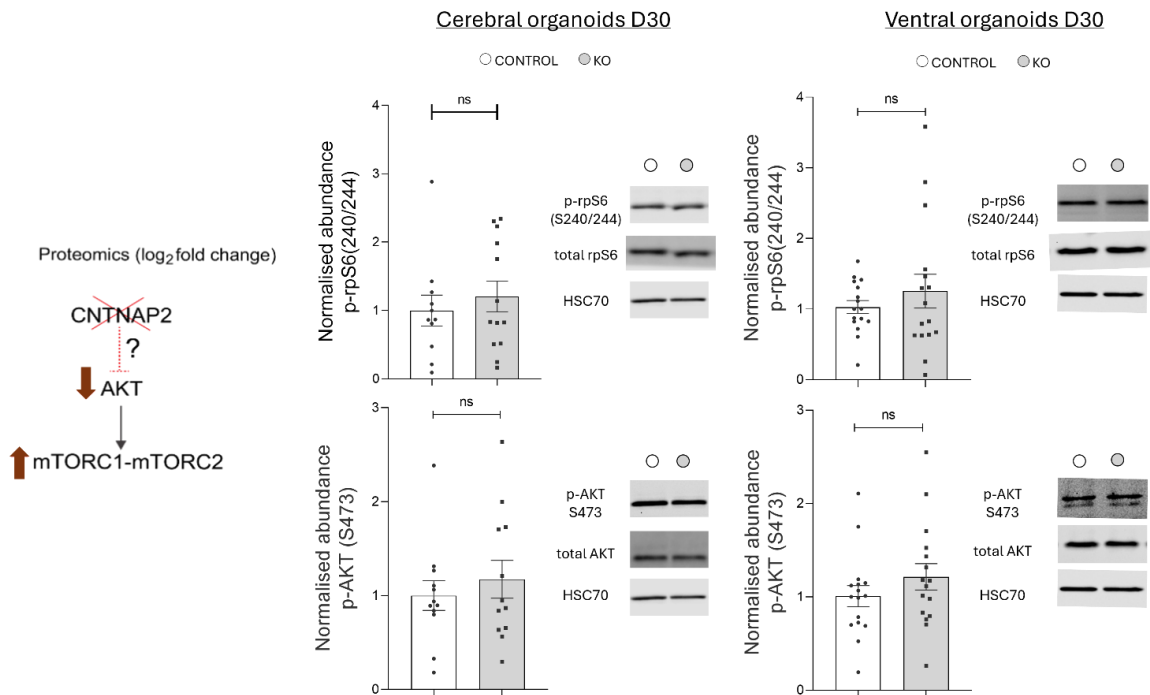


Figure 40 | Left: Illustration of possible mechanism for AKT/mTOR activation downstream of *CNTNAP2* loss of function. Right: Immunoblot analysis of AKT/mTOR signaling in D30 control and KO cerebral and ventral organoids. Quantification of phospho-rpS6 (S240/244) and phospho-AKT (S473) for the indicated groups ($n = 11-13$ /group, 4 separate organoid batches for D30 considering cerebral organoids, $n = 3-5$ /group, 4 separate organoid batches for D30 considering ventral organoids). KO values were normalized to the control mean for both cerebral and ventral organoids. Representative immunoblots of cerebral and ventral organoids probed with antisera against the indicated proteins are shown. HSC70 was used as the loading control. Regarding cerebral organoids samples, Student's t test was performed for the analysis (Normalised Phospho-S6 expression: Control: 1 ± 0.225 KO: 1.206 ± 0.224 ; $p=0.527$ and Normalised Phospho-AKT expression: Control: 1 ± 0.158 KO: 1.173 ± 0.201 ; $p=0.506$). In relation to ventral organoids samples, Man Whitney test was performed for Normalised Phospho-S6 expression (Control 1.028 ± 0.09274 ; KO 1.255 ± 0.2394 ; $p=0.9852$) and Student's t test was performed for Normalised Phospho-AKT expression (Control 1.008 ± 0.1132 ; KO 1.215 ± 0.1409 ; $p=0.2621$).

Discussion

This study aimed to investigate the role of *CNTNAP2* in early brain development using human brain organoid models derived from control and *CNTNAP2* knockout hiPSC lines. Through a combination of techniques, such as immunofluorescence, confocal imaging, and Western blot analyses, we examined critical markers of excitatory and inhibitory neurons as well as key effectors of the PI3K/AKT/mTOR signaling pathway. Our findings revealed notable alterations in neuronal differentiation and molecular signaling, highlighting the impact of *CNTNAP2* deletion on the balance between excitatory and inhibitory neuronal populations. While significant changes were observed in markers such as TBR1 and GSH2, no differences were detected in the expression of mTOR pathway effectors in both cerebral and ventral organoids at day 30. Together with recent results published in Chalkiadaki et al. [117] for D60 dorsal organoid, whereby AKT/mTOR is hyperactivated, our study at D30 raises the possibility of mTOR-independent mechanisms downstream of *CNTNAP2* during early cortical development. These results contribute to our understanding of how *CNTNAP2* influences cortical development and its potential role in neurodevelopmental disorders, however they are not sufficient to draw definitive conclusions. Thus, further investigation is required to fully understand the implications of *CNTNAP2* deletion on cortical development.

The XCL1 cell line used in this study is a well characterized and suitable for differentiation tests for iPSCs and for generating allelic match differentiated cells [118]. Despite its reliability, this cell line presents certain limitations, particularly in the context of this project. Firstly, XCL1 is a male human pluripotent stem cell line, offering no insight into female iPSCs or potential sex-specific differences that could influence the results. Secondly, drawing robust conclusions would require testing more than one cell line to ensure the reproducibility and generalizability of the findings. Finally, there is a potential risk of off-target effects associated with genome editing, meaning that some observed results may not solely reflect the knockout of *CNTNAP2* but could also arise from unintended alterations introduced during the editing process. Moreover, we did not detect significant *CNTNAP2* protein or mRNA expression (Fig. 21) in this model, however we only tested one antibody and one set of primers. Chalkiadaki et al. [117] have tested additional antibodies and primer pairs targeting different parts of the protein or mRNA sequence respectively. In patients harboring *CNTNAP2* mutations, mRNA but no protein is detected, thus our model only recapitulates *CNTNAP2* protein deficiency.

In addition, we did not examine if our Zinc-Finger model is indeed a loss-of-function model. *CNTNAP2* is a neuronal cell adhesion molecule involved in synapse formation, axonal myelination, and neural network connectivity, playing a crucial role in brain development and function. Loss of function mutations in *CNTNAP2* should disrupt neuronal migration, synaptic transmission, and interneuron connectivity, leading to neurodevelopmental disorders such as autism spectrum disorder (ASD), epilepsy, and language impairments [83]. This should probably involve changes in juxtaparanodes, lipid rafts and pre-synapses, areas where *CNTNAP2* is expressed and where it interacts with TAG-1 [119,120]. We did not elucidate this mechanism.

In our dorsal forebrain model, we observed significant differences in KO and control, including changes in organoid size, concomitant with disorganization and alterations in the size and perimeter of ventricular zone-like structures. Notably, the accelerated cell cycle in KO organoids suggests an increased proliferation rate, which we hypothesize may lead to cellular stress or lethality. This is further supported by the reduced expression of TBR1, a

critical marker of deep-layer cortical neurons (Fig. 26). TBR1 plays a pivotal role in neuronal differentiation and has been found to interact with forkhead transcription factor FOXP2, a gene strongly associated with language and speech development [121]. FOXP2 directly binds to regulatory regions of the CNTNAP2 locus, repressing its expression, and is known to regulate both excitatory and inhibitory neuron development [122]. Mutations in TBR1 linked to sporadic autism spectrum disorder (ASD) disrupt this interaction, highlighting the interplay between these genes [123,124]. In our study, RNA sequencing revealed pro-interneuronal gene expression, which, together with the reduced TBR1-positive cells in CNTNAP2 KO organoids, may reflect disrupted FOXP2/CNTNAP2/TBR1-mediated regulatory mechanisms. In addition, PAX6 homozygous deletion in human iPSCs led to upregulation of GABAergic interneuron-related transcriptional programs (DLX1/2/5/6, GSX2, GAD1/2). Thus, CNTNAP2 loss of function may engender transcriptional dysregulation, which is critical for cortical proliferation and differentiation and the maintenance of the glutamatergic/GABAergic progenitor pool balance [125].

In Chalkiadaki et al., we further performed proteomic and spatial transcriptomic analysis [117]. The results revealed that ablation of CNTNAP2 significantly alters the proteomic landscape of CNTNAP2 KO compared with control samples. 377 unique peptides were downregulated and 110 upregulated in KO organoids (fold change and p-value). Given the link between CNTNAP2 and ASD, the dataset was cross-referenced with the Simons Foundation Autism Research Initiative (SFARI) autism gene database, revealing 31 overlapping genes. Among the most upregulated targets in the KO proteomic analysis were FOXG1, PAX6, Protein Kinase C Beta (PRKCB), and Solute Carrier Family 32 (GABA Vesicular Transporter) Member 1 (SLC32A1).

To elucidate pathways affected by CNTNAP2 deletion in human cerebral organoids, Gene Ontology (GO) analysis was conducted on genes encoding the differentially expressed peptides. Analysis of the 110 upregulated genes demonstrated significant enrichment in terms associated with 'nervous system development', 'synapse', 'neuron differentiation', 'neurogenesis' and 'generation of neurons'. In contrast, GO terms for the 377 downregulated genes were predominantly linked to the ECM, including 'organization', 'adhesion', and 'collagen'. Notably, the proteomic analysis of CNTNAP2 KO cerebral organoids revealed disruptions in glutamatergic and GABAergic synaptic pathways, indicating a potential imbalance between excitatory and inhibitory neurons.

Spatial transcriptomics analysis revealed significant alterations in mRNA expression between PAX6⁻/NESTIN⁺ and PAX6⁺/NESTIN⁺ cells. PAX6 was selected as a marker for neural progenitors, while NESTIN was used to ensure the capture of both cytoplasmic and nuclear RNAs. These findings, combined with the proteomic analysis, supported the conclusion that CNTNAP2 knockout influences protein expression, particularly proteins associated with the excitatory/inhibitory neuronal balance. We observed a small overlap between transcriptomics-proteomics GO categories. Indeed, there was a weak correlation between the proteomic and transcriptomic datasets, suggesting that posttranscriptional regulatory mechanisms, such as translational control may be involved.

To further study interneuronal early development, we employed ventral forebrain organoids. In this model we did not detect significant differences in organoid size on day 30 (Fig. 28). One potential explanation for this lack of observed changes is the early developmental stage in which the analysis was conducted. It is possible that at later time points, as the organoids

mature, the anticipated differences in size and other developmental characteristics may become more apparent. Further investigations at advanced stages of organoid maturation could provide additional insights into the effects of *CNTNAP2* loss on ventral forebrain development.

In both dorsal and ventral models, no significant changes in AKT/mTOR signaling effectors were observed, suggesting that the disruptions in *CNTNAP2* KO organoids may not be mediated by alterations in this pathway, at least at the analyzed developmental stage (D30). It is possible that mTOR pathway dysregulation manifests at later stages of organoid development or through subtler mechanisms that are not detectable by the markers used in this study. Alternatively, the observed phenotypic changes in *CNTNAP2* KO organoids may be driven by other pathways or upstream regulatory mechanisms that indirectly influence neuronal development. Another potential explanation for the lack of significant changes could be the limited resolution of Western blot analysis, where expression changes in specific sub-populations of cells might be diluted in bulk samples. Future studies incorporating longitudinal analyses, expanded exploration of related pathways and higher-resolution techniques, such as single-cell RNA sequencing or proteomics, could help uncover such localized or subtle effects and provide additional insights.

Overall, these findings underscore the utility of forebrain organoids—both dorsal and ventral—as valuable tools for investigating the functional consequences of *CNTNAP2* loss and its implications in ASD pathogenesis.

References

- [1] Zakrzewski W, Dobrzyński M, Szymonowicz M, Rybak Z. Stem cells: past, present, and future. *Stem Cell Res Ther* 2019;**10**:68. <https://doi.org/10.1186/s13287-019-1165-5>
- [2] Nava MM, Raimondi MT, Pietrabissa R. Controlling Self-Renewal and Differentiation of Stem Cells via Mechanical Cues. *BioMed Res Int* 2012;**2012**:797410. <https://doi.org/10.1155/2012/797410>
- [3] Molofsky AV, Pardal R, Morrison SJ. Diverse mechanisms regulate stem cell self-renewal. *Curr Opin Cell Biol* 2004;**16**:700–7. <https://doi.org/10.1016/j.ceb.2004.09.004>
- [4] Shenghui H, Nakada D, Morrison SJ. Mechanisms of Stem Cell Self-Renewal. *Annu Rev Cell Dev Biol* 2009;**25**:377–406. <https://doi.org/10.1146/annurev.cellbio.042308.113248>
- [5] Gattazzo F, Urciuolo A, Bonaldo P. Extracellular matrix: A dynamic microenvironment for stem cell niche. *Biochim Biophys Acta BBA - Gen Subj* 2014;**1840**:2506–19. <https://doi.org/10.1016/j.bbagen.2014.01.010>
- [6] Singh VK, Saini A, Kalsan M, Kumar N, Chandra R. Describing the Stem Cell Potency: The Various Methods of Functional Assessment and In silico Diagnostics. *Front Cell Dev Biol* 2016;**4**. <https://doi.org/10.3389/fcell.2016.00134>
- [7] Lu F, Zhang Y. Cell totipotency: molecular features, induction, and maintenance. *Natl Sci Rev* 2015;**2**:217–25. <https://doi.org/10.1093/nsr/nwv009>
- [8] Shi Y, Sun G, Zhao C, Stewart R. Neural stem cell self-renewal. *Crit Rev Oncol Hematol* 2008;**65**:43–53. <https://doi.org/10.1016/j.critrevonc.2007.06.004>
- [9] Sun Y, Chen CS, Fu J. Forcing Stem Cells to Behave: A Biophysical Perspective of the Cellular Microenvironment. *Annu Rev Biophys* 2012;**41**:519–42. <https://doi.org/10.1146/annurev-biophys-042910-155306>
- [10] Yamanaka S, Blau HM. Nuclear reprogramming to a pluripotent state by three approaches. *Nature* 2010;**465**:704–12. <https://doi.org/10.1038/nature09229>
- [11] Chehelgerdi M, Behdarvand Dehkordi F, Chehelgerdi M, Kabiri H, Salehian-Dehkordi H, Abdolvand M, et al. Exploring the promising potential of induced pluripotent stem cells in cancer research and therapy. *Mol Cancer* 2023;**22**:189. <https://doi.org/10.1186/s12943-023-01873-0>
- [12] Varzideh F, Gambardella J, Kansakar U, Jankauskas SS, Santulli G. Molecular Mechanisms Underlying Pluripotency and Self-Renewal of Embryonic Stem Cells. *Int J Mol Sci* 2023;**24**:8386. <https://doi.org/10.3390/ijms24098386>
- [13] Takahashi K, Yamanaka S. Induction of Pluripotent Stem Cells from Mouse Embryonic and Adult Fibroblast Cultures by Defined Factors. *Cell* 2006;**126**:663–76. <https://doi.org/10.1016/j.cell.2006.07.024>
- [14] Yamanaka S, Li J, Kania G, Elliott S, Wersto RP, Van Eyk J, et al. Pluripotency of embryonic stem cells. *Cell Tissue Res* 2008;**331**:5–22. <https://doi.org/10.1007/s00441-007-0520-5>
- [15] Jaenisch R, Young R. Stem Cells, the Molecular Circuitry of Pluripotency and Nuclear Reprogramming. *Cell* 2008;**132**:567–82. <https://doi.org/10.1016/j.cell.2008.01.015>
- [16] Acharya P, Choi NY, Shrestha S, Jeong S, Lee M. Brain organoids: A revolutionary tool for modeling neurological disorders and development of therapeutics. *Biotechnol Bioeng* 2024;**121**:489–506. <https://doi.org/10.1002/bit.28606>
- [17] Ho B, Pek N, Soh B-S. Disease Modeling Using 3D Organoids Derived from Human Induced Pluripotent Stem Cells. *Int J Mol Sci* 2018;**19**:936. <https://doi.org/10.3390/ijms19040936>
- [18] Barré-Sinoussi F, Montagutelli X. Animal models are essential to biological research: issues and perspectives. *Future Sci OA* 2015;**1**:FSO63. <https://doi.org/10.4155/fso.15.63>

- [19] Kim J, Koo B-K, Knoblich JA. Human organoids: model systems for human biology and medicine. *Nat Rev Mol Cell Biol* 2020;**21**:571–84. <https://doi.org/10.1038/s41580-020-0259-3>
- [20] Hofer M, Lutolf MP. Engineering organoids. *Nat Rev Mater* 2021;**6**:402–20. <https://doi.org/10.1038/s41578-021-00279-y>
- [21] Andrews MG, Kriegstein AR. Challenges of Organoid Research. *Annu Rev Neurosci* 2022;**45**:23–39. <https://doi.org/10.1146/annurev-neuro-111020-090812>
- [22] Heinzelmann E, Piraino F, Costa M, Roch A, Norkin M, Garnier V, et al. iPSC-derived and Patient-Derived Organoids: Applications and challenges in scalability and reproducibility as pre-clinical models. *Curr Res Toxicol* 2024;**7**:100197. <https://doi.org/10.1016/j.crtox.2024.100197>
- [23] Yang S, Hu H, Kung H, Zou R, Dai Y, Hu Y, et al. Organoids: The current status and biomedical applications. *MedComm* 2023;**4**:e274. <https://doi.org/10.1002/mco2.274>
- [24] Verstegen MMA, Coppes RP, Beghin A, De Coppi P, Gerli MFM, de Graeff N, et al. Clinical applications of human organoids. *Nat Med* 2025:1–13. <https://doi.org/10.1038/s41591-024-03489-3>
- [25] Yao Q, Cheng S, Pan Q, Yu J, Cao G, Li L, et al. Organoids: development and applications in disease models, drug discovery, precision medicine, and regenerative medicine. *MedComm* 2024;**5**:e735. <https://doi.org/10.1002/mco2.735>
- [26] Lancaster MA, Huch M. Disease modelling in human organoids. *Dis Model Mech* 2019;**12**:dmm039347. <https://doi.org/10.1242/dmm.039347>
- [27] McCauley HA, Wells JM. Pluripotent stem cell-derived organoids: using principles of developmental biology to grow human tissues in a dish. *Dev Camb Engl* 2017;**144**:958–62. <https://doi.org/10.1242/dev.140731>
- [28] Mulder LA, Depla JA, Sridhar A, Wolthers K, Pajkrt D, Vieira De Sá R. A beginner’s guide on the use of brain organoids for neuroscientists: a systematic review. *Stem Cell Res Ther* 2023;**14**:87. <https://doi.org/10.1186/s13287-023-03302-x>
- [29] Eichmüller OL, Knoblich JA. Human cerebral organoids — a new tool for clinical neurology research. *Nat Rev Neurol* 2022;**18**:661–80. <https://doi.org/10.1038/s41582-022-00723-9>
- [30] Quadrato G, Arlotta P. Present and future of modeling human brain development in 3D organoids. *Curr Opin Cell Biol* 2017;**49**:47–52. <https://doi.org/10.1016/j.ceb.2017.11.010>
- [31] Chang Y, Kim J, Park H, Choi H, Kim J. Modelling neurodegenerative diseases with 3D brain organoids. *Biol Rev* 2020;**95**:1497–509. <https://doi.org/10.1111/brv.12626>
- [32] Kim S, Chang M-Y. Application of Human Brain Organoids—Opportunities and Challenges in Modeling Human Brain Development and Neurodevelopmental Diseases. *Int J Mol Sci* 2023;**24**:12528. <https://doi.org/10.3390/ijms241512528>
- [33] Wang H. Modeling Neurological Diseases With Human Brain Organoids. *Front Synaptic Neurosci* 2018;**10**. <https://doi.org/10.3389/fnsyn.2018.00015>
- [34] Guy B, Zhang JS, Duncan LH, Johnston RJ. Human neural organoids: Models for developmental neurobiology and disease. *Dev Biol* 2021;**478**:102–21. <https://doi.org/10.1016/j.ydbio.2021.06.012>
- [35] Hébert JM, Fishell G. The genetics of early telencephalon patterning: some assembly required. *Nat Rev Neurosci* 2008;**9**:678–85. <https://doi.org/10.1038/nrn2463>
- [36] Bagley JA, Reumann D, Bian S, Lévi-Strauss J, Knoblich JA. Fused cerebral organoids model interactions between brain regions. *Nat Methods* 2017;**14**:743–51. <https://doi.org/10.1038/nmeth.4304>
- [37] Zhou Y, Song H, Ming G. Genetics of human brain development. *Nat Rev Genet* 2024;**25**:26–45. <https://doi.org/10.1038/s41576-023-00626-5>

- [38] Kelley KW, Paşca SP. Human brain organogenesis: Toward a cellular understanding of development and disease. *Cell* 2022;**185**:42–61. <https://doi.org/10.1016/j.cell.2021.10.003>
- [39] Fleiss B, Stolp H, Mezger V, Gressens P. Central Nervous System Development. In: Gleason S, editor. *Avery's Dis. Newborn 11th Ed.* Elsevier EdGleason-TS-1620242, Elsevier; 2023, p. Chapter: CH052
- [40] (PDF) The first five years: Starting early. *Early Childhood Series No. 2.* 2011. ResearchGate n.d. https://www.researchgate.net/publication/293132955_The_first_five_years_Starting_early_Early_Childhood_Series_No_2_2011 (accessed January 26, 2025)
- [41] Kuwar Chhetri P, Das JM. *Neuroanatomy, Neural Tube Development and Stages.* StatPearls, Treasure Island (FL): StatPearls Publishing; 2025
- [42] Gammill LS, Bronner-Fraser M. Neural crest specification: migrating into genomics. *Nat Rev Neurosci* 2003;**4**:795–805. <https://doi.org/10.1038/nrn1219>
- [43] Agirman G, Broix L, Nguyen L. Cerebral cortex development: an outside-in perspective. *FEBS Lett* 2017;**591**:3978–92. <https://doi.org/10.1002/1873-3468.12924>
- [44] Hatanaka Y, Hirata T. How Do Cortical Excitatory Neurons Terminate Their Migration at the Right Place? Critical Roles of Environmental Elements. *Front Cell Dev Biol* 2020;**8**:596708. <https://doi.org/10.3389/fcell.2020.596708>
- [45] Hébert JM. Unraveling the Molecular Pathways That Regulate Early Telencephalon Development. *Curr. Top. Dev. Biol.* 2005;**69**:17–37. [https://doi.org/10.1016/S0070-2153\(05\)69002-3](https://doi.org/10.1016/S0070-2153(05)69002-3)
- [46] Yang Z. The Principle of Cortical Development and Evolution. *Neurosci Bull* 2024. <https://doi.org/10.1007/s12264-024-01259-2>
- [47] Villalba A, Götz M, Borrell V. The regulation of cortical neurogenesis. *Curr. Top. Dev. Biol.*, 2021;**144**:1–66. <https://doi.org/10.1016/bs.ctdb.2020.10.003>
- [48] Agirman G, Broix L, Nguyen L. Cerebral cortex development: an outside-in perspective. *FEBS Lett* 2017;**591**:3978–92. <https://doi.org/10.1002/1873-3468.12924>
- [49] Insolera R, Bazzi H, Shao W, Anderson KV, Shi S-H. Cortical neurogenesis in the absence of centrioles. *Nat Neurosci* 2014;**17**:1528–35. <https://doi.org/10.1038/nn.3831>
- [50] Akula SK, Exposito-Alonso D, Walsh CA. Shaping the brain: The emergence of cortical structure and folding. *Dev Cell* 2023;**58**:2836–49. <https://doi.org/10.1016/j.devcel.2023.11.004>
- [51] Stepien BK, Vaid S, Huttner WB. Length of the Neurogenic Period—A Key Determinant for the Generation of Upper-Layer Neurons During Neocortex Development and Evolution. *Front Cell Dev Biol* 2021;**9**:676911. <https://doi.org/10.3389/fcell.2021.676911>
- [52] Faux C, Rakic S, Andrews W, Britto JM. Neurons on the Move: Migration and Lamination of Cortical Interneurons. *Neurosignals* 2012;**20**:168–89. <https://doi.org/10.1159/000334489>
- [53] Xiang Y, Tanaka Y, Patterson B, Kang Y-J, Govindaiah G, Roselaar N, et al. Fusion of Regionally Specified hPSC-Derived Organoids Models Human Brain Development and Interneuron Migration. *Cell Stem Cell* 2017;**21**:383-398.e7. <https://doi.org/10.1016/j.stem.2017.07.007>
- [54] Spruston N. Pyramidal neurons: dendritic structure and synaptic integration. *Nat Rev Neurosci* 2008;**9**:206–21. <https://doi.org/10.1038/nrn2286>
- [55] Lodato S, Rouaux C, Quast KB, Jantrachotechatchawan C, Studer M, Hensch TK, et al. Excitatory Projection Neuron Subtypes Control the Distribution of Local Inhibitory Interneurons in the Cerebral Cortex. *Neuron* 2011;**69**:763–79. <https://doi.org/10.1016/j.neuron.2011.01.015>

- [56] Costa MR, MÃ¼ller U. Specification of excitatory neurons in the developing cerebral cortex: progenitor diversity and environmental influences. *Front Cell Neurosci* 2015;**8**. <https://doi.org/10.3389/fncel.2014.00449>
- [57] Delgado RN, Allen DE, Keefe MG, Mancina Leon WR, Ziffra RS, Crouch EE, et al. Individual human cortical progenitors can produce excitatory and inhibitory neurons. *Nature* 2022;**601**:397–403. <https://doi.org/10.1038/s41586-021-04230-7>
- [58] The Petilla Interneuron Nomenclature Group (PING). Petilla terminology: nomenclature of features of GABAergic interneurons of the cerebral cortex. *Nat Rev Neurosci* 2008;**9**:557–68. <https://doi.org/10.1038/nrn2402>
- [59] Kepecs A, Fishell G. Interneuron cell types are fit to function. *Nature* 2014;**505**:318–26. <https://doi.org/10.1038/nature12983>
- [60] Fishell G, Kepecs A. Interneuron Types as Attractors and Controllers. *Annu Rev Neurosci* 2020;**43**:1–30. <https://doi.org/10.1146/annurev-neuro-070918-050421>
- [61] Christodoulou O, Maragkos I, Antonakou V, Denaxa M. The development of MGE-derived cortical interneurons: An Lhx6 tale. *Int J Dev Biol* 2022;**66**:43–9. <https://doi.org/10.1387/ijdb.210185md>
- [62] Bandler RC, Mayer C, Fishell G. Cortical interneuron specification: the juncture of genes, time and geometry. *Curr Opin Neurobiol* 2017;**42**:17–24. <https://doi.org/10.1016/j.conb.2016.10.003>
- [63] Batista-Brito R, Ward C, Fishell G. The generation of cortical interneurons. Patterning Cell Type Specif. Dev. CNS PNS, *Comprehensive Developmental Neuroscience* 2020;**20**:461–79. <https://doi.org/10.1016/B978-0-12-814405-3.00020-5>
- [64] Englund C, Fink A, Lau C, Pham D, Daza RAM, Bulfone A, et al. Pax6, Tbr2, and Tbr1 Are Expressed Sequentially by Radial Glia, Intermediate Progenitor Cells, and Postmitotic Neurons in Developing Neocortex. *J Neurosci* 2005;**25**:247–51. <https://doi.org/10.1523/JNEUROSCI.2899-04.2005>
- [65] Gomes AR, Fernandes TG, Vaz SH, Silva TP, Bekman EP, Xapelli S, et al. Modeling Rett Syndrome With Human Patient-Specific Forebrain Organoids. *Front Cell Dev Biol* 2020;**8**:610427. <https://doi.org/10.3389/fcell.2020.610427>
- [66] Reumann D, Krauditsch C, Novatchkova M, Sozzi E, Wong SN, Zabolocki M, et al. In vitro modeling of the human dopaminergic system using spatially arranged ventral midbrain–striatum–cortex assembloids. *Nat Methods* 2023;**20**:2034–47. <https://doi.org/10.1038/s41592-023-02080-x>
- [67] Fetit R, Barbato MI, Theil T, Pratt T, Price DJ. 16p11.2 deletion accelerates subpallial maturation and increases variability in human iPSC-derived ventral telencephalic organoids. *Development* 2023;**150**:dev201227. <https://doi.org/10.1242/dev.201227>
- [68] Walsh CA, Morrow EM, Rubenstein JLR. Autism and Brain Development. *Cell* 2008;**135**:396–400. <https://doi.org/10.1016/j.cell.2008.10.015>
- [69] Wang L, Wang B, Wu C, Wang J, Sun M. Autism Spectrum Disorder: Neurodevelopmental Risk Factors, Biological Mechanism, and Precision Therapy. *Int J Mol Sci* 2023;**24**:1819. <https://doi.org/10.3390/ijms24031819>
- [70] Sharma SR, Gonda X, Tarazi FI. Autism Spectrum Disorder: Classification, diagnosis and therapy. *Pharmacol Ther* 2018;**190**:91–104. <https://doi.org/10.1016/j.pharmthera.2018.05.007>
- [71] Lim HK, Yoon JH, Song M. Autism Spectrum Disorder Genes: Disease-Related Networks and Compensatory Strategies. *Front Mol Neurosci* 2022;**15**:922840. <https://doi.org/10.3389/fnmol.2022.922840>
- [72] Doldur-Balli F, Imamura T, Veatch OJ, Gong NN, Lim DC, Hart MP, et al. Synaptic dysfunction connects autism spectrum disorder and sleep disturbances: A perspective from studies in model organisms. *Sleep Med Rev* 2022;**62**:101595. <https://doi.org/10.1016/j.smr.2022.101595>

- [73] Zhang J, Cai F, Lu R, Xing X, Xu L, Wu K, et al. CNTNAP2 intracellular domain (CICD) generated by γ -secretase cleavage improves autism-related behaviors. *Signal Transduct Target Ther* 2023;**8**:219. <https://doi.org/10.1038/s41392-023-01431-6>
- [74] Contractor A, Ethell IM, Portera-Cailliau C. Cortical interneurons in autism. *Nat Neurosci* 2021;**24**:1648–59. <https://doi.org/10.1038/s41593-021-00967-6>
- [75] Kereszturi É. Diversity and Classification of Genetic Variations in Autism Spectrum Disorder. *Int J Mol Sci* 2023;**24**:16768. <https://doi.org/10.3390/ijms242316768>
- [76] Modabbernia A, Velthorst E, Reichenberg A. Environmental risk factors for autism: an evidence-based review of systematic reviews and meta-analyses. *Mol Autism* 2017;**8**:13. <https://doi.org/10.1186/s13229-017-0121-4>
- [77] Boksha IS, Prokhorova TA, Tereshkina EB, Savushkina OK, Burbaeva GSh. Protein Phosphorylation Signaling Cascades in Autism: The Role of mTOR Pathway. *Biochem Mosc* 2021;**86**:577–96. <https://doi.org/10.1134/S0006297921050072>
- [78] Courchesne E, Pierce K, Schumann CM, Redcay E, Buckwalter JA, Kennedy DP, et al. Mapping Early Brain Development in Autism. *Neuron* 2007;**56**:399–413. <https://doi.org/10.1016/j.neuron.2007.10.016>
- [79] Peñagarikano O, Geschwind DH. What does CNTNAP2 reveal about autism spectrum disorder? *Trends Mol Med* 2012;**18**:156–63. <https://doi.org/10.1016/j.molmed.2012.01.003>
- [80] St. George-Hyslop F, Kivisild T, Livesey FJ. The role of contactin-associated protein-like 2 in neurodevelopmental disease and human cerebral cortex evolution. *Front Mol Neurosci* 2022;**15**:1017144. <https://doi.org/10.3389/fnmol.2022.1017144>
- [81] D’Onofrio G, Accogli A, Severino M, Caliskan H, Kokotović T, Blazekovic A, et al. Genotype–phenotype correlation in contactin-associated protein-like 2 (CNTNAP-2) developmental disorder. *Hum Genet* 2023;**142**:909–25. <https://doi.org/10.1007/s00439-023-02552-2>
- [82] Lu Z, Reddy MVVVS, Liu J, Kalichava A, Liu J, Zhang L, et al. Molecular Architecture of Contactin-associated Protein-like 2 (CNTNAP2) and Its Interaction with Contactin 2 (CNTN2). *J Biol Chem* 2016;**291**:24133–47. <https://doi.org/10.1074/jbc.M116.748236>
- [83] Peñagarikano O, Abrahams BS, Herman EI, Winden KD, Gdalyahu A, Dong H, et al. Absence of CNTNAP2 Leads to Epilepsy, Neuronal Migration Abnormalities, and Core Autism-Related Deficits. *Cell* 2011;**147**:235–46. <https://doi.org/10.1016/j.cell.2011.08.040>
- [84] St George-Hyslop F, Haneklaus M, Kivisild T, Livesey FJ. Loss of CNTNAP2 Alters Human Cortical Excitatory Neuron Differentiation and Neural Network Development. *Biol Psychiatry* 2023;**94**:780–91. <https://doi.org/10.1016/j.biopsych.2023.03.014>
- [85] Canali G, Garcia M, Hivert B, Pinatel D, Goullancourt A, Oguievetskaia K, et al. Genetic variants in autism-related CNTNAP2 impair axonal growth of cortical neurons. *Hum Mol Genet* 2018;**27**:1941–54. <https://doi.org/10.1093/hmg/ddy102>
- [86] Fernandes D, Santos SD, Coutinho E, Whitt JL, Beltrão N, Rondão T, et al. Disrupted AMPA Receptor Function upon Genetic- or Antibody-Mediated Loss of Autism-Associated CASPR2. *Cereb Cortex* 2019;**29**:4919–31. <https://doi.org/10.1093/cercor/bhz032>
- [87] Poliak S, Salomon D, Elhanany H, Sabanay H, Kiernan B, Pevny L, et al. Juxtaparanodal clustering of *Shaker*-like K⁺ channels in myelinated axons depends on Caspr2 and TAG-1. *J Cell Biol* 2003;**162**:1149–60. <https://doi.org/10.1083/jcb.200305018>
- [88] Poliak S, Peles E. The local differentiation of myelinated axons at nodes of Ranvier. *Nat Rev Neurosci* 2003;**4**:968–80. <https://doi.org/10.1038/nrn1253>
- [89] Pinatel D, Hivert B, Boucraut J, Saint-Martin M, Rogemond V, Zoupi L, et al. Inhibitory axons are targeted in hippocampal cell culture by anti-Caspr2 autoantibodies

- associated with limbic encephalitis. *Front Cell Neurosci* 2015;**9**:265. <https://doi.org/10.3389/fncel.2015.00265>
- [90] Barcia G, Scorrano G, Rio M, Gitiaux C, Hully M, Poirier K, et al. Exploring the clinical spectrum of CNTNAP2-related neurodevelopmental disorders: A case series and a literature appraisal. *Eur J Med Genet* 2024;**72**:104979. <https://doi.org/10.1016/j.ejmg.2024.104979>
- [91] Poot M. Connecting the CNTNAP2 Networks with Neurodevelopmental Disorders. *Mol Syndromol* 2015;**6**:7–22. <https://doi.org/10.1159/000371594>
- [92] Toma C, Pierce KD, Shaw AD, Heath A, Mitchell PB, Schofield PR, et al. Comprehensive cross-disorder analyses of CNTNAP2 suggest it is unlikely to be a primary risk gene for psychiatric disorders. *PLoS Genet* 2018;**14**:e1007535. <https://doi.org/10.1371/journal.pgen.1007535>
- [93] Gandhi T, Canepa CR, Adeyelu TT, Adeniyi PA, Lee CC. Neuroanatomical Alterations in the CNTNAP2 Mouse Model of Autism Spectrum Disorder. *Brain Sci* 2023;**13**:891. <https://doi.org/10.3390/brainsci13060891>
- [94] Paterno R, Marafija JR, Ramsay H, Li T, Salvati KA, Baraban SC. Hippocampal gamma and sharp-wave ripple oscillations are altered in a Cntnap2 mouse model of autism spectrum disorder. *Cell Rep* 2021;**37**:109970. <https://doi.org/10.1016/j.celrep.2021.109970>
- [95] Ahmed NY, Knowles R, Liu L, Yan Y, Li X, Schumann U, et al. Developmental deficits of MGE-derived interneurons in the Cntnap2 knockout mouse model of autism spectrum disorder. *Front Cell Dev Biol* 2023;**11**:1112062. <https://doi.org/10.3389/fcell.2023.1112062>
- [96] Jang WE, Park JH, Park G, Bang G, Na CH, Kim JY, et al. Cntnap2-dependent molecular networks in autism spectrum disorder revealed through an integrative multi-omics analysis. *Mol Psychiatry* 2023;**28**:810–21. <https://doi.org/10.1038/s41380-022-01822-1>
- [97] Scott KE, Kazazian K, Mann RS, Möhrle D, Schormans AL, Schmid S, et al. Loss of Cntnap2 in the Rat Causes Autism-Related Alterations in Social Interactions, Stereotypic Behavior, and Sensory Processing. *Autism Res* 2020;**13**:1698–717. <https://doi.org/10.1002/aur.2364>
- [98] George-Hyslop FS, Haneklaus M, Kivisild T, Livesey FJ. Loss of CNTNAP2 Alters Human Cortical Excitatory Neuron Differentiation and Neural Network Development. *Biol Psychiatry* 2023;**94**:780–91. <https://doi.org/10.1016/j.biopsych.2023.03.014>
- [99] Tariq K, Cullen E, Getz SA, Conching AKS, Goyette AR, Prina ML, et al. Disruption of mTORC1 rescues neuronal overgrowth and synapse function dysregulated by Pten loss. *Cell Rep* 2022;**41**:111574. <https://doi.org/10.1016/j.celrep.2022.111574>
- [100] Huang J, Chen L, Wu J, Ai D, Zhang J-Q, Chen T-G, et al. Targeting the PI3K/AKT/mTOR Signaling Pathway in the Treatment of Human Diseases: Current Status, Trends, and Solutions. *J Med Chem* 2022;**65**:16033–61. <https://doi.org/10.1021/acs.jmedchem.2c01070>
- [101] Nussinov R, Yavuz BR, Arici MK, Demirel HC, Zhang M, Liu Y, et al. Neurodevelopmental disorders, like cancer, are connected to impaired chromatin remodelers, PI3K/mTOR, and PAK1-regulated MAPK. *Biophys Rev* 2023;**15**:163–81. <https://doi.org/10.1007/s12551-023-01054-9>
- [102] Sharma A, Mehan S. Targeting PI3K-AKT/mTOR signaling in the prevention of autism. *Neurochem Int* 2021;**147**:105067. <https://doi.org/10.1016/j.neuint.2021.105067>
- [103] Wang L, Zhou K, Fu Z, Yu D, Huang H, Zang X, et al. Brain Development and Akt Signaling: the Crossroads of Signaling Pathway and Neurodevelopmental Diseases. *J Mol Neurosci* 2017;**61**:379–84. <https://doi.org/10.1007/s12031-016-0872-y>

- [104] Statoulla E, Chalkiadaki K, Karozis D, Gkogkas CG. Regulation of mRNA translation in stem cells; links to brain disorders. *Cell Signal* 2021;**88**:110166. <https://doi.org/10.1016/j.cellsig.2021.110166>
- [105] Ma Q, Chen G, Li Y, Guo Z, Zhang X. The molecular genetics of PI3K/PTEN/AKT/mTOR pathway in the malformations of cortical development. *Genes Dis* 2024;**11**:101021. <https://doi.org/10.1016/j.gendis.2023.04.041>
- [106] Andrews MG, Subramanian L, Kriegstein AR. mTOR signaling regulates the morphology and migration of outer radial glia in developing human cortex. *eLife* 2020;**9**:e58737. <https://doi.org/10.7554/eLife.58737>
- [107] Thomas SD, Jha NK, Ojha S, Sadek B. mTOR Signaling Disruption and Its Association with the Development of Autism Spectrum Disorder. *Molecules* 2023;**28**:1889. <https://doi.org/10.3390/molecules28041889>
- [108] Xing X, Zhang J, Wu K, Cao B, Li X, Jiang F, et al. Suppression of Akt-mTOR pathway rescued the social behavior in Cntnap2-deficient mice. *Sci Rep* 2019;**9**:3041. <https://doi.org/10.1038/s41598-019-39434-5>
- [109] Boksha IS, Prokhorova TA, Tereshkina EB, Savushkina OK, Burbaeva GSh. Protein Phosphorylation Signaling Cascades in Autism: The Role of mTOR Pathway. *Biochem Mosc* 2021;**86**:577–96. <https://doi.org/10.1134/S0006297921050072>
- [110] Zhao H, Mao X, Zhu C, Zou X, Peng F, Yang W, et al. GABAergic System Dysfunction in Autism Spectrum Disorders. *Front Cell Dev Biol* 2022;**9**:781327. <https://doi.org/10.3389/fcell.2021.781327>
- [111] Hoffman EJ, Turner KJ, Fernandez JM, Cifuentes D, Ghosh M, Ijaz S, et al. Estrogens Suppress a Behavioral Phenotype in Zebrafish Mutants of the Autism Risk Gene, CNTNAP2. *Neuron* 2016;**89**:725–33. <https://doi.org/10.1016/j.neuron.2015.12.039>
- [112] St George-Hyslop F, Haneklaus M, Kivisild T, Livesey FJ. Loss of CNTNAP2 Alters Human Cortical Excitatory Neuron Differentiation and Neural Network Development. *Biol Psychiatry* 2023;**94**:780–91. <https://doi.org/10.1016/j.biopsych.2023.03.014>
- [113] Xing X, Zhang J, Wu K, Cao B, Li X, Jiang F, et al. Suppression of Akt-mTOR pathway rescued the social behavior in Cntnap2-deficient mice. *Sci Rep* 2019;**9**:3041. <https://doi.org/10.1038/s41598-019-39434-5>
- [114] Lancaster MA, Renner M, Martin C-A, Wenzel D, Bicknell LS, Hurles ME, et al. Cerebral organoids model human brain development and microcephaly. *Nature* 2013;**501**:373–9. <https://doi.org/10.1038/nature12517>
- [115] Akula SK, Exposito-Alonso D, Walsh CA. Shaping the brain: The emergence of cortical structure and folding. *Dev Cell* 2023;**58**:2836–49. <https://doi.org/10.1016/j.devcel.2023.11.004>
- [116] Pigoni M, Uzquiano A, Paulsen B, Kedaigle AJ, Yang SM, Symvoulidis P, et al. Cell-type specific defects in *PTEN* -mutant cortical organoids converge on abnormal circuit activity. *Hum Mol Genet* 2023;**32**:2773–86. <https://doi.org/10.1093/hmg/ddad107>
- [117] Chalkiadaki K, Statoulla E, Zafeiri M, Voudouri G, Amvrosiadis T, Typou A, et al. GABA/Glutamate Neuron Differentiation Imbalance and Increased AKT/mTOR Signaling in CNTNAP2–/– Cerebral Organoids. *Biol Psychiatry Glob Open Sci* 2025;**5**:100413. <https://doi.org/10.1016/j.bpsgos.2024.100413>
- [118] Welcome to XCell Science n.d. <https://www.xcellscience.com/control-lines/xcl-1> (accessed January 26, 2025)
- [119] Traka M, Dupree JL, Popko B, Karagogeos D. The Neuronal Adhesion Protein TAG-1 Is Expressed by Schwann Cells and Oligodendrocytes and Is Localized to the Juxtaparanodal Region of Myelinated Fibers. *J Neurosci* 2002;**22**:3016–24. <https://doi.org/10.1523/JNEUROSCI.22-08-03016.2002>

- [120] Falivelli G, De Jaco A, Favaloro FL, Kim H, Wilson J, Dubi N, et al. Inherited genetic variants in autism-related CNTNAP2 show perturbed trafficking and ATF6 activation. *Hum Mol Genet* 2012;**21**:4761–73. <https://doi.org/10.1093/hmg/dds320>
- [121] Deriziotis P, O’Roak BJ, Graham SA, Estruch SB, Dimitropoulou D, Bernier RA, et al. De novo TBR1 mutations in sporadic autism disrupt protein functions. *Nat Commun* 2014;**5**:4954. <https://doi.org/10.1038/ncomms5954>
- [122] Vernes SC, Newbury DF, Abrahams BS, Winchester L, Nicod J, Groszer M, et al. A Functional Genetic Link between Distinct Developmental Language Disorders. *N Engl J Med* 2008;**359**:2337–45. <https://doi.org/10.1056/NEJMoa0802828>
- [123] Chiu Y, Li M, Liu Y, Ding J, Yu J, Wang T. Foxp2 regulates neuronal differentiation and neuronal subtype specification. *Dev Neurobiol* 2014;**74**:723–38. <https://doi.org/10.1002/dneu.22166>
- [124] Vernes SC, Newbury DF, Abrahams BS, Winchester L, Nicod J, Groszer M, et al. A Functional Genetic Link between Distinct Developmental Language Disorders. *N Engl J Med* 2008;**359**:2337–45. <https://doi.org/10.1056/NEJMoa0802828>
- [125] Chan WK, Negro D, Munro VM, Marshall H, Kozić Z, Brown M, et al. Loss of PAX6 alters the excitatory/inhibitory neuronal ratio in human cerebral organoids. *bioRxiv* 2023. <https://doi.org/10.1101/2023.07.31.551262>